

EUROFER 97
Tensile, Charpy, Creep and
Structural Tests

**M. Rieth, M. Schirra, A. Falkenstein, P. Graf,
S. Heger, H. Kempe, R. Lindau,
H. Zimmermann**

**Institut für Materialforschung
Programm Kernfusion**

Forschungszentrum Karlsruhe

in der Helmholtz-Gemeinschaft

Wissenschaftliche Berichte

FZKA 6911

EUROFER 97

Tensile, Charpy, Creep and Structural Tests

M. Rieth, M. Schirra, A. Falkenstein, P. Graf, S. Heger,

H. Kempe, R. Lindau, H. Zimmermann

Institut für Materialforschung

Programm Kernfusion

Forschungszentrum Karlsruhe GmbH, Karlsruhe

2003

Impressum der Print-Ausgabe:

**Als Manuskript gedruckt
Für diesen Bericht behalten wir uns alle Rechte vor**

**Forschungszentrum Karlsruhe GmbH
Postfach 3640, 76021 Karlsruhe**

**Mitglied der Hermann von Helmholtz-Gemeinschaft
Deutscher Forschungszentren (HGF)**

ISSN 0947-8620

Abstract

EUROFER 97 – the European reference material for the first wall of a DEMO fusion reactor – was produced as 3.5 t batch of rods and plates. Following the history of the development activities from conventional martensitic 12 % Cr steel, MANET and OPTIFER up to the low or reduced activation (RAFM) EUROFER steel, results obtained from experiments on specimens from rods (\varnothing 100 mm) and plates (14 mm) are presented for a basic characterization. Physical and mechanical properties are compared with those of OPTIFER-1W and the F82H-mod 2% W steel.

The transition behaviour was determined by plotting a continuous TTT (time temperature transition) diagram. In addition, extension coefficients were determined from room temperature up to 1000 °C.

Hardening tests at temperatures from 850 °C to 1120 °C illustrated the range of maximum hardness as well as grain size development. Tempering tests and additional annealing experiments from 300 °C to 875 °C allowed characterizing tempering behaviour and stability.

Charpy properties were examined for various heat treatments and specimen types between 60 °C and -100 °C. Further, ductility criteria like FATT, DBTT and 68 J were determined. Particular attention was paid to the influence of grain size and O₂ content.

Tensile strength was measured for several heat treatments between room temperature and 700 °C.

Long-term ageing was investigated by means of stabilization annealing experiments. These were carried out with various temperature/time combinations including tensile tests. In EUROFER tensile strength was hardly affected by the different heat treatments while the ductility criteria showed only a moderate increase in temperature. Therefore, it can be concluded that EUROFER is not susceptible to ageing.

Creep and creep rupture properties were investigated in the temperature range of 450 °C to 650 °C. So far, creep times of up to 15000 h have been covered by the experiments. The status of the test program allows for an extrapolation of the 1 % yield limits and times to rupture to a period of 20000 h. Creep behaviour and stress exponents can be determined reliably for the experimental stress range. However, for the design relevant low stress range (= 100 MPa) up to 550 °C creep data are still lacking.

Therefore, special creep tests at 500 °C and 550 °C were started in 2001. They are aimed at the experimental determination of design relevant yield limits (0.01-1%) and minimum creep rate behaviour.

EUROFER 97: Zug-, Kerbschlag-, Kriechversuche und Strukturuntersuchungen

Zusammenfassung

Der europäische Referenzwerkstoff EUROFER für die Erste Wand eines DEMO-Fusionsreaktors ist als 3,5 t-Charge in verschiedenen Halbzeugabmessungen hergestellt worden. Nach dem historischen Vorspann über die Entwicklungslinie vom konventionellen martensitischen 12% Cr-Stahl über MANET und OPTIFER zum reduziert-aktivierenden EUROFER, werden die Ergebnisse der Versuche an 2 Halbzeugabmessungen ($\varnothing 100$ mm und 14 mm Blech) zur Basis-Charakterisierung beschrieben. Die physikalischen und mechanischen Eigenschaften werden mit denen von OPTIFER-1W und dem 2%W-Stahl F82H-mod verglichen.

Zur Klärung des Umwandlungsverhaltens wurde ein kontinuierliches Zeit-Temperatur-Umwandlungsschaubild erstellt und die Ausdehnungskoeffizienten für RT-1000°C bestimmt. Härteversuche im Temperaturbereich 850-1120°C zeigen den Bereich der maximalen Härteannahme und die Korngrößenentwicklung. Anlassversuche und zusätzliche Glühversuche im T-Bereich 300-875°C geben Aufschluss über das Anlassverhalten und die zusätzlichen Glühversuche über die Anlassbeständigkeit. Das Kerbschlagzähigkeitsverhalten wird für verschiedene Vergütungszustände und Proben aus 2 verschiedenen Halbzeugen für den Prüftemperaturbereich +60 bis -100°C beschrieben und die Duktilitätskriterien FATT-DBTT-68 J bestimmt. Auf den Einfluss der Korngröße und des O₂-Gehaltes wird besonders hingewiesen. Die Zugfestigkeitseigenschaften für verschiedene Vergütungszustände wurden im Prüftemperaturbereich RT-700°C bestimmt.

Das Alterungsverhalten der Vergütungsstruktur, infolge langzeitiger Temperatureinwirkung, wurde durch Stabilisierungsglühungen mit verschiedenen T/t-Kombinationen auf die Zugfestigkeitseigenschaften untersucht. EUROFER zeigt bei den Zugfestigkeitseigenschaften praktisch kaum einen Einfluss der Glühbehandlungen und bei den Kerbschlagzähigkeitseigenschaften nur eine moderate Erhöhung der Temperaturen für die Zähigkeitskriterien, d.h., EUROFER ist nicht alterungsanfällig.

Das Zeitstandfestigkeits- und Kriechverhalten wird im T-Bereich 450-650°C untersucht, und bisher ist der Versuchszeitraum bis rd. 15000 h experimentell abgedeckt. Der bisherige Stand des Versuchsprogramms erlaubt die Festlegung der Mindestwerte für die 1% Zeit-Dehngrenzen und die Zeitstandfestigkeit für 20000 h Einsatzzeit. Das Kriechverhalten mit dem daraus abgeleiteten Spannungsexponenten kann für den experimentell abgedeckten Spannungsbereich sicher angegeben werden.

CONTENTS

1	Introduction.....	1
2	History.....	1
3	Test Material.....	3
4	Test Results.....	4
4.1	Transition Behaviour.....	4
4.2	Hardening and Annealing Behaviour.....	5
4.3	Charpy Properties.....	8
4.4	Tensile Properties.....	10
4.5	Ageing Behaviour.....	11
4.5.1	Tensile Test Results.....	11
4.5.2	Charpy Test Results.....	12
4.6	Creep and Creep Rupture Behaviour.....	12
4.6.1	Creep and Creep Rupture Tests at 450-650 °C.....	13
4.6.2	Creep Tests in the Low Stress Range at 500 °C and 550 °C.....	17
5	Summary.....	19
6	Literature.....	20
7	Tables	
8	Figures	

1 Introduction

Materials development is one of the technological key topics for the realization of future fusion reactors. In particular, first wall materials with low activation potential, high temperature and corrosion resistance as well as insensitivity for neutron irradiation are of highest interest [1, 2]. Due to their chemical composition such low or reduced activation alloys show much faster deactivation behaviour after operation (decrease of irradiation rate [Sv/h] and decay heat [W/kg]). For the nuclear waste management this is of particular significance because the major part of radioactivity comes from structural materials (helium as product of nuclear fusion is not radioactive). Therefore, environmental and security criteria have a high priority [3].

Activation calculations have shown that in principle different metals could be used as base for low activation alloys like, for example, V, Cr, Ti, Fe. But beside low activation aspects also physical and mechanical properties as well as production and processing technology are of decisive significance. So the short time till realization of ITER allows only for iron base alloys, i.e. martensitic 8-11 % CrWVTa steels, for the use as structural material [4].

With the development of EUROFER as European reference material for a future DEMO reactor a major milestone has been reached. Therefore, it seems to be appropriate to give an overview of the different developmental steps that led to EUROFER 97.

2 History

Development of the low activation alloys started from the high temperature 12 % Cr steels. For decades they had been applied in the construction of conventional plants, power plants, and turbines. Consequently, their production and processing technology was well established [5-10] contrary to the longer-term development of vanadium based alloys, for instance.

In 1965, development activities of the Forschungszentrum Karlsruhe / Institute for Materials Research (FZK / IMF) started with the Nb-free steel 1.4922 used in plant construction and the Nb-stabilized 1.4914 used for aircraft engines [11]. Within the fast breeder project, a modified version of the 1.4914 steel with improved toughness was developed for use as fuel element wrapper after various problems had been dealt with and solved (Fig. 1, stage I). This line of development is presented in detail in [12-14].

In a next step, a potential first-wall alloy was developed for the planned Next European Torus (NET) facility within the framework of the nuclear fusion project. This material was referred to as MANET (Martensite for NET) (see Fig. 1, stage II) [15-21]. By optimizing the chemical composition, high-temperature stability and transition behaviour were improved. At the same time, the embrittlement behaviour was more favourable due to a finer grain. New findings with respect to the N/Al ratio resulted in a δ -ferrite free, more stable structure, optimized precipitation behaviour, and improved creep toughness [22-25].

History

Based on this experience, the first, so-called low-activation alloys CeTa and TaHf were produced in 1986. For these, the alloying elements with long decay times due to high activation by neutron irradiation (Nb, Mo, Ni, Al) had been substituted by Ta, W, and Ce [4b, 26]. The alloys were specified along the lines of international development programs. A variety of CrMnWVNTa experimental alloys (LA series) had already been produced and tested in particular by the Culham Laboratory / British Steel, UK [27, 28].

The specification of the alloys was based on activation calculations which, at that time, were characterized by contradictions regarding element activation due to different spectra, computation methods, and nuclear data libraries. In some cases, for example, only simple neutron induced collision processes were taken into account. Only with the introduction of sequential reactions by S. Cierjacks [29-32], their international acceptance [4b] and further adaptation efforts well founded project related statements could be made with respect to the element and alloys activation. So generally accepted decay curves could be plotted, as shown by the three examples in Fig. 2 [33, 34]. As a consequence, several alloying elements were rejected or limited (Hf, Ta, W) and new upper limits were obtained for all radiologically undesired tramp elements. Part of these limits is found to be in the ppm and sub-ppm range and cannot yet be achieved metallurgically and analytically. This is the reason why this stage of development is also referred to as reduced activation (RAFM = Reduced Activation Martensitic) steels.

With this guidelines, the development line of the OPTIFER (Optimized Ferrite) alloys started at FZK in 1992 within the framework of the European Long-term Programme [35-37] (Fig. 1, stage III). The OPTIFER alloys are 9.5 % Cr-Mn-V-Ta steels with 1 % W or W free variants with germanium [38] (Table 1).

Parallel to the work on OPTIFER, a Japanese version of an 8 % Cr-Mn-V steel with 2 % W has been investigated since 1994. This RAFM steel, called F82H-mod, was produced as a batch of 5 tons by JAERI / NKK and made available as plate material by IEA to European laboratories for joint examinations (round robin tests) [39].

Based on the physical, mechanical, and structural data obtained for OPTIFER and F82H-mod [40, 41] combined with the findings made by various European institutes with regard to low activation alloys (UK, F), BATMAN alloys (I), and OPTIMAX steels (CH) [18], a specification was set up for a European reference alloy (Table 2a). For comparison, Table 2b shows analytical data for OPTIFER (1W) and F82H-mod (2W).

Motivation points for this industrial heat had been:

- Gathering experience with the industrial production of a high purity steel and comparison with experimental heat production details.
- Gathering information about forming properties, homogeneity of mechanical and structural properties, and targeting specified mechanical and microstructural characteristics.
- Gaining technological results from the production of a test blanket module with respect to forming and weldability.

- The most important mechanical and metallurgical properties as well as the irradiation performance should be characterized within a common testing program by the European associations.

The alloy, designated EUROFER 97, has been available to European laboratories for various development activities since 1999 (Fig. 36).

Further perspectives of developmental work with respect to EUROFER-ODS or V-alloys are shown in [42-45] including international comments.

This report includes data of EUROFER 97 that has been produced within the frame of basic characterization tests at FZK / IMF I in 2001. First results are published in [46-49].

3 Test Material

After an European ITB the EUROFER production offer of Böhler Edelstahl GmbH, Austria was accepted by the European Commission. Different plates, rods, pipes and welding wires were delivered with a total weight of 3.5 t. The according heats were arc-molten in vacuum and after that re-molten again. The production steps are described in [50].

All specimens used for the basic characterisation have been fabricated from Ø 100 mm forged rods (heat E 83699) and 14 mm rolled plates (heat E 83698). The chemical composition according to the producer of these heats is given in Table 3 (A). The alloying elements (a) are well within the specification except of the Ta content which is too high but results in a finer grain. An FZK/IMF chemical analysis of heat 83698 (B) and published compositions of three heats with 5 different dimensions (C) agree well the producer data [51]. The desired values for critical elements with respect to low activation (c) like Ni and Nb could not yet be met. The metallurgical problems are discussed more detailed in [50].

The difference between the desired and real values for the content of the critical high activation elements (c) becomes clear when comparing the analysis data with the desired maximum limits [32-34]. Figure 3 shows the real contents of the OPTIFER, F82H-mod and EUROFER heats. But it is also clear that there has been a large progress since the start of the low activation materials development. Especially the most critical element (Nb) has been reduced from 100-200 ppm at the beginning down to 1-5 ppm for OPTIFER-Xb.

Figure 4 shows the results of activation calculations using the real values of the chemical analysis of the different alloys. In this connection, the hypothetical steel EUROFER-ref. (?) refers to EUROFER with a chemical composition as specified. The dominant influence of Nb can be seen by comparing the deactivation curves for F82H-mod (1-2 ppm Nb, ▽) and for

EUROFER with 10-15 ppm Nb (?). The progress of the low activation alloys development with respect to waste disposal can also be clearly seen. While the conventional steels (AISI 316, MANET) would have to be handled as highly radioactive waste even after more than 100 years, EUROFER and F82H-mod could be considered as low-level radioactive [34, 39, 42].

The EUROFER material as delivered has been heat treated according to the producer as follows:

rod: \varnothing 100 mm: 979°C 1h 51 min/air + 739°C 3h 42min/air,
plate: 14 mm: 980°C 27 min/air + 760°C 90 min/air.

The provided tempering protocol shows that the austenitization time of the \varnothing 100 mm rod includes heating up. But the holding time at 979°C was 1h 15 min. The reason for the different annealing temperatures (739°C and 760°C) was to achieve the same hardness for plates and rods. For the sake of simplicity, in the following we refer to the annealing treatments as follows:

rod \varnothing 100 : $980^{\circ}\text{C}/\text{air} + 740^{\circ}\text{C}/\text{air}$ and
plate 14 mm : $980^{\circ}\text{C}/\text{air} + 760^{\circ}\text{C}/\text{air}$.

Examples for the fully martensitic microstructure can be seen in Fig. 5. It shows metallographic pictures of the rod. Border and core zones with values for hardness and grain size are compiled. Further results from metallographic examinations of plates and rods are given in [52].

4 Test Results

4.1 Transition Behaviour

For proper heat treatments of hardening steels the knowledge of the according transition behaviour is of high significance. Continuous heating and cooling processes are most common in practise and, therefore, the continuous Time-Temperature Transition (TTT) diagram is more important than the isothermal TTT diagram [53]. By our order SAARSTAHL has created a TTT diagram for the EUROFER 97 steel for continuous cooling processes with an austenitization temperature of 980°C according to the reference hardening temperature (see Fig. 6). The transition temperatures are

$$A_{c1b} = 820^{\circ}\text{C} \quad M_s = 385^{\circ}\text{C} \quad \text{Pearlite formation for cooling rates} > 5^{\circ}\text{C}/\text{min}$$
$$A_{c1e} = 890^{\circ}\text{C} \quad M_f = 215^{\circ}\text{C}$$

One has to bear in mind that M_s , M_f and the formation of Pearlite depends on the austenitization temperature T_{Au} . Since the A_c points are determined during the heating phase they are independent of T_{Au} . This can be clearly seen in Fig. 7 where the TTT diagrams of different comparable steel types (see Table 1) are plotted for $T_{Au} < 1000^\circ$ (a) und $T_{Au} > 1000^\circ$ (b). Especially the region of Pearlite formation is shifted to slower cooling rates for higher austenitization temperatures [53]. Here EUROFER 97 shows practically the same transition behaviour as OPTIFER-V (B) and the tungsten free version OPTIFER-VI (D). In addition the expansion coefficient α has been determined from the dilatometer graphs for different intervals:

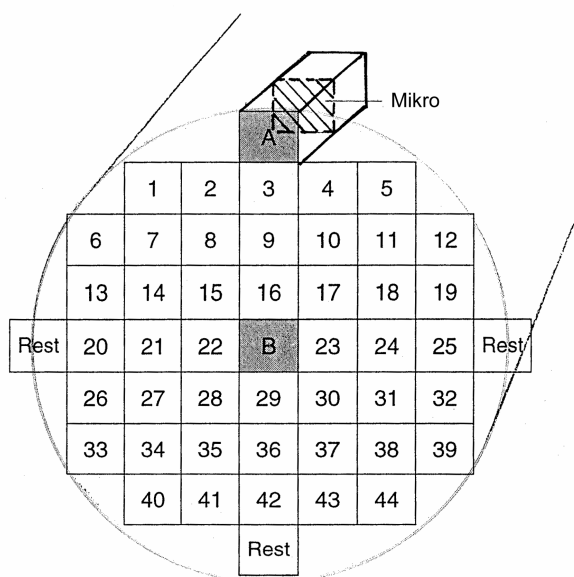
20-100 °C:	$\alpha = 12,23 \cdot 10^{-6}/^\circ\text{C}$	
20-200 °C:	= 12,04	
20-300 °C:	= 12,01	
20-400 °C:	= 12,14	> A_{c1}
20-500 °C:	= 12,33	$20 - 800 = 12,74 \cdot 10^{-6}/^\circ\text{C}$
20-600 °C:	= 12,56	$20 - 900 = 10,07$
20-700 °C:	= 12,79	$20 - 1000 = 11,26$

The so far unanswered question about the effect of longer isothermal holding times in the transitionless temperature region between Pearlite formation and onset of Martensite after further cooling down to room temperature (hardening) on the martensitic microstructure has been clarified by a test series using the F82H-mod steel [40]. This question is of significant relevance if – due to warping – larger or more complicated components can not be cooled down to room temperature at once. In such cases a stepwise cooling procedure or warm bath hardening is necessary.

A test series of F82H-mod specimens has been austenitized at 1040 °C and loaded into a furnace at 500 °C (Martensite formation temperature $M_s = 425^\circ\text{C}$). After different holding times of the subcooled Austenite (from 5 h to 10000 h) the specimens have been air cooled (Fig. 8). Metallographic postexaminations have shown the same complete martensitic microstructure with the same hardness level for all specimens – even for those with extreme holding times of 500-10000 h. The observed structure and hardness is the same like that after continuous cooling with a rate of 1.25 °C/min.

4.2 Hardening and Annealing Behaviour

Such complementary properties like toughness and strength may be controlled through grain size and hardness for hardening steels like EUROFER 97 by a suitable choice of hardening and/or annealing temperature. To determine the hardening and annealing behaviour specimens have been fabricated out of a 15 mm disc from a Ø100 mm rod (the layout is given below).



Specimens A and B have been used for metallographic examinations of the condition as delivered (Section 3). Specimens 1-7 have been austenitized in a quartz tube under vacuum for 30 minutes in the temperature range between 850 °C and 1120 °C to avoid decarbonisation and tinder. Cooling has been performed simply by removal of the furnace. Due to the small masses this results approximately in the same cooling rates like in air (T , t , V/V). Then the specimens have been bisected to determine hardness and grain size (transverse to the rod axis). As can bee seen from Fig. 9-Aa maximum hardness is reached for temperatures above 900 °C. The metallographic determination of the grain size shows only a moderate grain coarsening with rising austenitization temperatures (Fig. 9-Ab and Table below).

Results of Hardness Tests		HV30*)	Grainsize
Spec. No.	1 = 850°C 30' V/V	245	10 µm
	2 = 900°C 30' V/V	406	11
	3 = 950°C 30' V/V	421	13,5
	4 = 1000°C 30' V/V	430	14,3
	5 = 1040°C 30' V/V	412	21,4
	6 = 1080°C 30' V/V	412	48,1
	7 = 1120°C 30' V/V	400	52,5
*) Average of 3 Measurements			

The comparison with F82H-mod and different OPTIFER steel types shows a similar behaviour while differences in the slope and onset of the hardening curve result mainly from different C+N contents. The distinct lower hardness of OPTIFER-III with 1.6 % Ta is connected with the formation of primary carbides (Ta_3C) and, therefore, with a reduction of solved carbon [37]. The grain size (b) depends on the Ta content and – as shown in [40, 41] – Ta contents of less than 0.02 % (F82H-mod, OPTIFER-II) are not sufficient to yield an adequate fine grain. This is the reason why a lower bound of 0.05 % has been specified for EUROFER 97.

Prior to the annealing tests two different solution heat treatments have been performed, one at 1040 °C and the other at 980 °C. The resulting annealing curves are independent of the prior austenitization temperatures (Fig. 10A) and show the common secondary hardness maximum between 500 °C and 550 °C as well as the drop in hardness due to the annealing effect up to 800 °C. The following partial austenitization (exceeding of Ac_{1b}) starting from 850 °C causes a rise in hardness.

Results of Annealing Tests (Specimen No. 8-32)						
				b)	950°2hV/V+1040°30'V/V+750°2hV/V	206 grain size = 22,1 µm
a)	<u>1040°30'V/V</u>	+ 300°2h/L	HV30	= 419	c)	980°30'V/V + 300°2h/L
	"	+ 400°2h/L		= 420		" + 400°2h/L
	"	+ 500°2h/L		= 421		" + 500°2h/L
	"	+ 525°sh/L		= 435		" + 525°2h/L
	"	+ 550°2h/L		= 435		" + 550°2h/L
	"	+ 600°2h/L		= 352		" + 600°2h/L
	"	+ 650°2hV/V		= 300		" + 650°2hV/V
	"	+ 700°2hV/V		= 264		" + 700°2hV/V
	"	+ 750°2hV/V		= 210		" + 750°2hV/V
	"	+ 800°2hV/V		= 194		" + 800°2hV/V
	"	+ 850°2hV/V		= 307		" + 850°2hV/V
	"	+ 875°2hV/V		= 412		" + 875°2hV/V

The table above shows a specimen (b) for which a homogenization heat treatment at 950 °C has been performed prior to the hardening and annealing treatment. For forged materials such homogenization heat treatments have shown good results. But in the present case where we have a rather homogeneous initial condition there is no influence on the grain size (Fig. 9) and on the annealing hardness (Fig. 10) detectable.

The annealing curve of EUROFER 97 looks like that of OPTIFER-Ia and IVc (Fig. 10B) and in the technically relevant temperature range of 650-750 °C it is similar to that of the F82H-mod alloy [40].

A distinguished hardness and toughness level is controlled by the solution and annealing heat treatment. The later long-term use at raised temperatures acts like an additional annealing on the hardening condition (also called ageing) and lowers the initially selected hardness and toughness, respectively. This behaviour can not be seen in Fig. 10. It has to be completed by additional tests for annealing resistance (stabilization annealing). Extensive empirical examinations have shown the influence of annealing temperature and annealing time on the hardness. Both show a certain equivalence that has been described by Hollomon and Jaffe with a parameter $P = T_K(c+\log t)$ [54]. Later, this parameter has been used by Larson and Miller [55] to describe the creep rupture behaviour. With that it is possible – at least within certain boundaries – to extrapolate short-term hardness tests to longer periods.

Specimens in the condition as delivered from a 14 mm plate have been used to determine the so-called annealing master-curve for temperatures between 550 °C and 750 °C and for annealing times between 20 h and 3300 h. In addition two other specimens have been austenitized at 1075 °C and 950 °C and annealed at 750°C. Then they have been aged at 600 °C for 1050 h. The Hollomon-Jaffe parameter P for 600 °C / 1050 h has a value of 18.35. This is equivalent to 550 °C / 20000 h. The results of the hardness tests with the specimens are shown in Fig. 11 together with the Hollomon-Jaffe parameter. The annealing master-curve remains on the hardness level of the initial material up to a parameter value of P = 19. EUROFER 97 shows the same favourable behaviour like F82H-mod and OPTIFER which are also shown in the figure.

Therefore it is clear that metallographic examinations of the aged specimens have resulted in no major changes of the martensitic microstructure. Figures 12 and 13 show the initial microstructure after three different annealing heat treatments and after the stabilization treatment (600°C / 1050 h). It has been seen from metallographic examinations of different ferritic-martensitic steels that Cr contents of less than 10 % and heat treatments in the range of the α - γ -transition led to two-phase materials with the formation of α -Ferrite [56]. Also EUROFER with about 9 % Cr shows some per cent Ferrite after austenitization at 980 °C or 1040 °C and tempering at 850 °C (Fig. 14 a-c). The specimen tempered at 875 °C shows only few single Ferrite grains (Fig. 14 d). Since heat treatments are technological not relevant in the temperature range of the α - γ -transition the two-phase formation is only of metallurgical interest.

4.3 Charpy Properties

ISO-V specimens of a 14 mm EUROFER 97 plate have been tested after different heat treatments. The results are given in Fig. 15 and Table 4. Both, the condition as delivered (austenitized at 980 °C, symbol ●) and the condition with an austenitization temperature of 1040 °C (symbol ?) show – within the usual scattering – similar values for the toughness criteria (DBTT, FATT, 68 J, [57 c]). After austenitizing at 1075 °C, that is for a grain size of 45 μm the ductile-to-brittle transition is shifted to higher temperatures (! ?). An influence of the specimen orientation (transversal or longitudinal) on DBTT is not recognizable. Only differences in the upper shelf energy can be detected. This makes sense, because during manufacturing the plates have been shifted by 90° after each rolling step and, therefore, a distinctive rolling direction has been avoided. However, the scattering within test series with specimens of the same condition or between different plates is even more pronounced. The reported values from CIEMAT, Madrid for the plate #3 in the condition as delivered is clearly worse compared with plates #4, #5 and #6 [45].

The observed ductile-to-brittle transition behaviour is different depending on the prior heat treatment. For the condition as delivered and for the annealing temperature 1050 °C (● and ?) the transition is smooth while the other curves show a more or less extended step. Even though such behaviour has already been observed in the past for this type of steel [57 c] there is no reasonable explanation available. Also the scattering of the data makes a precise determination of the curve difficult (this extend of scattering has been observed with the F82H-mod steel too) because most often only one specimen per temperature is tested. Therefore we fabricated specimens from a EUROFER 97 Ø 100 mm rod transverse and longitudinal to the rod axis and performed five Charpy tests for a given test temperature in the

range between room temperature and -60 °C (Fig. 16, Table 5). In the case of this forged rod the influence of the specimen orientation can be seen quite clearly: the values for the longitudinal oriented specimens are much better.

The above mentioned step in the ductile-to-brittle transition is reproduced by drawing the average curves (details are given in Fig. 16 B).

The oxygen content (the concentrations are given in Table 1 for different alloys) is a further, quite essential influence on the Charpy properties which is most often neglected. Extensive Charpy tests – also with conventional martensitic 12 % Cr steels – have clearly shown a deterioration of the Charpy properties with an increasing O₂ content (Fig. 17) [57 b]. Based on these results for EUROFER 97 the O₂ content has been specified with less than 100 ppm.

The following table shows the EUROFER values for FATT and DBTT dependent on heat treatment and resulting grain size. For comparison F82H-mod and OPTIFER with different contents of O₂ are shown too.

		FATT	DBTT	Grain Size	O ₂
EUROFER 14 mm	as delivered = 980°+760° (transverse) = 1050°+750° (transverse) = 1075°+750° (transverse) = 1075°+750° (transverse)	-78° -72° -56° -54°	-70 -73 -56 -57	16 µm 26 µm 45 µm 11-16	10 ppm
Ø 100 mm	as delivered = 980°+740° (longitudinal) = 980°+740° (transverse)	-67 ^{*)} -49 ^{*)}	-70 ^{*)} -53 ^{*)}		13 ppm
F82H-mod [40]	as delivered = 1040°+750°	-35/-10	-42/-20	55 µm	103- 125 ppm
OPTIFER-IVc	= 960°+750° = 1075°+750	-	-35 -46	35 µm 103 µm	190
OPTIFER-V	= 950°+750 = 1075°+750 = 950°+750	-57 - -81	-72 -55 -88	14 µm 50 µm 12 µm	60

^{*)} Average Values

1) FATT: Fracture Appearance Transition Temperature (50 % crystalline fracture)

DBTT: Ductile Brittle Transition Temperature (Value at 50 % upper shelf energy)

68 J: Temperature at 68 J taken from Energy-Temperature curve

4.4 Tensile Properties

Tensile specimens have been fabricated from the Ø 100 mm rod and 14 mm plate in the condition as delivered (austenitization temperature 980 °C). The results of tensile tests performed in the temperature range from room temperature to 700 °C are compiled in Table 6. Further specimens with different applied heat treatments (1075 °C + 750 °C and 950 °C) have been tested for comparison with the OPTIFER alloys (Table 7).

From Fig. 18 it can be seen that tensile and yield strength of both conditions as delivered (●?) are different only at room temperature. The higher values of the Ø 100 mm rod result from the lower austenitization temperature. In the test temperature range of 300-600°C the results are nearly identical. The three conditions with higher (1075 °C) and lower (950 °C) austenitization temperatures also lead approximately to the same tensile strength. But the yield strength of the 950 °C condition (▽) is about 5-10 % lower in the whole test temperature range. Also the ductility values (total elongation A, uniform elongation Ag, reduction of fracture Z) are not or only weakly (but not systematically) influenced by the austenitization temperature. In Fig. 16f the ratio of yield and tensile strength is plotted which shows the technically usable fraction within the elastic strain (< 0.2 %). Since this is a result from Figs. 16 a and b, an explicit or strong influence of the austenitization temperature can also be not detected. The increase up to 600 °C and the following drop for temperatures above 650 °C has been observed not only for EUROFER but for all steels of this type.

A comparison of the present tensile test results with those of OPTIFER (W) and F82H-mod (partly shown in [45, 46, 47]) is given in Fig. 19. The hatched band includes the values for OPTIFER Ia, IVc, V with austenitization temperatures of 950 °C and 1075 °C and annealing temperatures of 750 °C (for a detailed description see [41, 57b]). The values for F82H-mod are plotted with the symbol ⊗. Here each point represents the average of different heat treatments (950 °C, 1000 °C, 1040 °C / 750 °C) which have practically no influence on tensile and yield strength [57b]. The EUROFER values appear at the lower end of the hatched ribbon. Tensile and yield strength of the Ø100 mm rod as delivered (austenitization at 980°C) agree with the OPTIFER-V values (950 °C) and the EUROFER 14 mm plate (950 °C, symbol ▽) with OPTIFER-IVc (950 °C).

All ductility values as well as the ratio of yield and tensile strength appear within a narrow scattering band as can be seen from Fig. 19 c-f.

It was shown that the change of the hardening temperature in the range of 950-1075 °C has no or only moderate influence on the tensile properties. This is supposed to be illustrated again by means of Fig. 20 for the F82H-mod steel. For testing temperatures between 700 °C and room temperature one can observe virtually the same values of $R_{p0.2}$ and R_m for austenitization temperatures down to 950 °C. Due to the two-phase formation starting at 875 °C ($A_{c1e} = 915$ °C) the values are much lower.

For the first time values are available also for the low temperature range down to -150 °C for a RAMF steel. Although tensile strength and yield stress increase strongly, uniform and total elongation increase. Only the reduction of fracture decreases from 78.5 % at room temperature to 60.2 % at -150 °C ([58], Table 11).

4.5 Ageing Behaviour

For martensitic steels hardness and toughness – which depend on the intended application – are determined by the hardening and annealing treatment. During a long-term exposure at higher temperatures the microstructure is annealed additionally. This is usually called ageing. Heat treatments applied to reduce or anticipate long-term form, measure and/or structural changes are designated as artificial ageing or stabilization (DIN 17014).

The maximum temperature load specified for the blanket module is 550 °C for 20000 h [59]. As mentioned in Sect. 4.2 it is possible to extrapolate from short tests at high temperatures to longer times at lower temperatures with the help of the annealing master curve and the Hollomon-Jaffe parameter [54]. With $P = T_K (18 + \log t)$ we have equivalence between 550 °C / 20000 h and 580 °C / 3300 h or 600 °C / 1050 h (Fig. 21). Extensive ageing test series have been performed at 550 °C and 600 °C for 5000 h to cover the parameter field around 550 °C / 20000 h.

In the frame of OPTIFER-IVc examinations [56, 57b] numerous temperature/time combinations have been already selected in order to determine how much the ageing temperature may be increased to reduce the necessary exposure times. Results of tensile and Charpy tests have shown that the difference in range between 550 °C / 5000 h and 625 °C / 5000 h is negligible small and the results have been the same even for $P = 18.36$ and $P = 18.94$. Therefore, and since the ageing effect is generally small for RAFM steels, we have chosen only two combinations for the EUROFER aging treatment (580 °C / 3300 h and 600 °C / 1050 h).

4.5.1 Tensile Test Results

We have performed tensile tests from room temperature to 600 °C with specimens from EUROFER Ø 100 mm rods (as delivered) that have been stabilized at 600 °C / 1050 h and 580 °C / 3300 h. In addition a third ageing treatment (600 °C / 1050 h, austenitized at 1075 °C) has been examined (Table 8). The comparison with results from unstabilized specimens shows that only for the condition as delivered (?) a slight decrease of the yield strength (3-5 %) at room temperature occurs (see Fig. 22). All other characteristic values are virtually equal with those of the unstabilized specimens.

These results agree well with examinations performed by CIEMAT. They used ageing treatments at temperatures of 400 °C and 500 °C for 1000 h and 5000 h [60].

There is also a good agreement with the results from aged specimens of F82H-mod and OPTIFER-IVc (Fig. 23). The aged 2 % W steel shows practically the same values as in the condition as delivered (Fig. 23 a). Tensile and yield strength of OPTIFER-IVc (1 % W) is reduced by about 10 % due to the different stabilization heat treatments (Fig. 23 b). But the absolute values are at the same level as those from F82H-mod and EUROFER. Therefore the ratio of yield and tensile strength is in good agreement too [57a, 57b].

4.5.2 Charpy Test Results

Up to now only CIEMAT has examined aged Charpy specimens in the condition as delivered and applied heating at 500°C / 5000 h [60]. As already mentioned in Sect. 4.3 there is significant scattering in the Charpy energy / temperature curve within the test series. Therefore the characteristic ductility values (DBTT, FATT, 68 J) are given as mean values which may deviate by ±10 °C (this has been shown for the example of F82H-mod in [57d]).

For a first estimation of the influence of ageing on the ductility criteria we give a comparison between the CIEMAT EUROFER, FZK F82H-mod and OPTIFER results in the table below.

EUROFER	DBTT [°C]	FATT [°C]	68 J [°C]
Plate as delivered			
CIEMAT	-62	-65	-70
FZK	-70	-78	-82
+500 °C / 5000 h, CIEMAT [60]	-58	-56	-70
<u>F82H-mod</u> [57d]	-42/-20	-35/-10	-52/-20
as delivered			
+550 °C / 5000 h	-34/-10	-31/0	-40/-10
+600 °C / 5000 h	-10/+8	-16/+5	-24/+4
<u>OPTIFER-IVc</u> [57d]			
1075 °C+750 °C	-60	-46	-66
+550 °C / 5000 h	-43	-37	-45
+580 °C / 3300 h and 600 °C /	-50	-35	-52
1050 h, respectively			
+600 °C / 5000 h	-43	-41	-45

The influence of ageing at 500 °C for 5000 h on EUROFER is small. On the other hand, with a Hollomon-Jaffe parameter of $P = 16.77$ we are still away from the target value of $P = 18.36$ (see Fig. 21). Here the values for F82H-mod and OPTIFER – which show a distinct trend – are more expressive. Independent of the scattering the results from F82H-mod show clearly that stabilization treatments in the range of $P = 18-19$ may improve the ductility criteria by about 10-15 °C.

4.6 Creep and Creep Rupture Behaviour

For the design of components which are long-term loaded at higher temperatures the creep and creep rupture behaviour of the according material is of high relevance where the necessary design-relevant characteristic values are extracted from creep and creep rupture tests (e.g. DIN 50118). We have performed creep rupture tests with specimens from EUROFER 97 14 mm plates and Ø 100 mm rods. The different heat treatments and base materials are given in the table below.

1)	\emptyset 100mm	as delivered (980°C+740°C)	Test temp.:	450-650°
2)	14 mm	as delivered (980°C+760°C)		450-650°
3)	\emptyset 100mm	1075°C30'/L+750°C2h/L		450-650°
4)	14 mm	1075°C30'/L+750°C2h/L		450-650°
5)	14 mm	950°C30'/L+750°C2h/L		450-650°
6)	\emptyset 100mm	as delivered +580°C 3300h		450-650°
7)	\emptyset 100mm	as delivered +600°C 1050h		450-650°
8)	\emptyset 100mm	1075°C+750°C+600°C 1050h		550-650°

Up to now creep rupture tests with specimens in conditions 1-5 are running for periods up to 10^4 h. In addition at each test temperature long-term tests have been started which are expected to cover rupture times between 20000-40000 h (see Tables 9-12). The tests with specimens of condition 6-8 (those with additional stabilization heat treatments) are finished with the exception of three tests (Table 13).

A second program covers creep test in the design relevant low stress regime (60-180 MPa) at temperatures of 500 °C and 550 °C with EUROFER specimens in the condition as delivered. Due to the low stresses in these cases no rupture can be expected within several ten or even hundred thousand hours. So only data of yield limits will be available which, however, are very important for the design.

4.6.1 Creep and Creep Rupture Tests at 450-650 °C

Figures 24 a and b show the resulting times for 1 % yield limit and rupture vs. stress for the different applied heat treatments. In the case of EUROFER scattering of the test results is relatively small. This has been examined in additional tests for 500 °C / 250 MPa and 550 °C / 190 MPa. It is significantly smaller as has been observed with F82H-mod specimens [58]. The results for specimens of condition 1 and 2 (●?) fit nicely to mean value curves. Also the results of condition 3 and 4 (?) fit nicely to mean value curves, but only for test temperatures of up to 550 °C. At higher temperatures (600 °C and 650 °C) a clear increase in rupture time is observed due to the coarser grain. The tests with specimens of condition 5 (x) with a reduced austenitization temperature of 950 °C tend to lower times. For comparison the according mean value curves from F82H-mod examinations [58] are drawn too. Due to the relatively large scattering of the F82H-mod results both steels may be considered as equivalent. Tests which are still running (?) will cover time periods longer than $2 \cdot 10^4$ h.

Figures 25 a and b show all available results in the yield limit and creep rupture master curve over the Larson-Miller parameter [55]. Additionally the comparison with F82H-mod and OPTIFER-W is shown.

For this representation the Larson-Miller Parameter $P = T_K (c + \log t)$ has been used with $c = 30$. An optimization of the c-value based on experimental results with EUROFER led to values of 27-33.8 in the case of the 1 % yield limit and 27.6-32.6 for rupture times (for a detailed description see [56]). For OPTIFER-W an average of $c = 28$ and for F82H-mod $c = 33$ has been determined [56, 58]. Therefore the choice of $c = 30$ in Fig. 25 seems to be appropriate.

Test Results

The EUROFER results for the condition as delivered with an austenitization temperature of 980 °C (?) agree almost with the results from F82H-mod. Only in the range of P = 26 -30 the EUROFER results tend to lower stress values.

The results of the different OPTIFER-W alloys [56] vary within the indicated tolerance (min.-max.) bars. They are in general higher compared to the results of EUROFER. The reason is the higher content of Cr (about 9.5 %) and has been already discussed in [56].

Extrapolated values of the 1 % yield limit and creep strength for a maximum load period of 20000 h at 400-600 °C are listed in Table 15. Here the influence of the austenitization temperature is not significant for EUROFER and F82H-mod [58]. But the OPTIFER alloys show a distinct effect, i.e. lower austenitization temperatures to improve the Charpy properties are accompanied by a deterioration of the creep properties.

A comparison between the reference conditions (1075 °C for OPTIFER and as delivered in the case of EUROFER and F82H-mod) shows only small differences in the minimum values. But OPTIFER-W owns a considerable potential for higher rupture times as can be seen in Fig. 25. The reason for this – especially for the 1 % yield limit – is the clearly retarded creep process in the strain range up to 1 %. The effect is shown in Fig. 26. For all three materials creep curves are plotted for the same stress levels at temperatures of 450-550 °C. The differences are also given in the table below. It lists 1 % yield limits which have been experimentally investigated during creep periods of up to 5000 h.

Test Temp.	R _{p1%/5000h} [MPa]		
	EUROFER	F82H-mod	OPTIFER-W
450 °C	280	280/290	370
500 °C	205	210/230	245/305
550 °C	155	150/185	210/225
600 °C	93	108/125	125/130

Finally, the design diagram for EUROFER (resulting from Tables 6 and 15) is shown in Fig. 27.

To describe creep behaviour yield limits in the range from 0.1-5 % (see Tables 9-13) and values of the minimum creep rate dependent on stress have been determined. Plotting the minimum creep rate $\dot{\epsilon}_{p\min}$ vs. the applied stress σ in log-log scale results in straight line for each test temperature – provided that there are no structural changes in the according material. Then the slope of these lines corresponds to the stress exponents $n = \frac{\Delta \log \dot{\epsilon}}{\Delta \log \sigma}$ based on Norton's Creep Law $\dot{\epsilon} = k \cdot \sigma^n$ [61].

Figure 28 shows reliable values from experiments available so far. The calculated values for n and k are given in Table 16. However, at the moment these values are valid only for the experimentally covered stress range. A final statement can only be given when all test are finished (values in parenthesis, Tables 10-13). Here the low stress long-term creep tests at 500 °C and 550 °C play an important role (see Sect. 4.6.2). For specimens of the condition with austenitization at 950 °C the number of tests is too small for quantitative predictions. For comparison the representation in Fig. 28 shows additional lines each for F82H-mod and OPTIFER. At 650 °C there is a stronger stress dependency for $\sigma > 80$ MPa compared to lower stresses. Therefore two values for n are given (see Table 16). The onset of this two-slope behaviour – caused by major structural changes – can just be seen in the case of EUROFER (●). To see whether this creep acceleration occurs also at 500 °C and 550 °C we have to wait for the end of the still running long-term tests.

The present creep data may also be used to determine values for the effective activation energy of the creep process according to $Q_K = R \Delta \log \dot{\varepsilon} / \Delta 1/T$ [62]. This is the slope of the line when plotting $\dot{\varepsilon}_{\text{ppm}}$ vs. $1/T$.

The averaged values from different stresses are given in the table below together with those of F82H-mod and OPTIFER [56].

Effective Activation Energy of the Creep Process Q_K

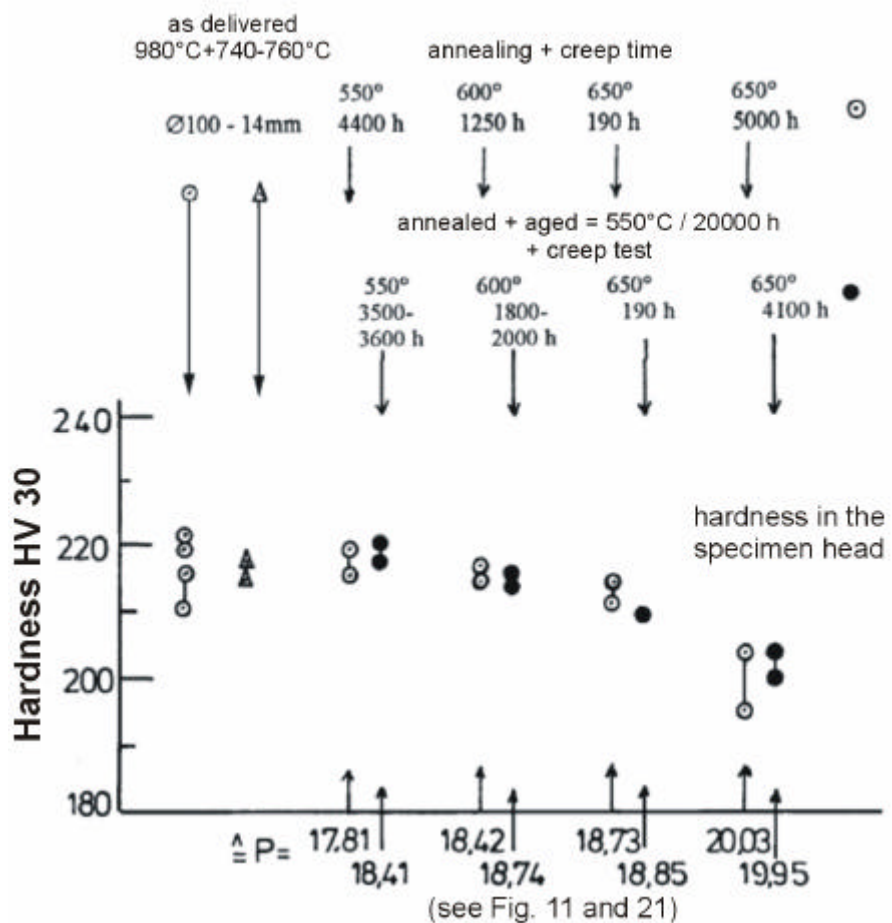
	Q_K [kcal/mol] (J/mol)	T [°C]
EUROFER '97	144 (604)	450 - 650
	133 (557)	450 - 650
OPTIFER-W [56]	160 (671)	450 – 650
F82H-mod [56]	149 (625)	450 - 700

The effect of stabilization heat treatments (which simulate long-term load at higher temperatures) on strength and toughness has already been discussed in Sect. 4.5. We have also tested creep specimens of the martensitic alloys with applied stabilization treatments in the range of the maximum operation temperature.

While creep tests may be considered as simulation of the operational condition prior stabilization treatments (ageing) add an additional load to the material. If, for example, a creep specimen in the annealed state is first aged at 580 °C / 3000 h (which corresponds to 550 °C / 20000 h, see Fig. 21) and is then tested in the creep facility at 550 °C for 10000 h, the microstructure will practically be stressed for 30000 h at 550 °C. This has to be kept in mind for the following discussion of the test results.

Specimens of EUROFER in the condition as delivered and with an austenitization treatment of 1075 °C have been stabilized at 600 °C / 1050 h and 580 °C / 3300 h (Table 13). Figures

29 a-c show the 1 % yield limit, time to rupture and minimum creep rate in comparison to the conditions without applied ageing treatment. All values of the aged specimens (?) and (?) fit nicely to the average curves of the according conditions without ageing (?!). That is, although the specimens have been loaded twice (ageing and creep) an ageing effect can be practically not detected. Therefore the results in Table 13 may be added to the data of Tables 9, 11 and 14. Metallographic examinations including hardness tests of the specimen heads with and without stabilization heat treatments at temperatures of 550-650 °C have shown no microstructural differences. As can be seen in the figure below, up to 650 °C the hardness values correspond nicely to those of the condition as delivered. Up to 600 °C there is no difference in hardness between the condition as delivered and the specimens that have been additionally aged. Only at 650 °C (time to rupture 190 h, P = 18.85) the additional heating starts to show a slight effect. For longer times to rupture ($P > 18.85$) both conditions show a clear decrease of the hardness. These as well as the other hardness values agree exactly with the annealing master curve in Fig. 11. So the results confirm a good ageing resistance of EUROFER 97.



With creep rupture tests characteristic ductility values (total elongation and reduction of fracture) are not only dependent on load time and temperature but also on the applied stress. Figure 30 shows values of the total elongation separately for each test temperature and dependent on time to rupture. For all EUROFER conditions there is no tendency of a decrease in elongation recognizable. But for a more qualified predication we should wait for the end of the still running long-term tests.

The results from specimens with applied stabilization heat treatments are also shown in Fig. 30 (???). These values too agree well with the unstabilized conditions. It is an additional proof for the good ageing resistance of EUROFER 97.

4.6.2 Creep Tests in the Low Stress Range at 500 °C and 550 °C

It has been already mentioned and explained that the maximum operating condition of components (1 % yield limit, time to rupture and creep rate at 550 °C for 20000 h) may be determined by experiments or close extrapolations. But unfortunately in the design range of up to 100 MPa and up to 550 °C there are no data available to describe the creep behaviour of martensitic steels. Also the tests performed at 550 °C for the current task cover just stresses down to 140-160 MPa and extrapolations for yield limits and creep rates to stresses below 100 MPa would be extremely uncertain.

It can be seen in Fig. 28 that at 650 °C the creep rate behaviour of F82H-mod as well as of EUROFER changes significantly in the low stress regime. That is, the measured creep rates in the low stress range are higher than extrapolated from higher stresses. Examinations in the past have shown a two slope behaviour in the case of the steel MANET-II [24] and a three slope behaviour for the martensitic 12 % Cr alloy X 18 CrMoVNb 12 1 [14] at 600 °C. Therefore the question arises whether EUROFER shows such a creep rate acceleration at low stresses even at the planned operating temperature of 550 °C or whether extrapolations (as indicated in Fig. 32 c) are valid. But this can only be cleared experimentally.

According to Fig. 24 the times to rupture for creep tests in this low stress regime up to 550 °C are well above 10⁵ h (> 12 years). Within test periods of ten years most often not even yield limits of 1 % are reached. And further, with creep rates in the range of 10⁻⁸/h to 10⁻¹⁰/h the strain measurement becomes rather difficult. So with creep tests using 25 mm specimens creep rates of 10⁻⁸/h would result in strains of only 0.00219 mm/year. Therefore we used special oversized specimens with lengths of 200 mm. This technique has already successfully been proved during a 10 year test series on the austenitic steel 316L(N) [63, 64]. The test assembly is given in Fig. 31.

The EUROFER long-term test program (phase II) in the low stress regime has been started at test temperature of 500 °C and 550 °C. The test parameters have been chosen to give a certain overlap to the standard creep program (phase I) as can be seen below.

MPa: 300 ← 500° → 220	
	230 -180-160-140-120-100 MPa
MPa: 260 ← 550° → 160	
	170 -120-100-80-70-60 MPa
Phase I	Phase II
(creep tests to rupture)	(tests without rupture)
specimen: Ø 5 x 25 and Ø 8 x 50 mm	Ø 8 x 200 mm (do x lo)

Test Results

Creep tests of phase II have been started in the second half of 2001 and therefore only few data are available (Table 14).

Usually, from creep rupture tests yield limits of 0.1-5 % can be extracted from the creep curves. But scattering is relatively high for the 0.1 and 0.2 % limits. Within phase II of the creep test series the use of oversized specimens enables us to extract yield limits even as low as 0.01 % [63].

Figure 32 shows the yield limits for 500 °C and 550 °C which have been acquired up to now. In the upper stress range yield limits from 0.1-5 % of phase I are plotted. The overlap with phase II can be clearly seen in the case of the 0.1 % yield limit from the tests at 500 °C / 230 MPa and 550 °C / 170 MPa.

Of course, after this short period in phase II there is no final conclusion about the creep behaviour possible. After certain time intervals (250 h, 500 h, 1000 h) the average creep rates are determined from the continuously registered creep curves and plotted vs. creep time (see scheme in Fig. 33). The overlap tests with 230 MPa and 170 MPa at 500 °C and 550 °C have already exceeded the second creep stage (a). Therefore they have been stopped without waiting for rupture. The other tests at lower stresses (c and d) will be continued until minimum creep rate is reached. If the minimum creep rate will not be reached (e) after the maximum planned test period (e.g. 50000 h), then only primary creep is covered by the experiment and no value will be available for the diagram in Fig. 32 c. Such insufficient test periods for minimum creep rate measurements affect the stress dependence which leads to invalid kinks in the stress vs. creep rate curves. This has been shown in [64] and in a compilation of creep results from literature [65] for the case of the 316L(N) steel.

The representation in Fig. 32c mirrors the minimum creep rate behaviour of EUROFER and F82H-mod as far as it has been verified experimentally up to now. The figure shows clearly which stress and creep rate ranges have still to be covered with the present test series. Further the uncertainty of simple extrapolations is indicated for 550 °C (?). Figures 34 a and b show the creep curves with the available data (February 2002). In Fig. 34 b the already mentioned scattering for very low stresses (60 MPa and 70 MPa) can be clearly seen. But after longer periods this disorder will be smoothed.

5 Summary

In the frame of the basic characterization the results from hardness tests have shown that EUROFER 97 can be considered as fully martensitic steel.

With respect to hardness and to a δ -ferrite free microstructure EUROFER 97 is comparable to F82H-mod and to the OPTIFER alloys. The δ -ferrite free microstructure results from the chromium content of 9 % or less. But there is still a certain potential. Based on the modified Schaeffler diagram and based on our experiences with the development of martensitic steels it has been shown that also Cr contents of up to 10.5 % lead to δ -ferrite free microstructure and in addition lead to higher strength. It has been shown further that for Cr contents of less than 9.5 % the structure becomes more instable and that heat treatments in the range of the α - γ -transition lead to the formation of α -ferrite [56]. Of course it is well known that a significant loss of corrosion resistance is accompanied by the decrease of the Cr content which is confirmed, for example, by the work of Knödler/Ennis for steels with 2.2-11 % Cr (including P92 with 9 % Cr) [66].

The assessment of strength and ductility (partly shown in [45, 46, 48, 67]) shows that EUROFER with 1 % W is equal to F82H-mod with 2 % W. But both steels are somewhat worse compared to OPTIFER-1W. Due to the higher W content of F82H-mod the formation of laves phases is favoured which deteriorates the ductility characteristic values significantly. But for a complete assessment we have to wait for the characterization of the irradiation performance.

Ageing resistance (change of structure and/or mechanical properties during long-term load at higher temperatures) is a very important criterion for material selection within certain designs. Extensive heat treatments with various temperature/time combinations covering the planned operating conditions (550 °C / 20000 h) have been performed. In this connection the hardness after annealing of all RAFM steels (OPTIFER, F82H-mod, EUROFER) has not been influenced by ageing. Only a slight change in tensile strength and Charpy toughness has been observed. But compared to conventional 12 % Cr steels [8] the loss of toughness is relatively small as can be seen in Fig. 35 for the case of F82H-mod and OPTIFER [57d]. Also creep rupture tests have shown no influence from ageing. Therefore prior ageing treatments can simply be added to the creep rupture values.

Acknowledgements

This work has been performed in the framework of the FUSION project of the Forschungszentrum Karlsruhe and was supported by the European Union within their Fusion Technology Programme.

6 Literature

- [1] I. Milch, E. Bogusch, W. Bahm, A. Möslang
“Kernfusion - Stand und Perspektiven“
atw 46, Jhg. 2001, Heft 11, Nov., S. 691; Heft 12, Dez., S. 794
atw 47, Jhg. 2002, Heft 2, Febr., S. 96, Heft 3, März, S. 167
- [2] Kernfusion im Forschungsverbund
Herrmann von Helmholtz-Gemeinschaft Deutscher Forschungseinrichtungen (HGF),
1996
- [3] U. Colombo, A. Jaumotte, E. Kennedy, C. Lopez-Martinez, M. Popp, C. Reece, H.
Schopper, E. Spitz, F. Troyon
"Report of the Fusion Programme Evaluation Board prepared for the Commission of
the European Communities", July 1990
- [4] Proceeding of the IEA workshops on Low-Activation-Materials
 - a) Ispra/Italien, 1.-3.10.1990
 - b) Culham/GB, 8.-12.4.1991
 - c) JAERI/Japan, 26.-28.10.1992
- [5] J.Z. Briggs, T.D. Parker
The Super 12% Cr Steels, Climax Molybdenum Company, New York, 1965
"Eigenschaften und Anwendung der modifizierten 12% Cr-Stähle“, Schweizer Archiv,
Juni 1967, S. 167-181
- [6] H. Wisniowski
"Hochwarmfeste 12%-Chromstähle"
DEW-Technische Berichte, Heft 2, 1969, S. 117-133
- [7] K. David
"Herstellung, Eigenschaften und Anwendung der hochwarmfesten 12% Cr-Stähle",
Vortrag KfK/IMF, Juli 1980
- [8] G. Kalwa
"Stand der Entwicklung und Anwendungstechnik des Werkstoffes X20CrMoV121",
9. MPA Seminar, Stuttgart, 13./14. Oktober 1983
- [9] W. Schoch
“100 Jahre Kraftwerkstechnik“.
VGB-Kraftwerkstechnik 63, Heft 7, Juli 1983, S. 614-637
- [10] D. Christianus, H. Fabritius, K. Forsch, B. Huchtemann, K.H. Keienburg, K.H. Meyer,
H. Weber
“Entwicklung warmfester Stähle im Dienste des Fortschrittes der Energietechnik“.
Stahl und Eisen 107 (1987) Nr. 14, 15, S. 697-705

- [11] Röchling HO-Katalog Hochwarmfeste Stähle und Legierungen 702.519/9.1969
VDEh-Werkstoffblatt 1.4914, Nov. 1973
- [12] K. Anderko
"Zur Eignung warmfester Vergütungsstähle mit 9-12% Cr für Komponenten im Kern
Schneller Reaktoren - ein Überblick", Journal of Nuclear Materials, 95 (1980), S. 31-43
- [13] K. Anderko, K. David, W. Ohly, M. Schirra, C. Wassilew
"Optimization work on Niobium stabilized 12% Cr martensitic steels for breeder and fu-
sion applications".
Topical Conf. on Ferritic Alloys for use in Nuclear Energy Technologies, Snowbird,
Utah, Program and Summaries, Juni 1983
- [14] M. Schirra
"Charakterisierende thermische und mechanische Untersuchungen an einem Nb-
legierten martensitischen 12% Cr-Stahl (W.-Nr. 1.4914) mit abgesenktem Stickstoffge-
halt".
KfK-Bericht 3640, August 1984
- [15] M. Schirra, S. Heger, H. Meinzer, B. Ritter, W. Schweiger
"Untersuchungen zum Vergütungsverhalten, Umwandlungsverhalten und der mechani-
schen Eigenschaften am martensitischen Stahl 1.4914 (NET-Charge MANET-I)".
KfK 4561, Juni 1989
- [16] R.L. Klueh, K. Ehrlich, F. Abe
"Ferritic/martensitic steels: promises and problems".
Journal of Nuclear Materials 191-194 (1992), S. 116-124
- [17] M. Schirra, P. Graf, S. Heger, H. Meinzer, W. Schweiger, H. Zimmermann
"MANET-II, Untersuchungsergebnisse zum Umwandlungs- und Vergütungsverhalten
und Prüfung mechanischer Eigenschaften".
KfK 5177, Mai 1993
- [18] K. Ehrlich, D.R. Harries, A. Möslang (Editors)
"Characterisation and Assessment of Ferritic/Martensitic Steels",
FZKA 5626, Februar 1997
- [19] M. Schirra, K. Ehrlich
"Development of a High-Strength Martensitic CrNiMoVNb steel with 10,5% Cr und
0,11% C (OPTIMAR-Type)".
Advanced Heat Resistant Steels for Power Generation, San Sebastian, España, April
27-29, 1998, Conf. Proceedings
- [20] K. Ehrlich, K. Anderko
"Metallische Werkstoffe als Erste-Wand-Werkstoffe für zukünftige Fusionsreaktoren",
Journal of Nuclear Materials 171 (1990), S. 139-149

Literature

- [21] R.L. Klueh, D.R. Harries
"High-Chromium Ferritic and Martensitic Steels for Nuclear Applications".
ASTM stock-number: MONO3, ISBN 0-8031-2090-7, 2001
- [22] M. Schirra, K. Anderko
"Anomalies in creep-curves of martensitic 9-14% chromium steels under long term loading".
steel research 6/90, p. 242/250
- [23] E. Materna-Morris, M. Schirra
"Mikrostrukturelle Untersuchungen zur Klärung von beobachteten Kriechanomalien in martensitischen 9-14% Chromstählen".
14. Vortragsveranstaltung der Arbeitsgemeinschaft Warmfeste Stähle und der Arbeitsgemeinschaft Hochtemperaturwerkstoffe, Düsseldorf, 19.11.91
- [24] M. Schirra, S. Heger, A. Falkenstein
"Das Zeitstandfestigkeits- und Kriechverhalten des martensitischen Stahles MANET II".
FZKA 5722, Okt. 1996
- [25] M. Schirra, S. Heger
"Der Einfluss des Delta-Ferrit-Gehaltes auf die Vergütungseigenschaften und das Zugfestigkeits- und Zeitstandverhalten eines Cr-Ni-MoV-Nb-Stahles mit 9-14% Chrom".
KfK 5080, Febr. 1994
- [26] K. Anderko, K. Ehrlich, L. Schäfer, M. Schirra
"Ceta, ein Entwicklungsschritt zu einem schwach aktivierbaren martensitischen Stahl".
KfK 5060, Juni 1993
- [27] G.J. Butterworth, K.W. Tupholme, J. Orr, D. Dulieu
"A study of the prospects for development of low activation martensitic stainless steels for first wall and blanket structures in fusion reactors".
Culham Laboratory Report CLM-R264, 1986
- [28] K.W. Tupholme, D. Dulieu and G.J. Butterworth
"Investigations on low activation 9 and 12% Cr, V, W steels for nuclear fusion reactor components".
Culham Laboratory Report CLM-R271 (1986) and Proceedings of ICFRM-3, Karlsruhe, October
- [29] S. Cierjacks
Interner Bericht 1988
- [30] S. Cierjacks, Y. Hino
"The Importance of Sequential (x,n) Reactions on Element Activation of Fusion Reactor Materials".
Journal of Nuclear Materials 170 (1990), S. 134-139

- [31] S. Cierjacks
"Nuclear data needs for "Low-activation" fusion materials development".
Fusion Engineering and Design 13 (1990) S. 229-239
- [32] S. Cierjacks, P. Oblozinsky, B. Rzechorz
"Nuclear Data Libraries for the Treatment of Sequential (x,n) Reactions in Fusion Materials Activation Calculations".
KfK 4867, Juli 1991
- [33] S. Kelzenberg
"Berechnung und experimentelle Verifizierung von Materialaktivierungen in D-T-Fusionsreaktoren".
FZKA 5836, Nov. 1996
- [34] E. Daum
"Katalogisierung des Aktivierungsverhaltens aller stabilen Elemente mittels Fispact 97-Rechnungen für DEMO 1. Wand".
Aktivierungsverhalten aller stabilen Elemente in verschiedenen Bereichen des HCPB-Blankets".
Vergleich von Aktivierungsberechnungen von FISPACT '97".
Interne Berichte 1998 (PKF 107, 110, 108)
- [35] K. Ehrlich, S. Kelzenberg, H.D. Röhrlig, L. Schäfer, M. Schirra
"The Development of Ferritic-Martensitic Steels with Reduced Longterm Activation".
Proceedings of ICFRM-6, Stresa, I, 27.9.-1.10.93. Journal of Nuclear Materials 212-215 (1994), S. 678-683
- [36] K. Ehrlich, S. Cierjacks, S. Kelzenberg, A. Möslang
"The development of structural materials for reduced long-term activation".
17th Intern. Symposium, Sun Valley, Idaho, USA, June 20-23, 1994, to be published in ASTM-STP 1270
- [37] M. Schirra, K. Ehrlich, S. Heger, M.T. Hernández, J. Lapeña
"OPTIFER, ein weiterer Schritt zur Entwicklung niedrigaktivierender martensitischer Stähle".
FZKA 5624, Nov. 1995
- [38] M. Schirra, K. Ehrlich, L. Schäfer
"Germanium enthaltender Stahl und seine Verwendung".
Patent 4432516 v. 18.7.95
- [39] E. Daum, K. Ehrlich, M. Schirra (Editors)
"Proceedings of the Second Milestone Meeting of European Laboratories on the Development of Ferritic/Martensitic Steels for Fusion Technology",
Karlsruhe 1996, FZKA 5848, Mai 1997

Literature

- [40] M. Schirra, Ch. Adelhelm, P. Graf, S. Heger, H. Kempe, H. Zimmermann, M.P. Fernández, J. Lapeña
"Arbeiten zur Grundcharakterisierung am niedrigaktivierenden Stahl F82H-mod im Vergleich zu OPTIFER".
FZKA 6008, Dez. 1997
- [41] M. Schirra, S. Heger, H. Kempe, M. Klotz, H. Zimmermann, J. Lapeña
"Untersuchungen zu physikalischen und mechanischen Eigenschaften der OPTIFER-Legierungen".
FZKA 6167, April 1999
- [42] K. Ehrlich
"The development of structural materials for fusion reactors".
Phil. Trans. Royal Society, London A (1999) 357, 595-623
- [43] K. Ehrlich, E.E. Bloom, T. Kondo
"International strategy for fusion materials development".
Journal of Nuclear Materials 283-287 (2000) 79-88
- [44] K. Ehrlich
"Status and Prospects of European RAFM-Steel Development".
Materials Assessment Meeting Karlsruhe, June 5-8, 2001-12-12
- [45] 10th International Conference on Fusion Reactor Materials
ICFRM-10, 10-19 Oct. 2001, Baden-Baden, Germany
- [46] R. Lindau, M. Schirra
"Erste Ergebnisse zur Charakterisierung einer Großcharge des niedrigaktivierenden ferritisch-martensitischen Stahls EUROFER-92".
Jahrestagung Kerntechnik, Mai 2000, Bonn, Tagungsband ISSN 0720-9207, S. 613-616
- [47] K. Ehrlich, R. Lindau, A. Möslang, M. Schirra
IEA-Workshop on RAFM-Steel, Tokyo, 2. + 3. Nov. 2000.
EUROFER 97 and Development Strategy for RAFM Steels in Europe.
- [48] R. Lindau, M. Schirra
"Status of investigations on the thermal and mechanical behaviour of EUROFER 97".
Workshop on Data Base Evaluation of RAFM Steels, Brasimone, I, Nov. 27-28, 2000
- [49] M. Schirra, R. Lindau
"Untersuchungen zu physikalischen und mechanischen Eigenschaften des niedrigaktivierenden martensitischen 9% Cr-Stahles EUROFER-97".
23. VDEh-Vortragsveranstaltung, 1.12.2000, Düsseldorf, Tagungsband S. 36-49
- [50] R. Schneider, P. Würzinger, G. Lichtenegger, H. Schweiger
"Metallurgie an den Grenzen höchster Reinheitsgrade und niedrigster Spurenelement-

gehalten".

BHM 145 (Jg. 2000) Heft 5, S. 199-203

[51] CEA/EURATOM, Annual Report 2000

[52] E.W. Schuring, H.E. Hofmans

"Metallographic characterisation of EUROFER 97 plate and bar materials".

ECN-C-00-108, October 2000

[53] H. Finkler, M. Schirra

"Transformation behaviour of the high temperature martensitic steels with 8-14% chromium".

Steel research 67 (1996) Nr. 8, S. 328-342 (englisch). FZKA 5607, Sept. 1995;

FZKA 6730, Juni 2002 (german)

[54] J.H. Hollomon, L.D. Jaffe

"Time-temperature Relations in Tempering Steel".

Transaction of the Am. Inst. of Mining and Met. Eng. 162/1945, pp. 233-249

[55] F.R. Larson, J. Miller

"A time-temperature relationship for rupture and creep stresses".

Trans. ASME 72 (1952, 765/75)

[56] M. Schirra, A. Falkenstein, S. Heger, J. Lapeña

"Das Zeitstandfestigkeits- und Kriechverhalten der niedrigaktivierenden OPTIFER-Legierungen".

FZKA 6464, Juli 2001

[57] Interne Berichte

a) PKF 118, Juli 1998 (F82H-mod)

b) PKF 152, Juni 2000 (IVc)

c) PKF 154, März 2000 (HT - mech. Eigenschaften)

d) PKF 159, Sept. 2000 (WB-Kerbschl.)

[58] M. Schirra, S. Heger, A. Falkenstein

"Das Zeitstandfestigkeits- und Kriechverhalten des niedrigaktivierenden martensitischen Stahles F82H-mod" (Abschlussbericht).

FZKA 6265, Mai 1999

[59] Schleisiek

Nuclear Fusion Project, Annual Report, Seite 68-69, FZKA 6050, Dez. 1997

[60] P. Fernández, A.M. Lancha, J. Lapeña, M. Serrano, M. Hernández-Mayoral

"Metallurgical properties of the reduced activation martensitic steel EUROFER '97 on as-received condition and after thermal aging".

Contribution 04PO12 in [45]

Literature

- [61] F.H. Norton
"The creep of steel at high temperatures".
Mc Graw Hill Publishing Co. Ltd. 1929
- [62] F. Garofalo
"Fundamentals of creep and creep-rupture in metals".
Macmillan Series in Materials Science, New York, 1965
- [63] M. Schirra, A. Falkenstein, S. Heger
"Experimentelle Ergebnisse zum Kriechverhalten des Strukturwerkstoffes 316-L (N)-DIN 1.4909 im niedrigen Spannungsbereich bei 550° und 600°C (Abschlussbericht)".
FZKA 6699, Februar 2002
- [64] M. Schirra
"Long-term studies on the creep behaviour of the structural material 316-L (N) in the low-stress range at 550° and 600°C.
9th Intern. Conf. on Creep and Fracture Engineering Materials and Structures, Swansea
1-6 April, 2001, Proceedings, p. 669-678
- [65] D. Lehmann
"Evaluation of stress to rupture and creep properties of type 316L (N) steel for design use".
Final report EUR 16168, 1995
- [66] R. Knödler, P.J. Ennis
"Oxidation of high-strength ferritic steels in steam at 650°C, preliminary results of COST 522 projects".
BALTICA-V-Condition and life management for power plants, Espoo, Finland, 2001,
VTT-Symposium, p. 355-364
- [67] M. Schirra
"Das Kriech- und Zeitstandfestigkeitsverhalten von EUROFER-97 im Vergleich zu F82H-mod und OPTIFER".
Beitrag Jahrestagung Kerntechnik, Mai 2001, Dresden

7 Tables

Table 1: Chemical Composition of the OPTIFER Alloys (without undesirable tramp elements)

Type	Heat	Cr wt. %	C →	Mn	V	Ta	W	Ge	P ppm	S →	B	N ₂	O ₂	Ce	Melting/Remarks
Ia	664	9.3	0.10	0.50	0.26	0.066	0.96	-	46	50	61	155	47	<10	SV4 = vacuum induction furnace + vacuum arc melting 25 kg heats 1. series with Bor desoxidation with Ce *) desoxidation with Y
Ib ^{*)}	667	9.5	0.12	0.49	0.234	0.163	0.98	-	40	10	63	62	87	410	
II	668	9.5	0.125	0.49	0.28	0.018	0.006	1.2	43	20	59	159	90	<10	
III	666	9.32	0.12	0.49	0.248	1.6	0.024	-	40	20	64	173			
IVa	986489	8.5	0.11	0.57	0.23	0.15	1.16	-	40	40	40	600	35		SV1 = open melting + vacuum arc melting 150 kg heats B free
IVb	986635	8.1	0.12	0.29	0.21	0.08	1.57	-		60	30	200		<20	
IVc	986778	9.05	0.13	0.52	0.25	0.09	1.00	-	40	30	-	540	190	<20	
(=Ia)	986779	9.35	0.12	0.54	0.26	0.07	1.03	-	40	30	-				
	986780	9.15	0.12	0.55	0.24	0.12	1.05	-	40	40	-				
	986781	9.35	0.12	0.57	0.26	0.08	1.00	-	30	50	-				
V (=Ia)	735	9.48	0.115	0.39	0.245	0.061	0.985	-	35	25	2	225	60		SV4 2. series Bor free 25 kg heats
VI (=II)	734	9.35	0.125	0.61	0.275	0.083	0.005	0.38	43	30	2	250	160	<100	
VII (=IVa+b)	736	8.38	0.09	0.37	0.205	0.069	1.03	-	36	25	2	263	170		
VIII	806	9.31	0.109	0.602	0.190	0.047	1.27	-	35 ^{*)}	17	82 ^{*)}	210	130	-	SV4 3. series 25 kg heats *) SAARSTAHL analysis
IX	803	9.27	0.12	0.374	0.209	0.040	1.40	-	30 ^{*)}	18	2 ^{*)}	280	60	-	
Xa	804	9.41	0.086	0.684	0.198	0.032	1.25	-	35 ^{*)}	21	2 ^{*)}	480	320	-	
Xb	824	9.15	0.09	0.42	0.195	0.088	1.06	-	15	30	5	235	99	-	
EUROFER	E83699	8.87	0.12	0.42	0.19	0.14	1.10	-	40	30	<5	180	13	-	Böhler-Kapfenberg
EUROFER	E83698	8.82	0.11	0.47	0.20	0.13	1.09	-	50	40	<10	200	10	-	acceptance certificate

Table 2a: Specification of the chemical composition of EUROFER 97

	Element	Minimum Value (wt. %)	Maximum Value (wt. %)	Remarks/Target
A)	Cr	8.50	9.50	9.0
	C	0.090	0.120	0.11
	Mn	0.20	0.60	0.4
	P		0.005	
	S		0.005	
	V	0.15	0.25	
	B		0.001	ALAP
	N ₂	0.015	0.045	0.03
	O ₂		0.01	
B)	W	1.0	1.2	
	Ta	0.05	0.09	
	Ti		0.01	
C)	Nb		0.001	ALAP
	Mo		0.005	ALAP
	Ni		0.005	ALAP
	Cu		0.005	ALAP
	Al		0.01	ALAP
	Si		0.050	
	Co		0.005	ALAP
	As+Sn+Sb+Zr		0.05	

A) basic composition

B) varied substitution elements

C) radiological undesirable tramp elements

ALAP = as low as possible

Table 2b: Chemical composition (mean real or specified)

	OPTIFER-(W)	F82H-mod (EU)
Fe	Basis	Basis
Cr	9.3 %	8.0 %
C	0.10 %	0.096 %
Mn	0.50 %	0.185 %
V	0.26 %	0.155 %
W	0.97 %	2.00 %
Ta	0.066 %	< 0.02 %
B	2-82 ppm	2 ppm
N ₂	62-600 ppm	70 ppm
O ₂	35-320 ppm	118 ppm
P	15-46 ppm	20 ppm
S	10-50 ppm	20 ppm

Table 3: Chemical composition

		A	B	C
	Specification	Producer analysis heat 83699/83698 (Ø100 mm/ 14 mm)	IMF analysis heat 83698 1.5 mm plate	CEA analysis 3 heats 5 sizes (see [51])
Cr	8.50-9.50 %	8.87/8.82 %	9.21 %	8.68-9.04 %
C	0.09-0.12	0.12/0.11	0.104	0.092-0.117
Mn	0.20-0.60	0.42/0.47	0.502	0.41-0.50
V	0.15-0.25	0.19/0.20	0.204	0.17-0.19
W	1.0-1.2	1.10/1.09	1.148	1.03-1.26
Ta	0.05-0.09	0.14/0.13	0.14	0.10-0.15
N ₂	0.015-0.045	0.018/0.020	0.0234	0.018-0.0226
O ₂	max. 0.01	0.0013/0.0010	<0.001	0.0005-0.0011
P	max. 0.005	0.004/0.005	<0.04	0.011-0.013
S	max. 0.005	0.003/0.004	0.004	<0.003
B	max. 0.001 ^{*)}	<0.0005/0.001	<0.01	<0.001
Ti	max. 0.01	0.008/0.005	0.004	0.001-0.005
Nb	max. 0.001 ^{*)}	<0.0010/0.0016	12 ppm	<20 ppm
Mo	max. 0.005 ^{*)}	<0.0010/0.0010	<8	<20-100
Ni	max. 0.005 ^{*)}	<0.007/0.0200	214	400-600
Cu	max. 0.005 ^{*)}	0.022/0.0016	35	30-400
Al	max. 0.01 ^{*)}	0.008/0.009	51	30-40
Si	max. 0.05 ^{*)}	0.07/0.04	430	300-600
Co	max. 0.005 ^{*)}	0.004/0.006	67	80-200
As+Sn+Sb+Zr	max. 0.05	<0.015/0.015		<65-145

^{*)} ALAP (as low as possible)

Table 4a: Charpy Tests							
Alloy: EUROFER (14mm)				Condition: a) as delivered=			
Heat-No.: E83698				980°C27'/air+760°C90'/air (transv.)			
Spec.: ISO-V				b) 1050°C30'/air + 750°C3h/air (transv.)			
IMF-Tests				c) 1075°C30'/air + 750°C2h/air (transv.)			
Test-Temp. °C	A _v J	cryst. area %	FATT/ DBTT °C	Test-Temp. °C	A _v J	cryst. area %	FATT/ DBTT °C
a) -100	12		-78 / -70	b) -40	213	24	-72 / -73
-80	75	51		-20	261		
-60	156	42		-20	243		
-40	189	31		+0	249		
-30	207	23		+0	240		
-20	246			RT	270		
-20	192			60	252		
-10	243			c) -60	15	100	-56 / -56
+0	240			-55	171	38	
RT	240			-50	165	35	
40	255			-45	156	35	
60	246			-40	195	24	
Prod. RT	215-220-221			-30	198	22	
+0	198-209-214			-30	180	25	
-20	190-204-216			-20	267	0	
				+0	267	0	
b) -90	33		-72 / -73	RT	270		
-80	105	68		40	276		
-60	180	33		60	300	T4a EU-14-1.doc	7/2000

Table 4b: Charpy Tests

Alloy: EUROFER (14mm)

Condition:

Heat-No.: E83698 plate:4/3

a) as del.+1075°C30'+750°C2h (longit.)

Spec.: ISO-V

b) as del.+1075°C30'+750°C2h (transv.)

IMF-Tests.

Test-Temp. °C	A _v J	cryst. area %	FATT/ DBTT °C	Test-Temp. °C	A _v J	cryst. area %	FATT/ DBTT °C
a) -80	15	100	-54 / -57	b) -60	15	100	-56 / -56
-70	15			-55	171	38	
-60	21	95		-50	165	35	
-55	168	38		-45	156	35	
-50	171	48		-40	195	24	
-40	183	0		-30	198	22	
-20	204			-30	180	25	
+0	234			-20	267	0	
RT	255			+0	267	0	
40	264			RT	270		
60	273			40	276		
				60	300		

Table 5a: Charpy Tests

Alloy: EUROFER-Æ100

Condition: as del.=980°C/air+740°C/air

Heat-No.:E83699

Spec.: ISO-V longitudinal

IMF-Vers.

T5a EU100-L.doc

2-2001

Test-Temp. °C	A _v J	cryst. area %	FATT/ DBTT °C	Test-Temp. °C	A _v J	cryst. area %	FATT/ DBTT °C
RT Ø251	246	0	-67/-70°	-35°	231	23	
	265	0	(Mittelwert)		Ø212	Ø24%	
	246	0	(min. -/-73°)		186	32	
	249	0	(max-54/-58°)		219	25	
	246	0			213	22	
					192	25	
	246	0		-40°	210	21	
	249	0			Ø204	Ø25%	
	258	0			183	42	
	252	0			168	44	
+-0° Ø253	258	0			171	37	
				-50°	186	31	
	231	7			Ø177	Ø39%	
	252	0			168	45	
	210	24			168	47	
	207	20		-60°	111	63	
	189	33			183	35	
	Ø218	Ø17%			162	43	
	210	24			Ø159	Ø46%	
	195	26					

Table 5b: Charpy Tests

Alloy: EUROFER-Æ100

Condition: as del.=980°C/air+740°C/air

Heat-No.:E83699

Spec.: ISO-V transverse

IMF-Vers.

T5b EU100-Q1.doc

2-2001

Test-Temp. °C	A _v J	cryst. area %	FATT/ DBTT °C	Test-Temp. °C	A _v J	cryst. area %	FATT/ DBTT °C
+60° RT	219	0	-49/-53	-20°	168	20	
	207	0	(Mittelwert)		186	25	
	225	0	(min-51/-55°)		189	25	
	228	0	(max-44/-45°)		165	28	
	237	0			174	16	
	210	0			Ø177	Ø23%	
	Ø222			-30°	168	32	
	213	0			141	38	
	235	0			147	35	
	219	0			171	33	
+-0°C -10°	204	0		-40°	159	37	
	228	0			Ø157	Ø35%	
	Ø220				150	41	
	192	0			135	44	
	174	18			153	42	
	237	0			153	36	
	222	0			153	37	
	207	18			Ø148	Ø40%	
	Ø207	Ø7%					Q2.doc→

Table 6

Alloy: EUROFER (\varnothing 100 and 14mm) **Cond. as del.:** a) $980^{\circ}\text{C} + 740^{\circ}\text{C}$ (\varnothing 100 mm)

Heat: E83699 and E83698

b) 980°C+760°C (14 mm plate)

Spec: Ø5x25mm (d_o x L_o)

Condition	Temp. °C	R _m N/mm ²	R _{p0,2} N/mm ²	A %	Ag %	Z %	R _{p0,2} /R _m	Rem.
a)	RT	671	568	21,4	4,59	76,3	0,85	
	300	544	479	17,5	2,70	78,8	0,88	
	400	503	453	18,0	2,36	78,0	0,90	
	500	424	404	22,4	1,20	87,3	0,95	
	600	291	284	32,4	0,84	94,3	0,98	
	700	163	133	36,0	2,50	96,6	0,82	
b)	RT	652	537	20,8	4,97	79,9	0,82	
	300	536	469	16,8	2,70	80,1	0,88	
	400	497	442	16,8	2,32	78,8	0,89	
	500	419	392	23,5	1,19	88,8	0,94	
	600	292	277	29,3	0,91	94,1	0,95	

Table 7

Alloy: EUROFER (E100 and 14mm) Condition: a) 1075°C30'V/V+750°C2hV/V

Heat: E83699 and E83698

b) 1075°C30'V/V+750°C2hV/V

Spec.: Ø5x25mm (d_o x L_o)

c) 950°C30'V/V+750°C2hV/V

Condition	Temp. °C	R _m N/mm ²	R _{p0,2} N/mm ²	A %	Ag %	Z %	R _{p0,2} /R _m	Rem.
a)	RT	627	513	23,2	5,16	79,7	0,82	Ø100
	300	519	456	16,4	2,78	77,9	0,88	
	400	487	447	16,7	2,03	76,5	0,92	
	500	404	384	25,0	1,26	86,6	0,95	
	600	284	278	28,4	0,79	94,7	0,98	
b)	RT	630	519	23,0	5,00	79,8	0,82	14mm
	300	521	460	20,5	2,51	79,8	0,88	
	400	481	434	20,5	2,23	77,6	0,90	
	500	409	391	23,2	0,91	87,1	0,96	
	600	290	284	29,4	0,61	93,9	0,98	
c)	RT	624	495	24,0	6,08	81,7	0,79	14mm
	300	511	432	21,1	3,60	78,8	0,85	
	400	474	417	20,9	2,88	77,3	0,88	
	500	399	374	25,0	1,39	88,5	0,94	
	600	280	265	30,2	0,90	95,4	0,95	

Table 8

Alloy: EUROFER ($\varnothing 100$)

Condition: a) as del. (980°C+740°C) +600°C1050h

Heat: E83699

b) -----“----- +580°C3300h

Spec.: 5x25mm ($d_o \times L_o$)

c) **1075°C+750°C +600°1050h**

(P=18,36)

Condition	Temp. °C	R _m N/mm ²	R _{p0,2} N/mm ²	A %	Ag %	Z %	R _{p0,2} /R _m	Rem.
a)	RT	666	547	21,4	5,14	77,5	0,82	
	300	537	472	17,3	3,03	78,2	0,88	
	400	503	454	17,5	2,67	76,9	0,90	
	500	422	401	23,8	1,44	87,7	0,95	
	600	296	283	32,7	0,92	94,6	0,96	
b)	RT	660	541	22,2	5,35	77,3	0,82	
	400	503	450	18,0	2,44	78,8	0,89	
	500	425	399	23,4	1,1	87,0	0,94	
c)	RT	624	506	22,0	5,68	76,9	0,81	
	300	503	436	16,8	2,77	77,5	0,87	
	400	468	420	18,4	2,77	76,9	0,90	
	500	400	378	23,2	1,46	88,4	0,95	
	600	284	274	26,4	0,65	93,9	0,96	

Table 9**Creep Rupture Tests**

ZSV-No=Test in Vacuum

T9 EU-100-1.doc

1-2002

Alloy, Heat, Condition	Test No.	J °C	S _o MPa	t _m h	e _o %	t _{ef0,1%} h	t _{ef0,2%} h	t _{ef0,5%} h	t _{ef1%} h	t _{ef2%} h	t _{ef5%} h	Spec. doxLo	A _u %	Z _u %	e _{pmin(abs)} x10 ⁻⁶ /h
EUROFER-Ø100	3968	450	360	265	0,26	0,5	3	19	60	144	245	5x25	24,0	84,1	113
E83699	3970		340	811	0,22	2	7	48	168	419	736	5x25	26,8	78,8	38
as delivered	3986		300		0,20	6	42	565	2570			8x50			(1,2)
(-980°C+740°C)	3967	500	300	76	0,22	0,4	1,2	5,8	16	48	67	5x25	26,8	89,6	442
	3969		260	1587	0,20	1	4	37	150	485	1292	5x25	30,8	87,1	28
	4021		250	3419	0,16	1	6	55	233	861	2765	8x50	21,4	88,7	13
	4025		250	3730	0,18	1	6	53	235	868	3034	8x50	24,4	90,3	12
	4039		250	3153	0,17	2	7,5	52	216	803	2537	8x50	22,2	88,7	14
	4040		250	2539	0,16	2	5	46	173	610	1973	8x50	22,6	90,5	19
	3974		240	10222	0,16	2	12	111	480	2190	8955	8x50	20,0	95,0	3,4
	3989		220		0,28	3	25	285	1830			8x50			(0,3)
	3965	550	260	15	0,16	/	0,2	1	2,6	7	13	5x25	34,4	91,0	2400
	3966		240	50	0,16	0,2	0,4	1,8	6	18	42	5x25	28,8	91,0	850
	ZSV2745		200	895	0,16	0,25	1	7	36	184	856	5x25	31,6	91,1	46
	4013		190	2760	0,14	0,75	3,5	26	130	656	2294	8x50	22,0	91,0	15
	4022		190	2641	0,14	0,75	3	27	129	660	2255	8x50	21,8	90,3	15
	4036		190	2650	0,14	1	4	31	143	713	2362	8x50	19,8	92,5	14
	4037		190	2691	0,14	0,5	3	27	129	669	2282	8x50	21,6	90,3	15
	4041		190	2523	0,14	0,5	3	27	131	663	2218	8x50	20,4	88,7	13
	ZSV2735		180	4372	0,12	1,5	7	70	306	1393	3685	8x50	23,8	90,3	9
	3988		160		0,12	3	25	360	3720			8x50			(0,5)
	3997	600	160	172	0,14	0,3	1	6,5	22	64	139	5x25	32,8	92,2	230
	ZSV2742		140	512	0,12	0,5	1	5	34	170	400	5x25	33,6	92,2	69
	ZSV2746		120	1251	0,12	0,25	1	17	166	548	1050	5x25	30,4	93,3	24
	ZSV2737		100	8920	0,06	2,5	17	560	2530	5615		8x50	24,4	91,8	2,2
	3972	650	100	197	0,12	0,25	1	9	36	88	157	5x25	50,4	96,0	175
	ZSV2736		80	926	0,12	0,5	2,5	55	208	469	785	5x25	37,6	95,2	25
	ZSV2780		70	1963	0,16	1	17	185	552	1104	1699	8x50	42,8	96,0	14
	ZSV2775		60	4971	0,04	10	72	500	1440	2918	4447	8x50	32,6	95,6	5,1
	ZSV2763		50		0,06	33	350	2845	6505	12312		8x50			1,2

Table 10

Creep Rupture Tests

ZSV-No=Test in Vacuum

T10 U-14-1.doc

1-2002

Table 11

Creep Rupture Tests

ZSV-No= Test in Vacuum

T11 EU-100-2.doc

1-2002

Table 12

Creep Rupture Tests

ZSV-No= Test in Vacuum

T12 EU-14-2.doc

3-2002

Table 13**Creep Rupture Tests**

ZSV-No= Test in Vacuum

T13 EU-Alt-1.doc

1-2002

Alloy, Heat, Condition	Test No.	J °C	S _o MPa	t _m h	e _o %	t _{ef0,1%} h	t _{ef0,2%} h	t _{ef0,5%} h	t _{ef1%} h	t _{ef2%} h	t _{ef5%} h	Spec. doxLo	A _u %	Z _u %	e _{pmin(abs)} x10 ⁻⁶ /h
EUROFER-Ø100	ZSV2764	450	310	7106	0,20	1,5	10	138	845	2940	6327	5x25	25,2	88,5	5
E83699	4027	500	260	1988	0,16	1	4	40	199	690	1723		28,0	87,1	20
as delivered	4006	550	220	299	0,12	0,25	1,5	8	31	106	250		34,8	89,8	128
+580°C3300h	ZSV2782		200	1054	0,16	0,25	0,5	10	69	312	858		30,0	92,2	36
	ZSV2779		180	3488	0,04	1,5	13	235	1030	2505	3439		29,6	87,2	5,5
	ZSV2777	600	120	1827	0,12	0,5	3	53	292	838	1542		32,8	93,3	18
	ZSV2765	650	80	879	0,12	0,5	2	19	120	380	728		40,0	94,3	36
as delivered	ZSV2757	450	350	402	0,32	0,5	2,5	19	70	187	355	5x25	31,2	87,2	83
+600°C1050h	4001		310		0,34	2	12	195	1340	5680					2,1
	3985	500	280	370	0,20	0,5	2	13	49	148	319		30,8	85,7	100
	ZSV2758		260	1712	0,24	0,5	2	26	139	553	1449		30,4	89,7	22
	3998		220		0,14	12	76	860	6310						(0,3)
	4004	550	220	273	0,16	0,5	1	7,5	29	96	227		36,4	88,5	145
	3984		200	1092	0,20	0,75	4	32	129	415	934		24,0	89,8	35
	ZSV2755		180	3624	0,12	0,5	2,5	37	230	1088	3035		28,8	93,3	11
	4026		160		0,12	14	65	670	4250						(0,9)
	ZSV2754	600	140	358	0,16	0,5	1	8	44	137	290		34,4	94,3	103
	ZSV2773		130	826	0,12	0,5	2	21	108	340	682		33,6	93,3	41
	ZSV2761		120	1991	0,12	0,5	2,5	50	307	918	1685		33,2	92,3	15
	3994	650	100	187	0,12	0,5	2,3	14	41	87	151		49,6	94,3	190
	ZSV2759		80	585	0,08	0,25	2	27	114	282	486		40,4	94,3	52
	ZSV2760		60	4047	0,08	1	9	220	1000	2340	3618		50,8	96,0	6,7
EUROFER-Ø100	3999	550	200	1357	0,12	1	4	35	170	625	1260	5x25	28,8	87,1	23
E83699	3993		180	6798	0,12	1,5	7	70	500	2565	6546		27,6	88,5	4,3
1075°C															
+600°C1050h	ZSV2776	600	140	1840	0,16	0,5	1,5	35	365	1085	1769		24,4	92,3	12
	ZSV2778	650	100	361	0,08	1,5	16	100	210	308	357		33,6	95,1	34
	ZSV2768		80	2148	0,12	1	22	290	780	1427	1990		35,2	92,2	10

Table 14

Creep Rupture Tests

ZSV-No= Test in Vacuum

T14 EU-LZ-KR.doc 7-02

Table 15: Minimum Values for 550 °C / 20000 h (annealed + aged)

Alloy Condition	1 % yield limit R _{p1%} [MPa]					Creep strength R _m [MPa]				
	400 °C	450 °C	500 °C	550 °C	600 °C	400 °C	450 °C	500 °C	550 °C	600 °C
OPTIFER (1 % W) 1075 °C + 750 °C 2h	350	270	200	142	83	370	310	235	165	103
950 °C + 750 °C 2h	330	245	160	93	53	365	280	195	120	68
OPTIFER (Ge) 1075 °C + 750 °C 2h	270	210	150	105	63	305	250	185	130	78
950 °C + 750 °C 2h	260	190	108	55	-	300	220	140	75	-
F82H-mod (2 % W) as del. = 1040 °C + 750 °C	340	260	190	130	80	345	270	220	160	95
EUROFER 97 (1 % W) as del. = 980 °C + 740-760 °C	340	255	185	120	75	360	290	220	150	90
1075 °C + 750 °C	340	250	190	135	85	350	280	215	165	105
950 °C + 750 °C	340	250	180	115	70	350	280	210	160	83

Table 16: n and k values (Norton) for EUROFER 97

	T [°C]	n	k	s range [MPa]		n		n
EUROFER as delivered 980 °C + 740-760 °C	450	25	$2 \cdot 10^{-67}$	360-320	F82H-mod 950-1000 °C + 750 °C	29	OPTIFER-W 900-950 °C + 750 °C	23
	500	23	$7 \cdot 10^{-60}$	300-230		23		16
	550	18	10^{-45}	260-170		18		16
	600	10	$3 \cdot 10^{-25}$	160-100		12.5		11
	650	6.2	$5 \cdot 10^{-16}$	90-50		8.4/5		6
1075 °C + 750 °C	450	25	$2 \cdot 10^{-67}$	350-310	1040 °C + 750 °C	29	1075 °C + 750 °C	24
	500					23		21
	550	21	10^{-52}	220-180		18		20
	600					12.5		15
	650	6.5	$6 \cdot 10^{-17}$	120-60		8.4/5		5.5

8 Figures

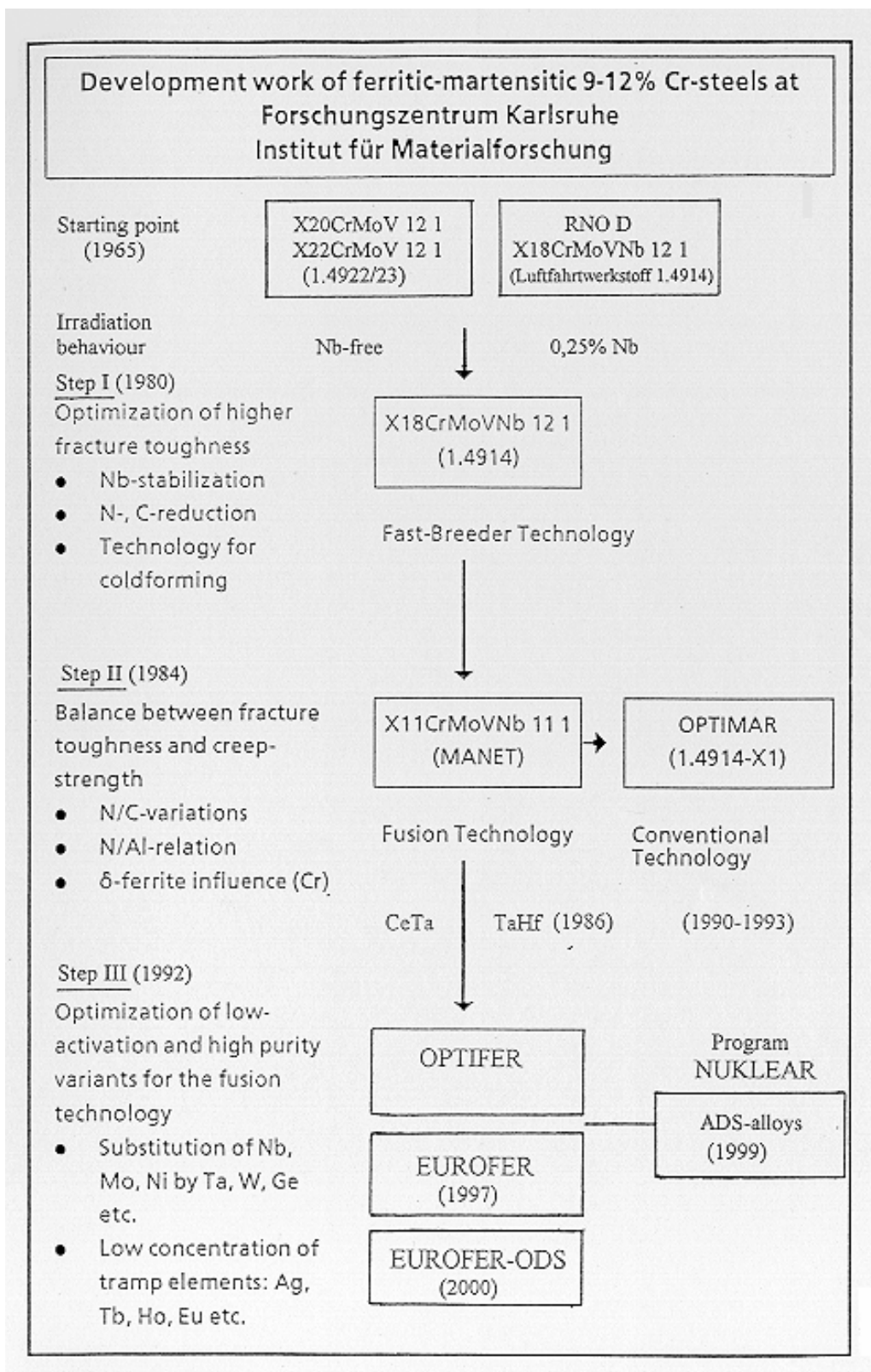


Fig. 1: Development work of 9-12 % Cr steels at FZK/IMF

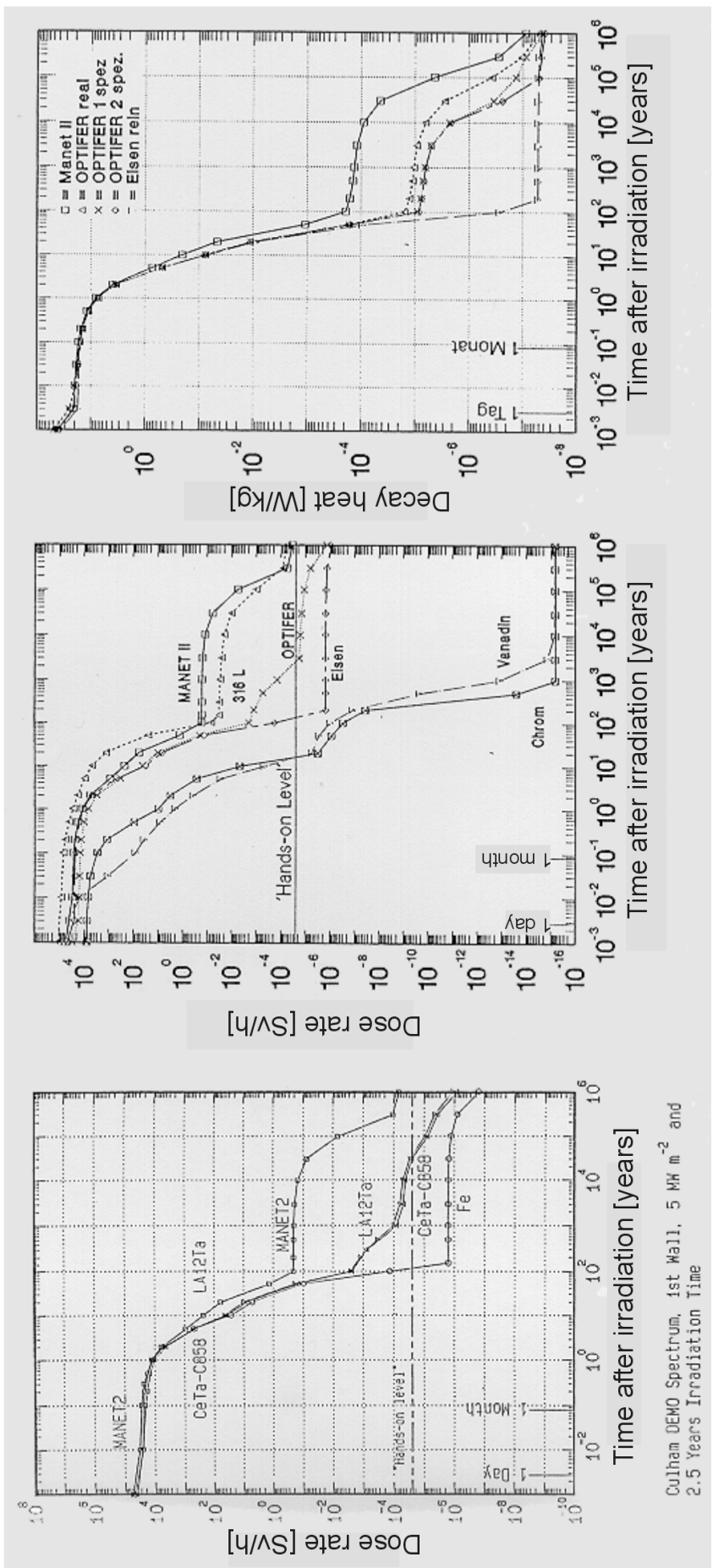


Fig. 2: Deactivation Curves

Culham DEMO Spectrum, 1st Wall, 5 MW m^{-2} and
2.5 Years Irradiation Time

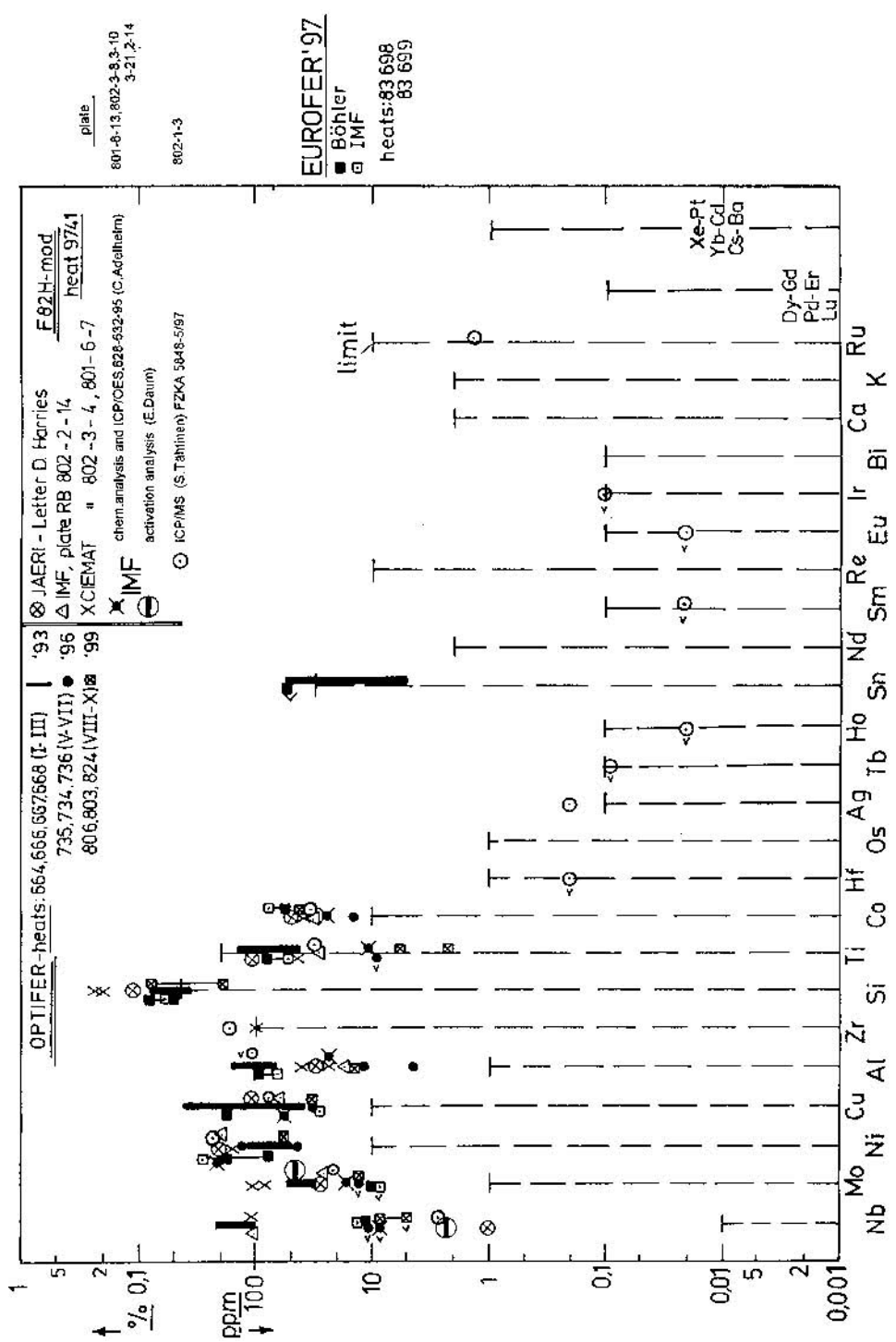


Fig. 3: Undesirable tramp elements in LA steels

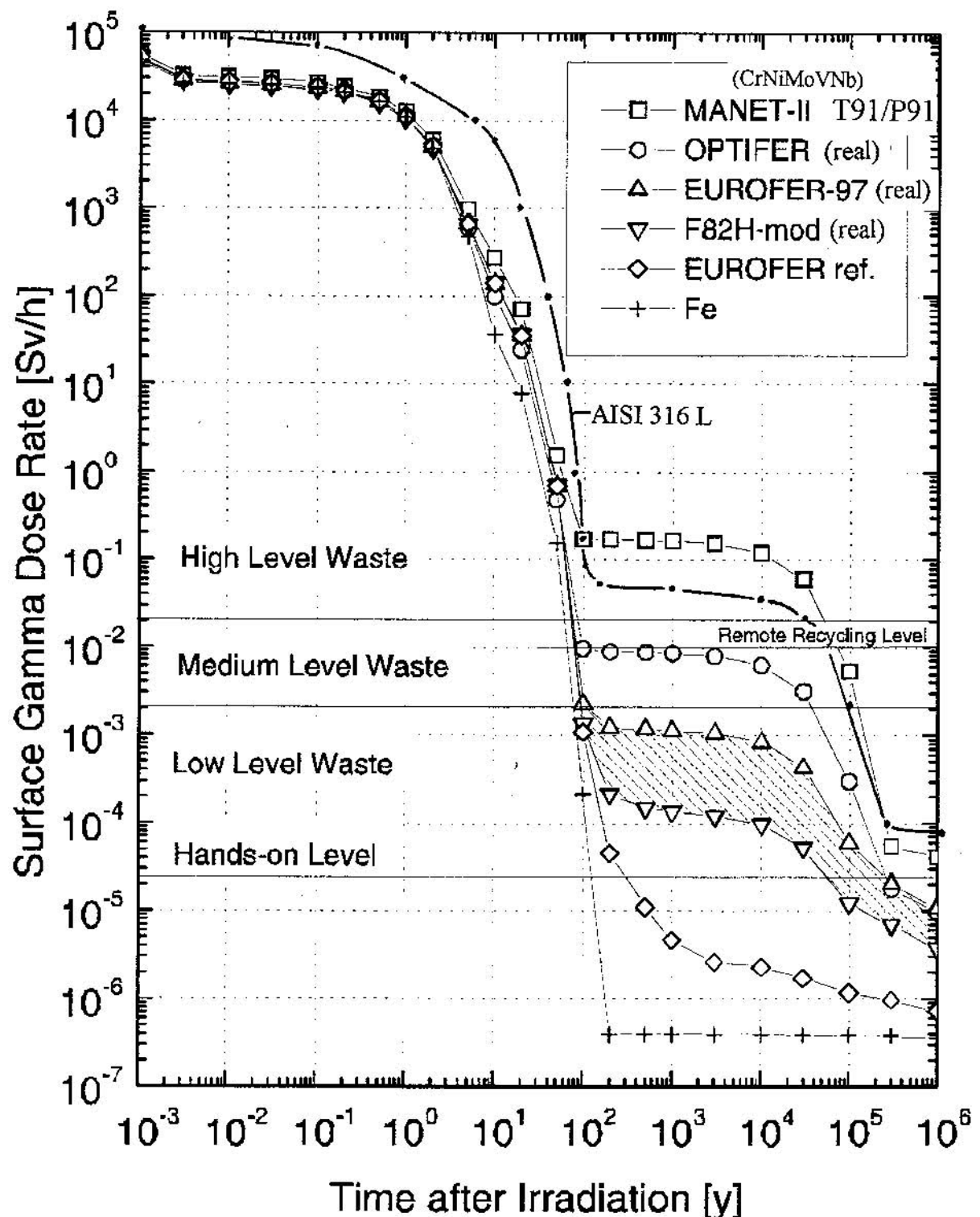
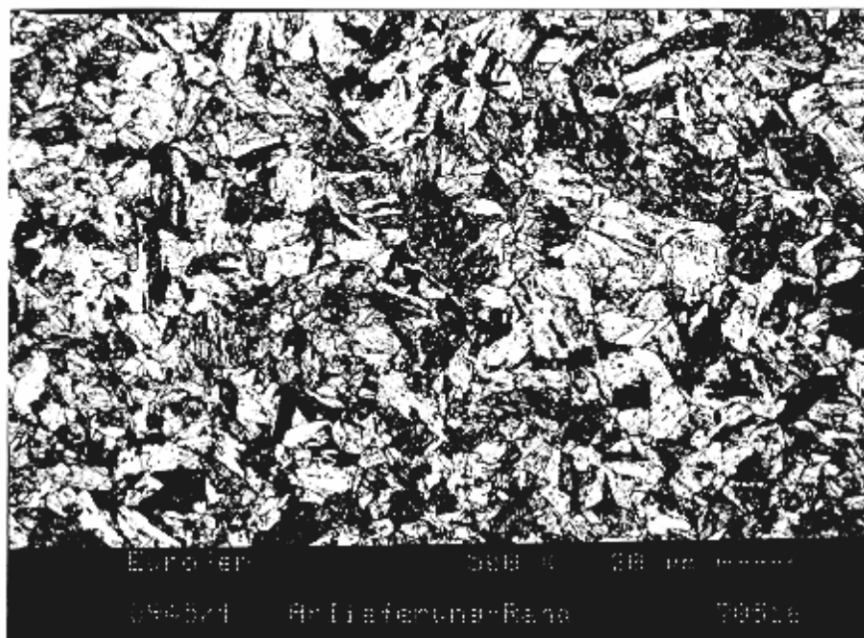


Fig. 4: Deactivation Curves

EUROFER Ø100 mm

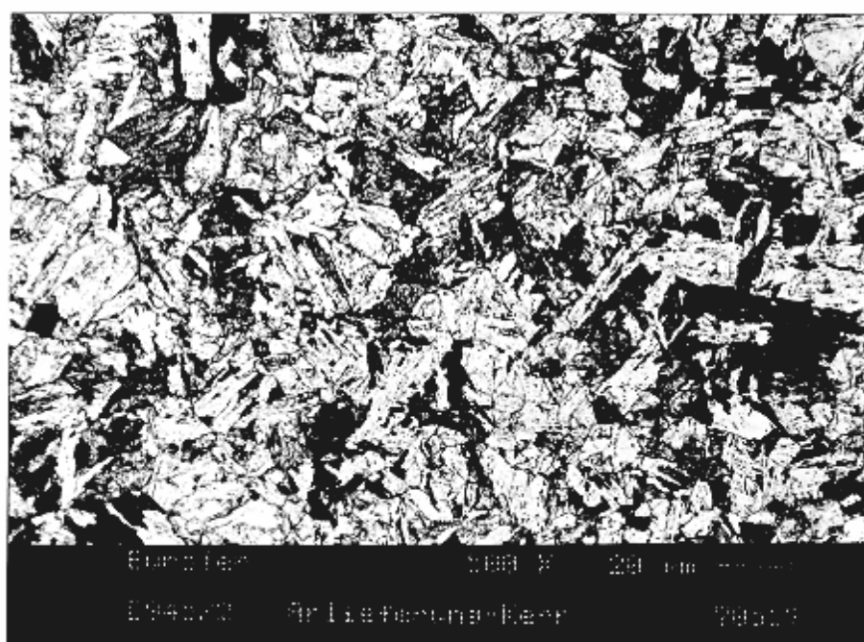
Condition as delivered

Specimen from border zone



HV30 = 210-216 grain size = 16.5 μm (ASTM 9)

Specimen from core zone



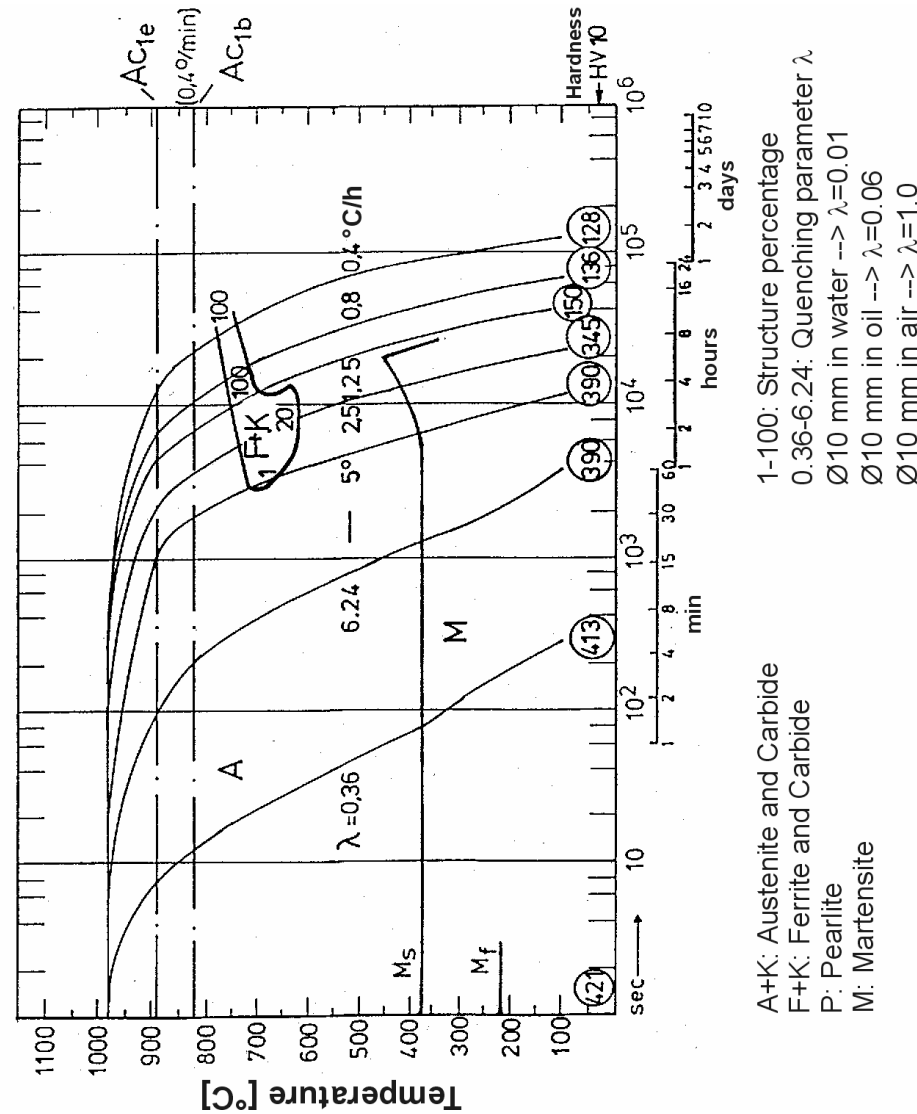
HV30 = 219-221 grain size = 16.5 μm (ASTM 9)

Fig. 5: Microstructure of EUROFER 97 as delivered

EUROFER 97

austenitization: 980°C 20 min
grain size after quenching: 8-8.5 ASTM

heat E83699



- 1-100: Structure percentage
0 36-6 24: Quenching parameter λ .
 Ø10 mm in water $\rightarrow \lambda=0.01$
 Ø10 mm in oil $\rightarrow \lambda=0.06$
 Ø10 mm in air $\rightarrow \lambda=1.0$

Fig. 6: Continuous TTT Diagram

Influence of the austenitization temperature on the transition behaviour of low activation 8-10 % Cr steels

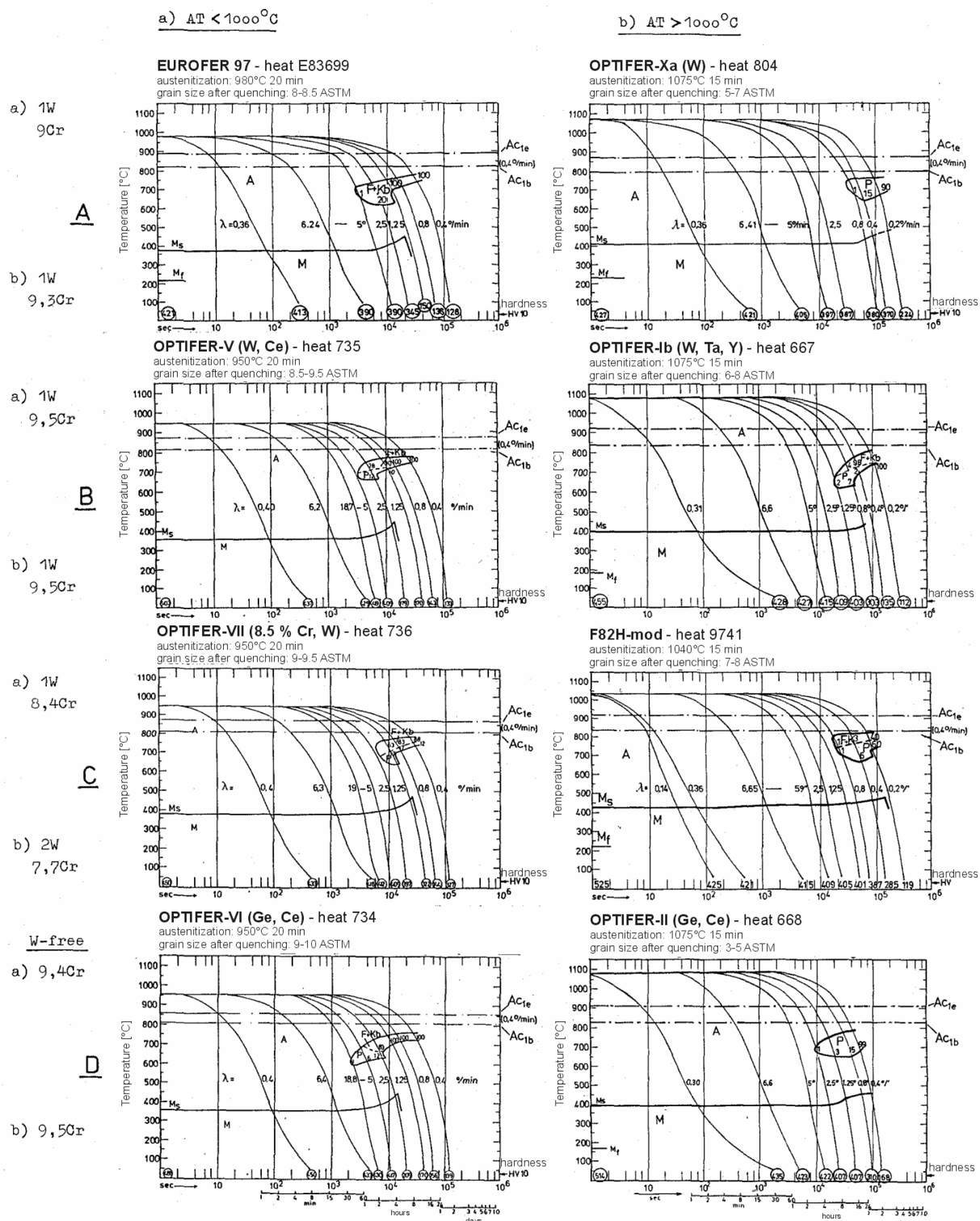
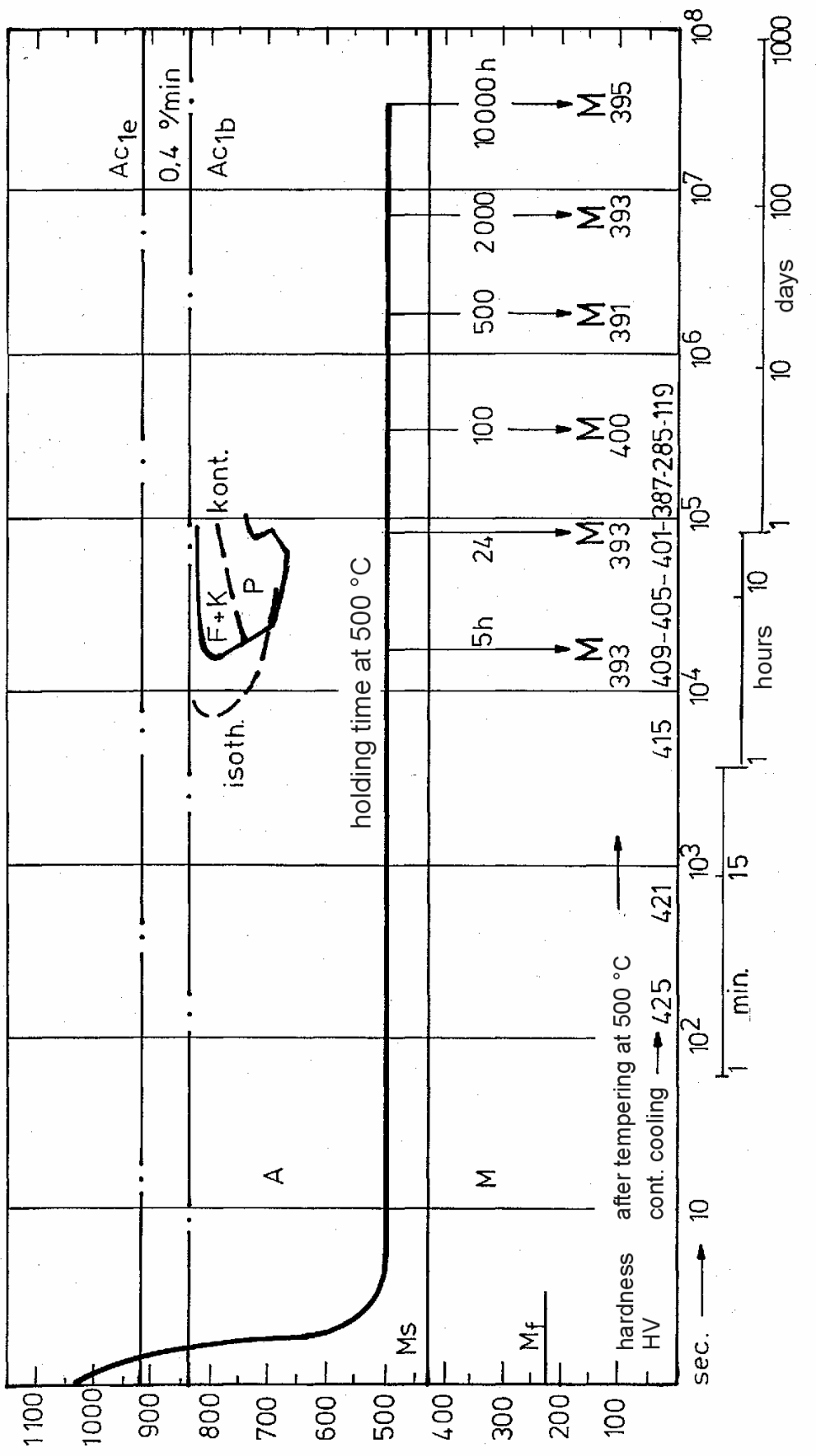


Fig. 7: Continuous TTT Diagrams of different 8-10 % Cr Steels

F82H-mod
austenitization: 1040°C 30 min



M: metallographic result after holding at 500 °C

Fig. 8: Influence of long isothermal holding times on the structure formation

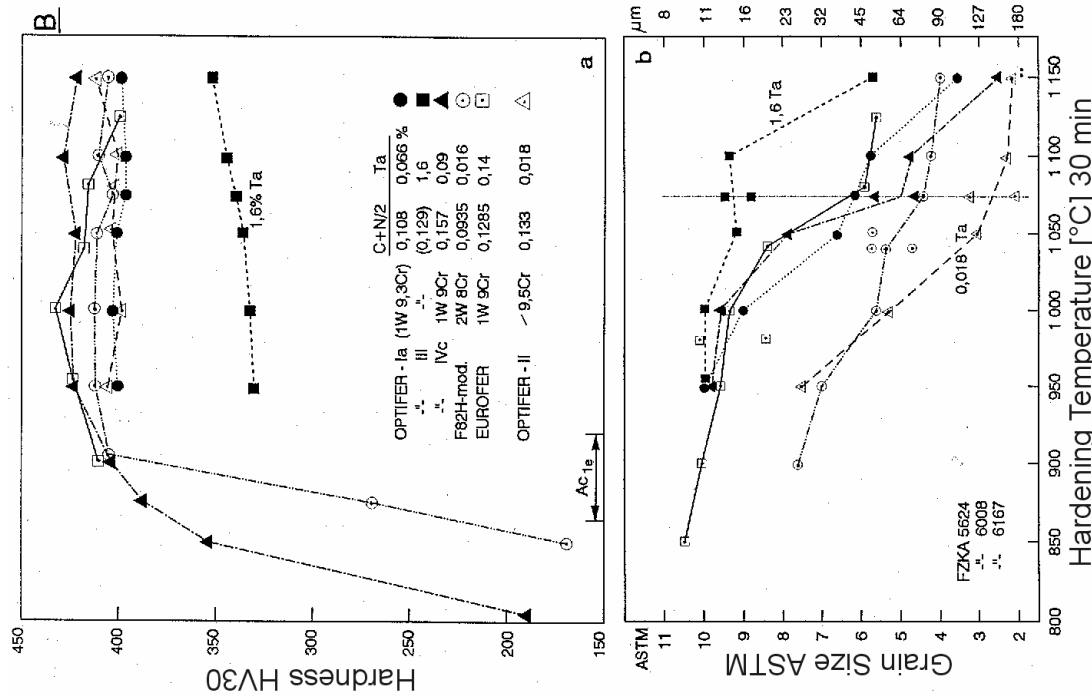
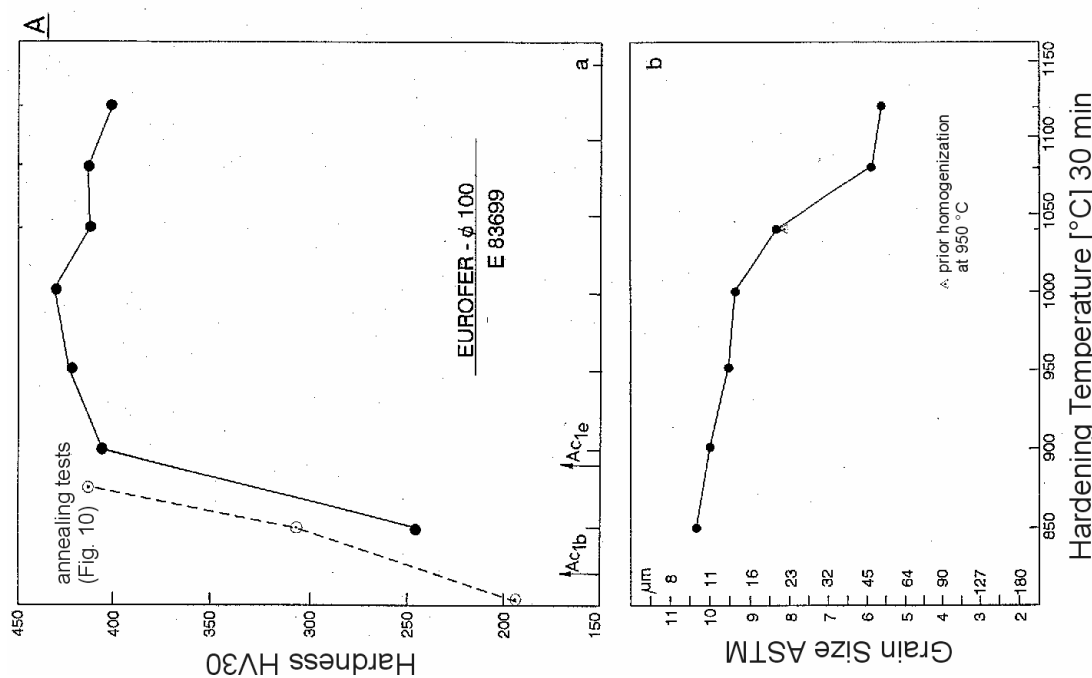


Fig. 9: Hardening Diagram and Influence of C-N-Ta Content on Hardening a) and Grain Size b)

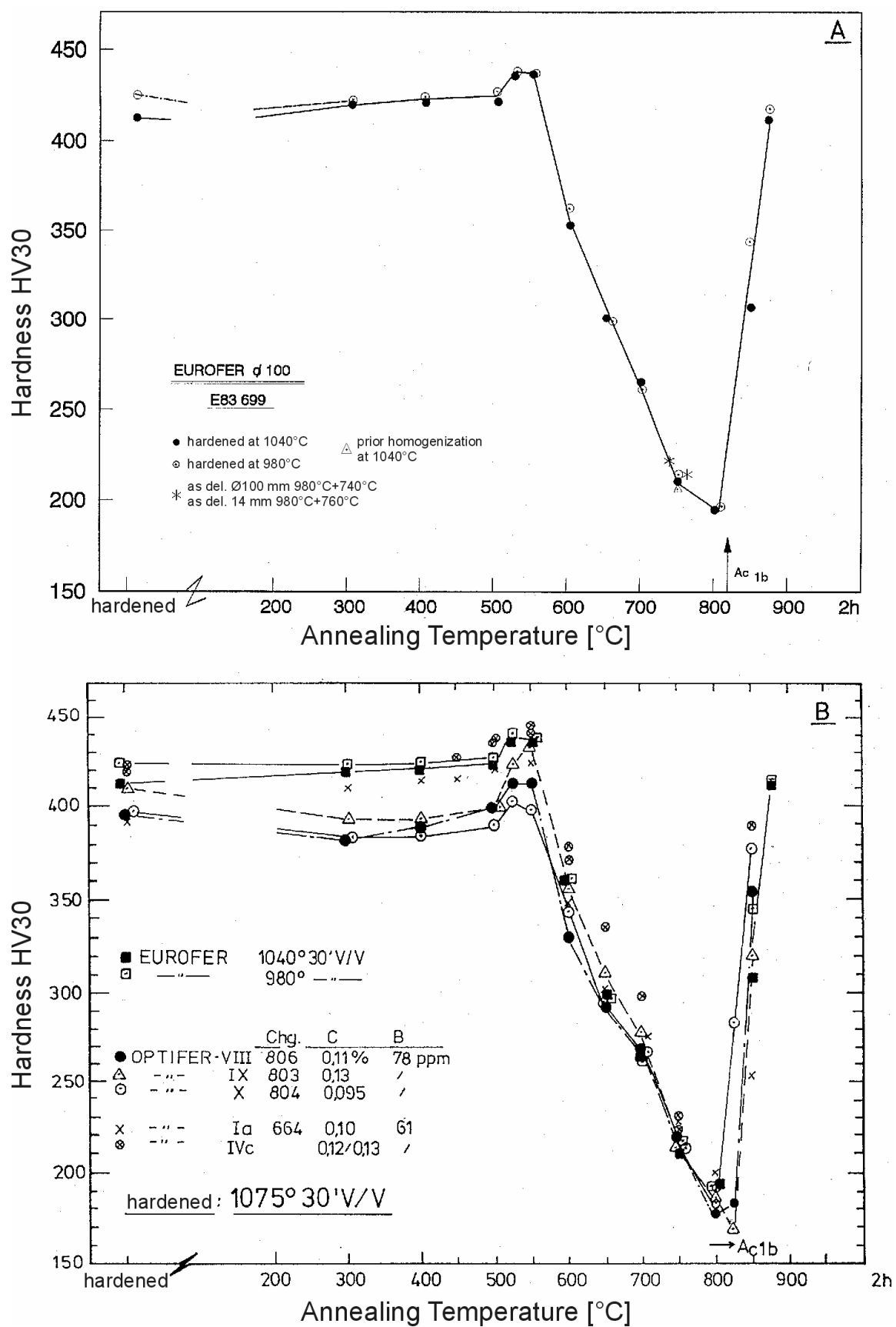


Fig. 10: Annealing Diagram

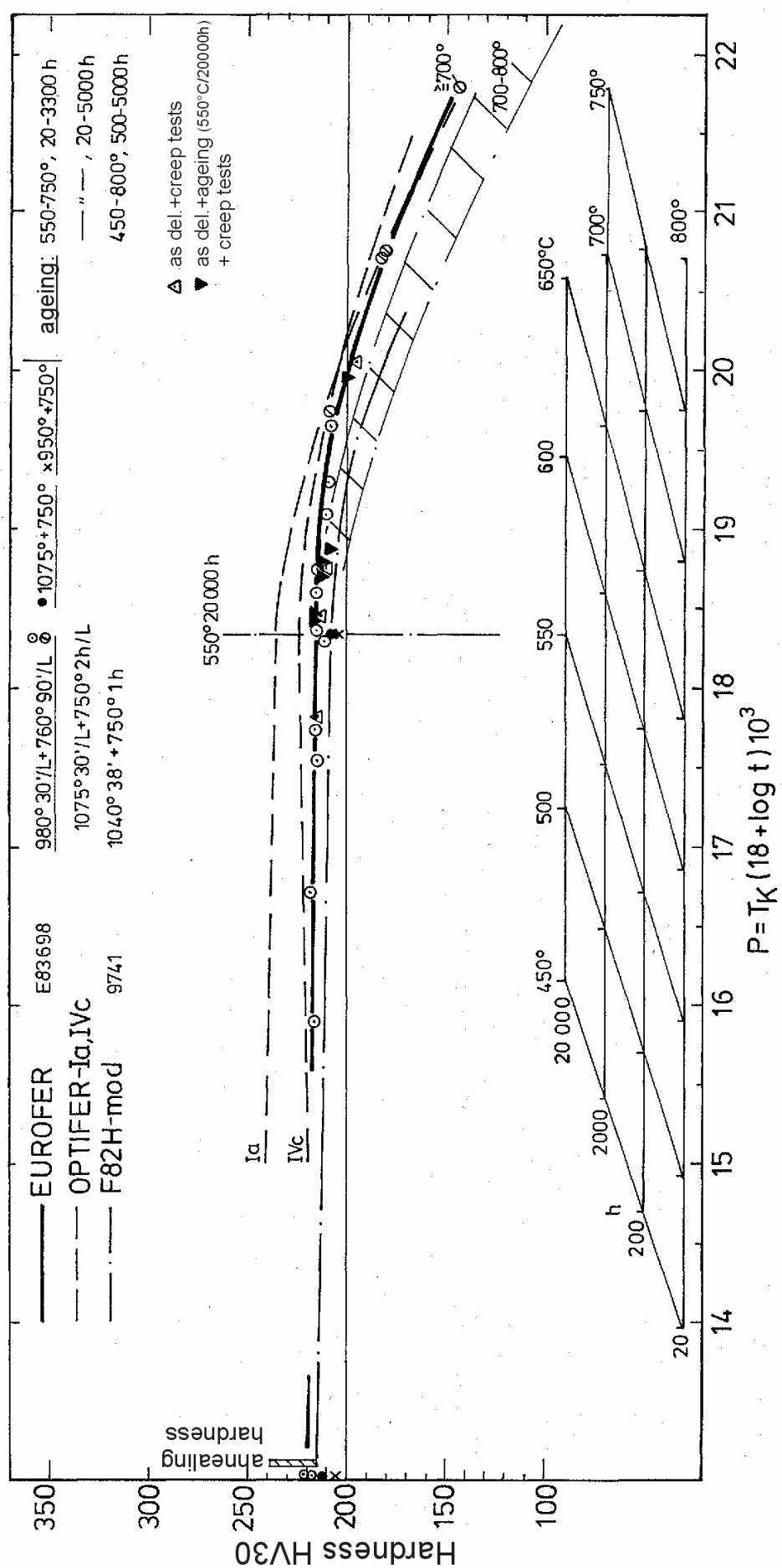
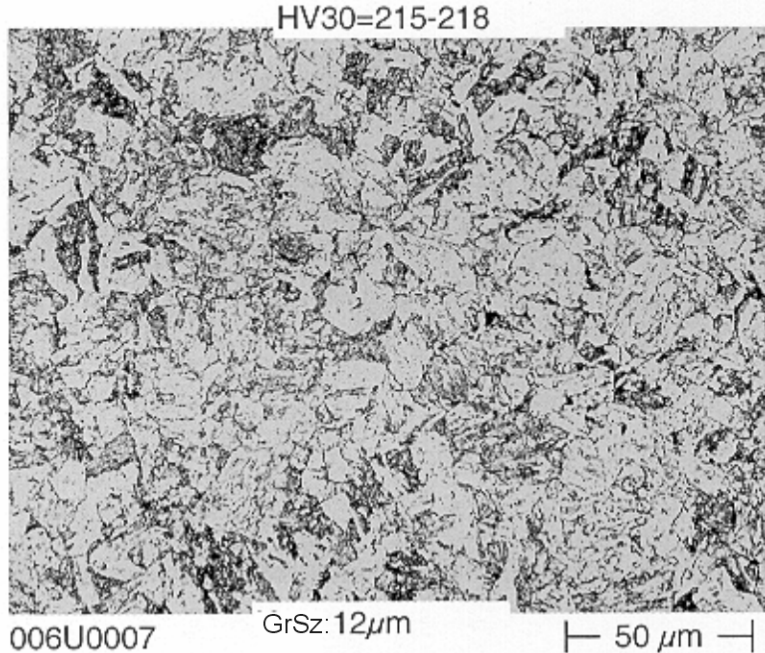


Fig. 11: Annealing Master Curve (Hollomon-Jaffe)

EUROFER heat E83968 14 mm plate

D968/1
as delivered



D968/14
as del.+600°C 1050h

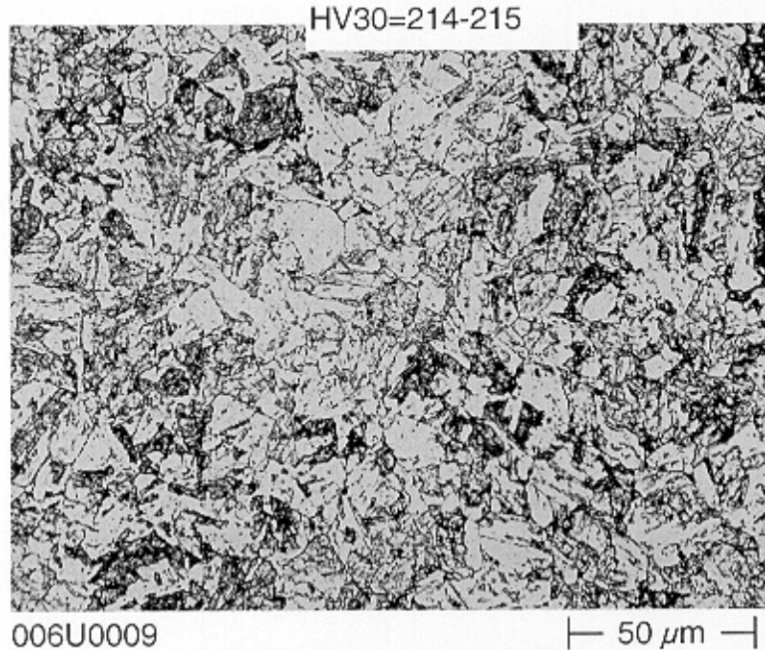


Fig. 12: Microstructure of EUFORFER as delivered and in the aged condition

EUROFER heat E83968 14 mm plate

D987/1

1075°C 30min V/V + 750°C 2h V/V

HV30=210-213



006U0001 Kgr.: 28µm

D987/2

950°C 30min V/V +750°C 2h V/V

HV30=205-207



006U0002 Kgr.: 13µm

D987/3

1075°C+750°C+600°C 1050h

HV30=207-209



006U0004

D987/4

950°C+750°C+600°C 1050h

HV30=205-207



006U0005

Fig. 13: Microstructure of EUROFER 97 after different heat treatments

EUROFER Ø100 mm

α -Ferrite formation between Ac_{1b} and Ac_{1e}

as delivered + 850°C

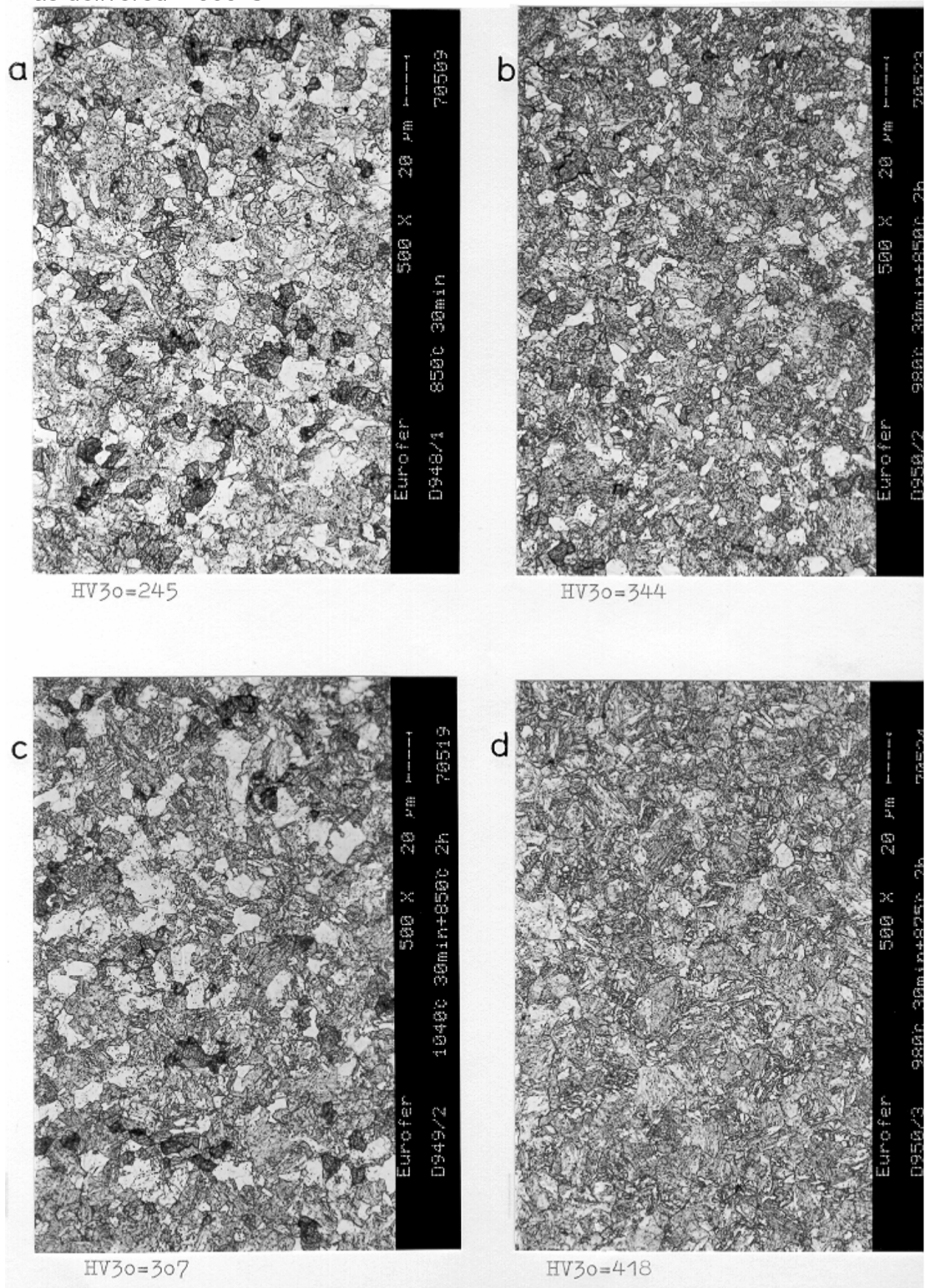


Fig. 14: Microstructure of EUROFER after heating between Ac_{1b} and Ac_{1e}

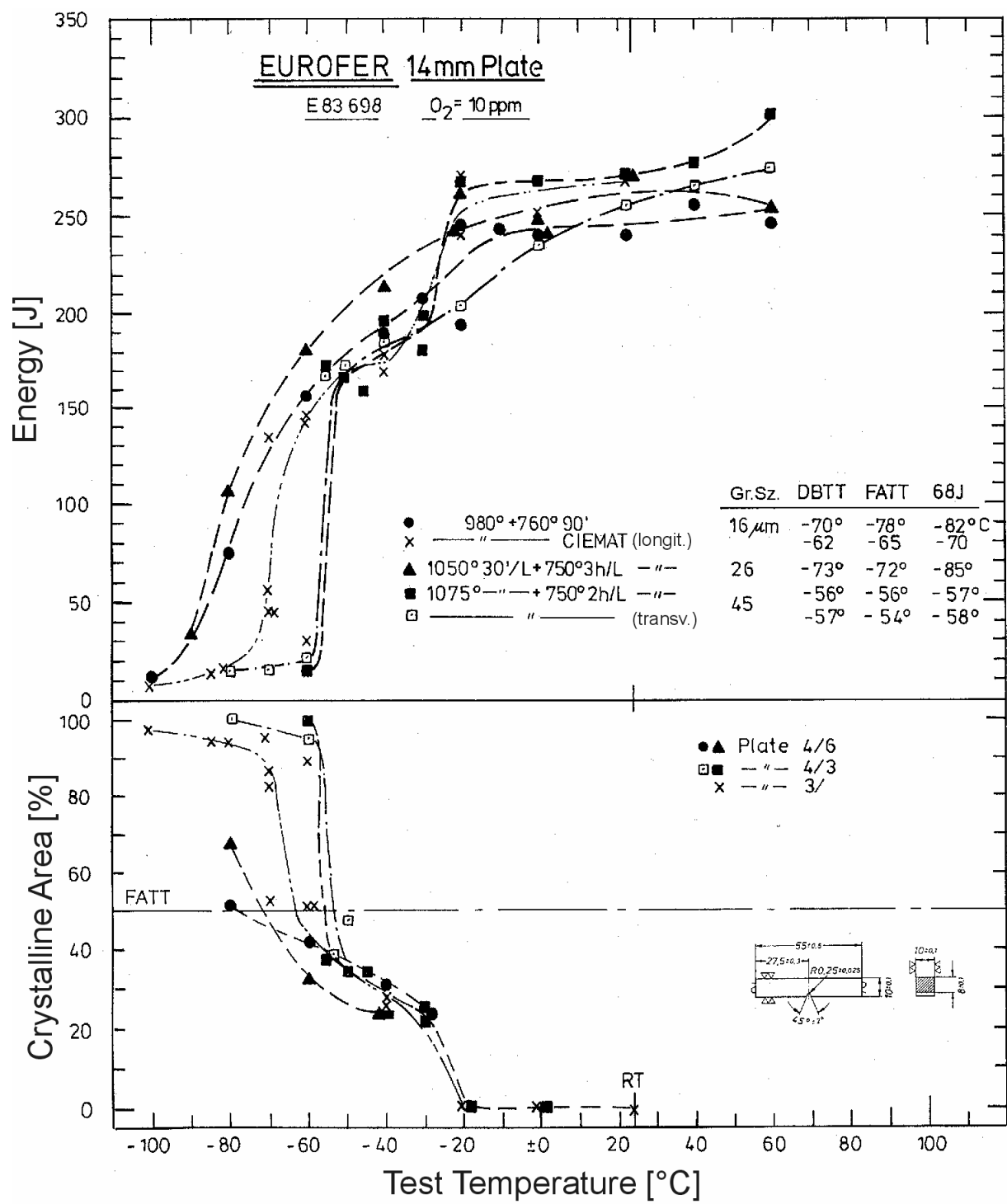


Fig. 15: Charpy Properties of EUROFER 97

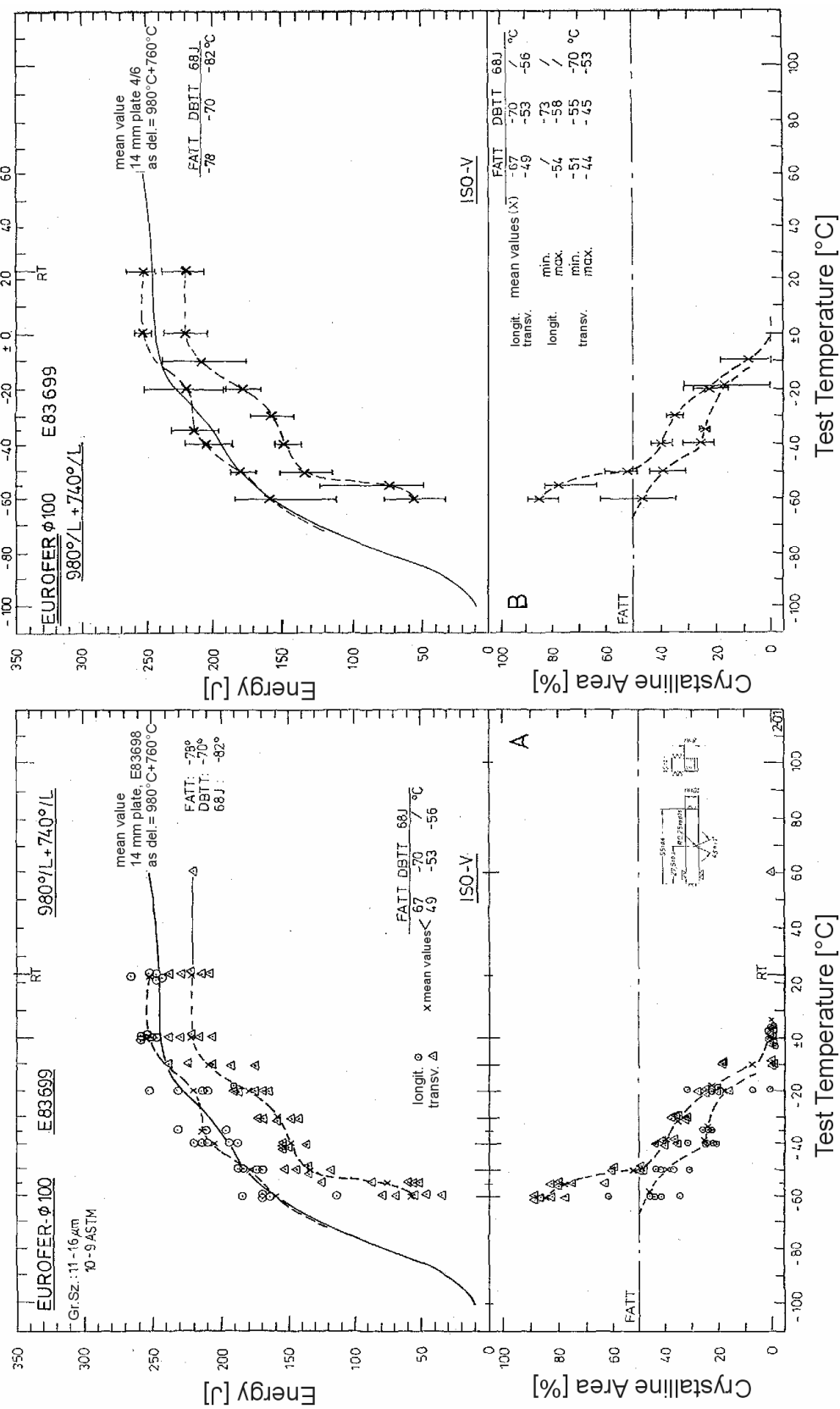


Fig. 16: Influence of Specimen Orientation on Charpy Properties of EUROFER 97

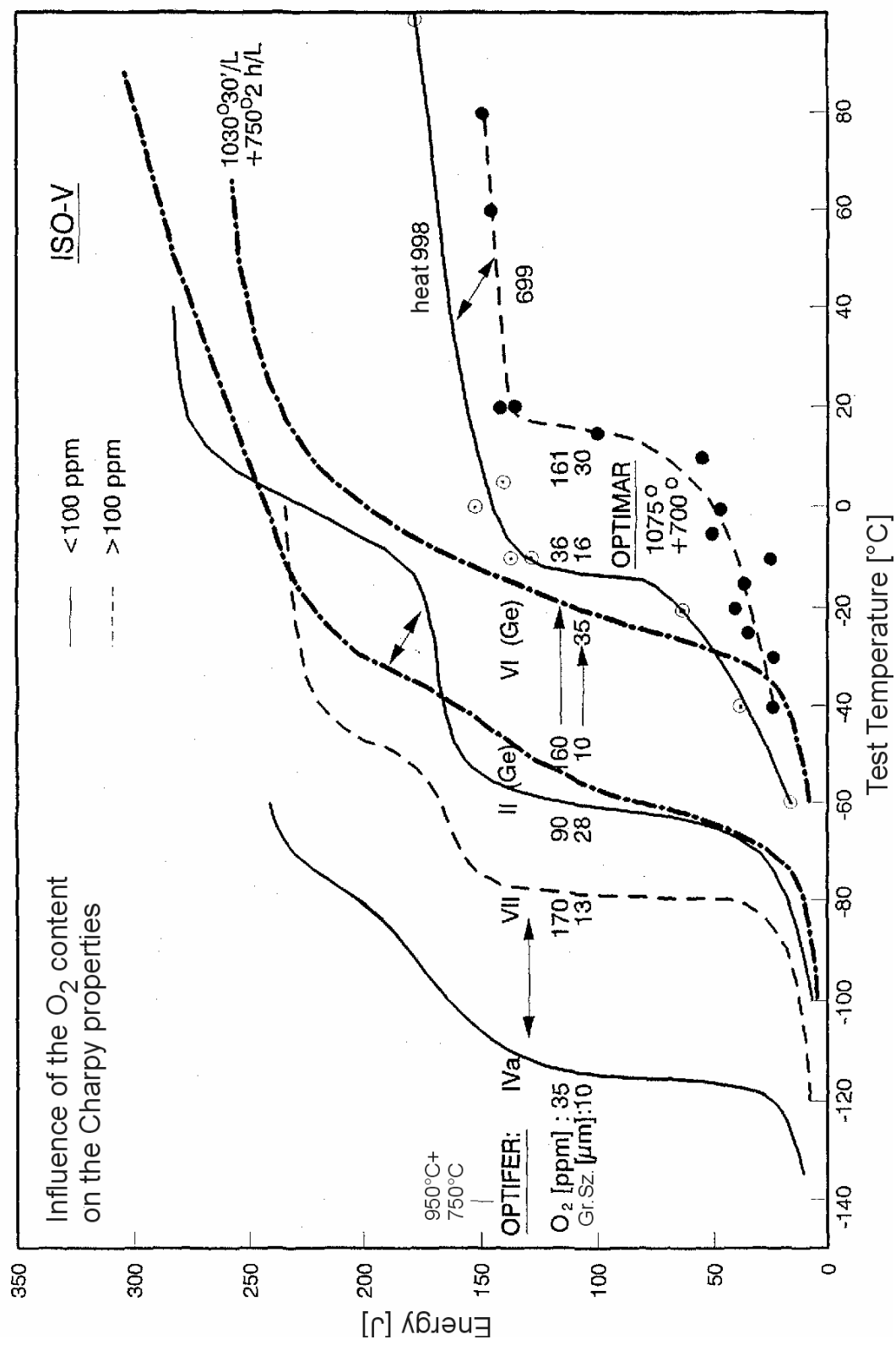


Fig. 17: Comparison of Charpy Properties of different Alloys and Influence of O₂ Content

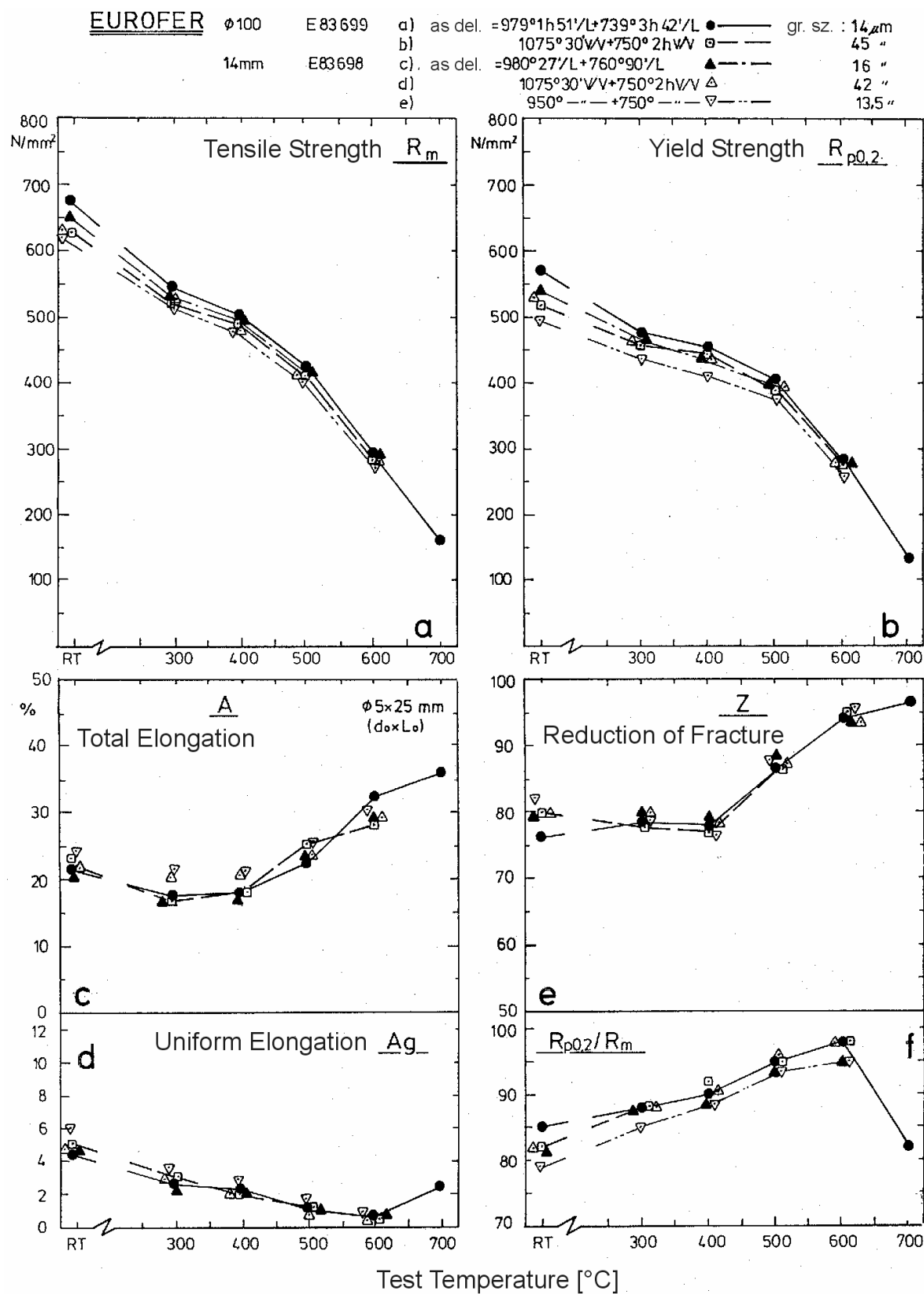


Fig. 18: Tensile Properties of EUROFER 97 (Influence of Annealing Treatment)

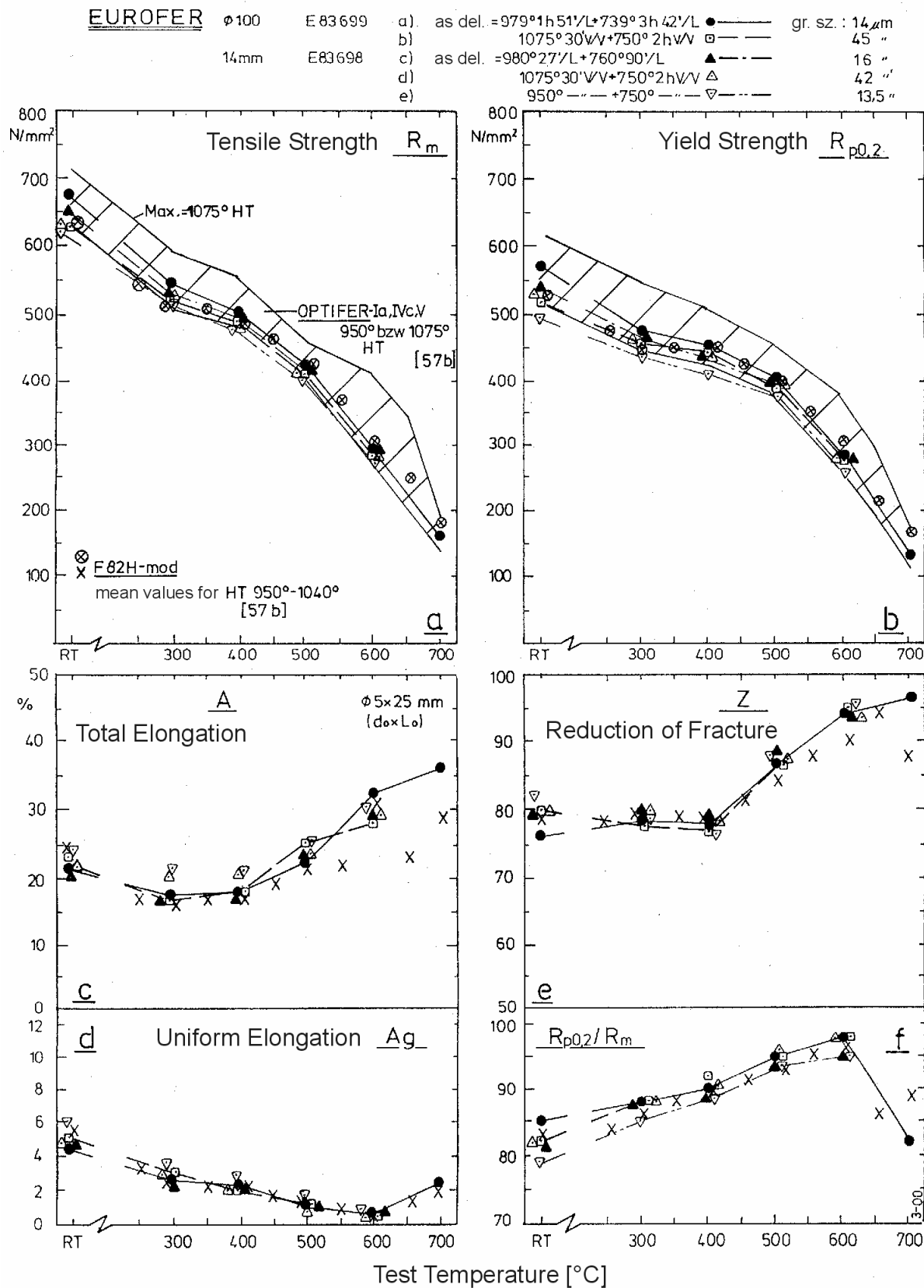
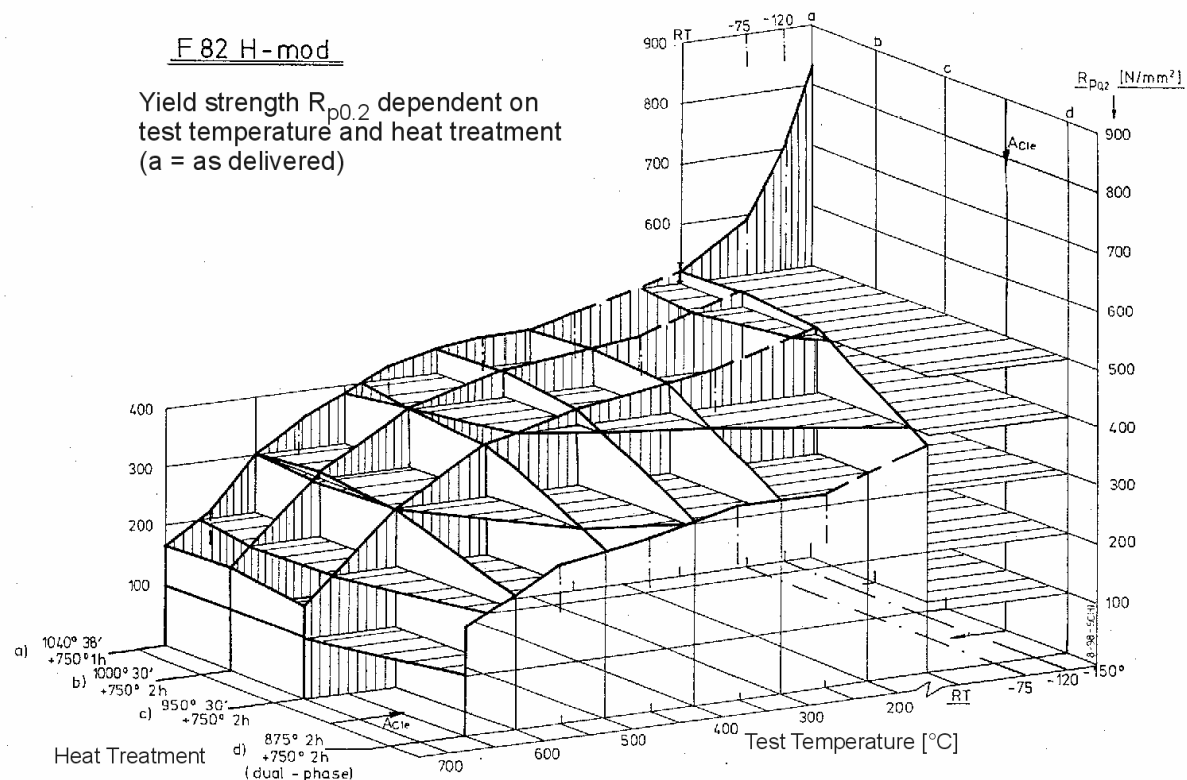


Fig. 19: Tensile properties of EUROFER compared to OPTIFER and F82H-mod

F 82 H-mod

Yield strength $R_{p0,2}$ dependent on test temperature and heat treatment
(a = as delivered)



Tensile strength R_m dependent on test temperature and heat treatment
(a = as delivered)

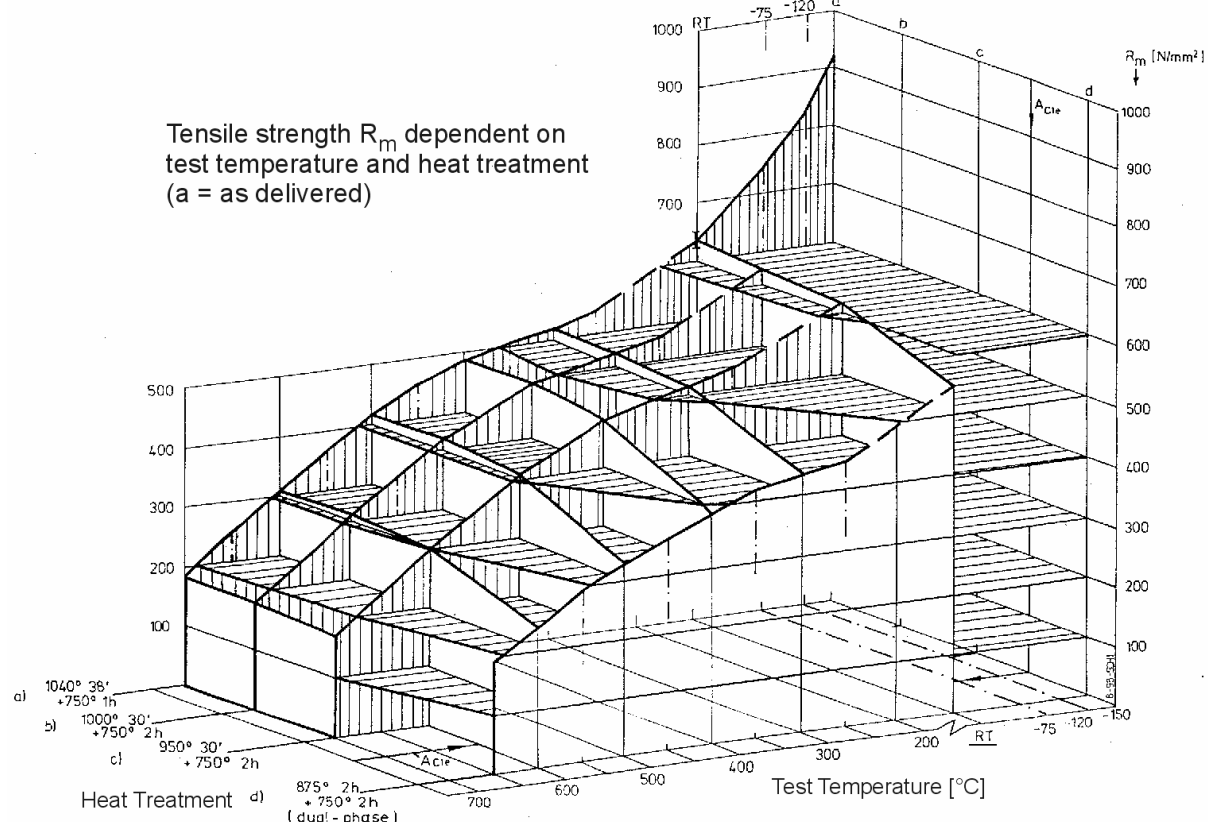
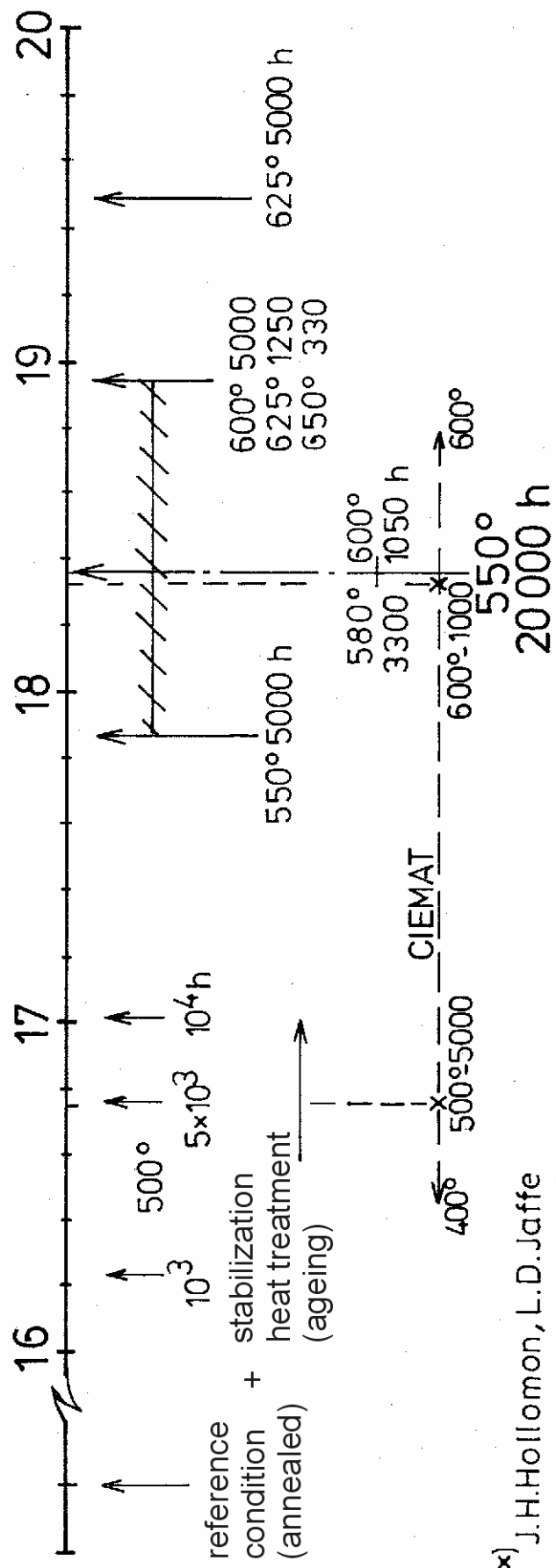


Fig. 20: Tensile and Yield Strength of F82H-mod depending on heat treatment and temperature

Hollomon-Jaffe -Parameter: $P = T_K (18 + \log t) 10^3$



x) J.H.Hollomon, L.D.Jaffe

"Time-temperature relations
in tempering steels."

Trans. of the Am.Inst. of Mining
and Mat. Eng. 162/1945 pp 223-249

Fig. 21: Explanation of the Hollomon-Jaffe Parameter for the case of ageing

EUROFER ϕ_{100} E 83 699

Influence of stabilization
heat treatments (ageing)

- a) as del. $\{= 980^\circ + 740^\circ\}$ ● —
- b) " " $+ 600^\circ 1050\text{ h}$ ○ —
- c) " " $+ 580^\circ 3300\text{ h}$ △ —
- d) $1075^\circ + 750^\circ$ ■ - - -
- e) " " $+ 600^\circ 1050\text{ h}$ □ - - -

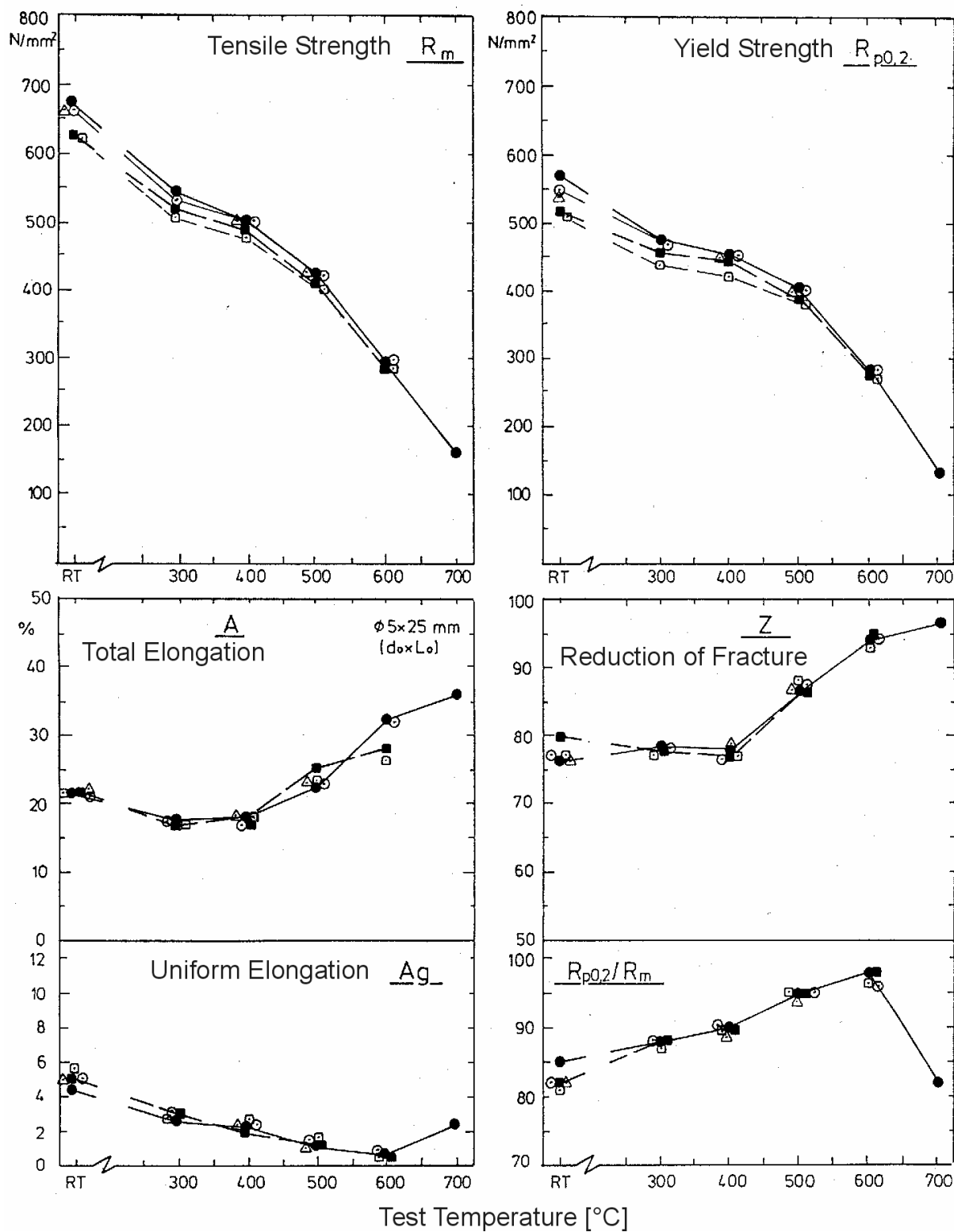


Fig. 22: Tensile Properties of EUROFER 97 after Ageing

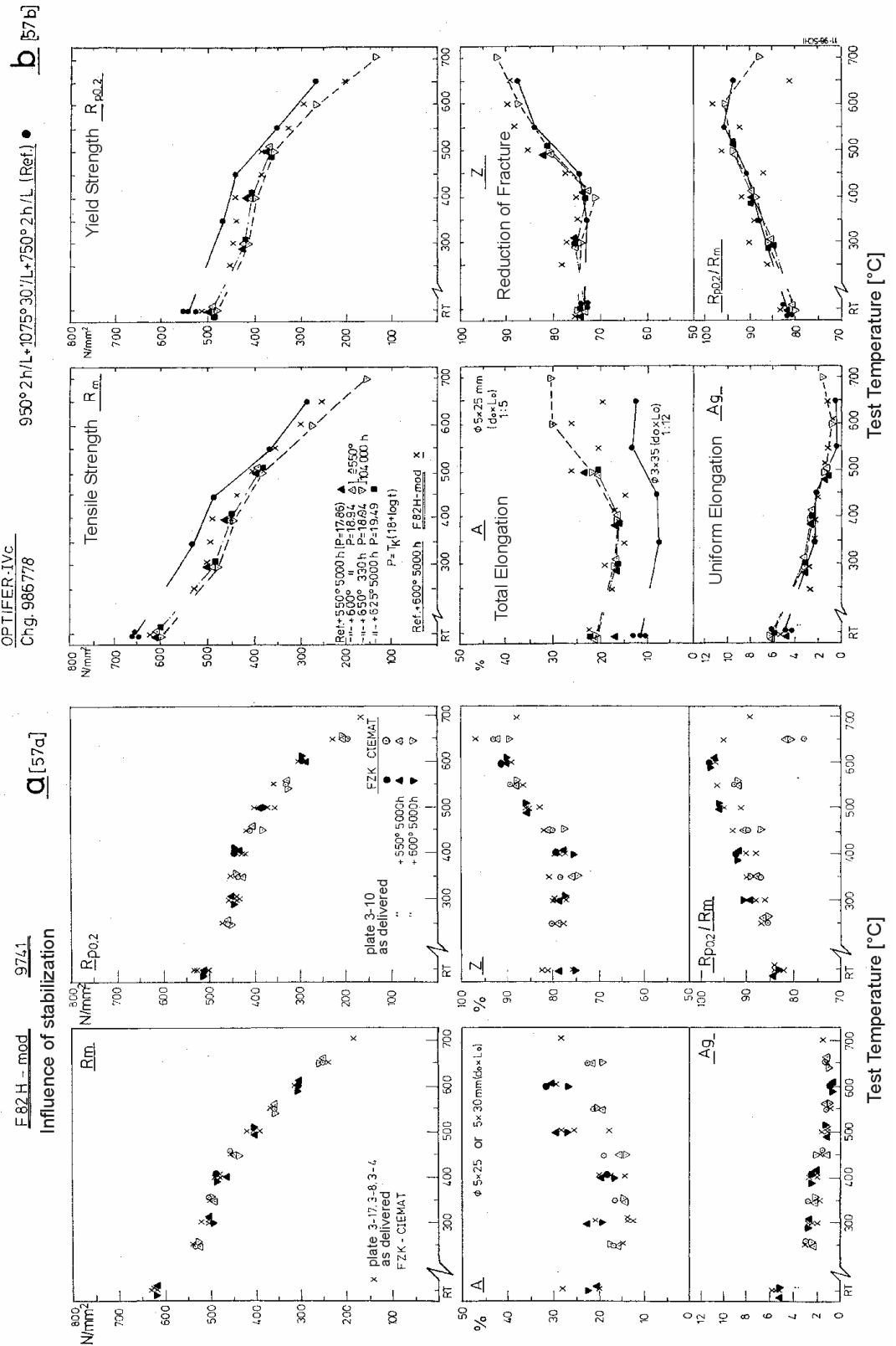


Fig. 23: Tensile properties after ageing and comparison with OPTIFER and F82H-mod.

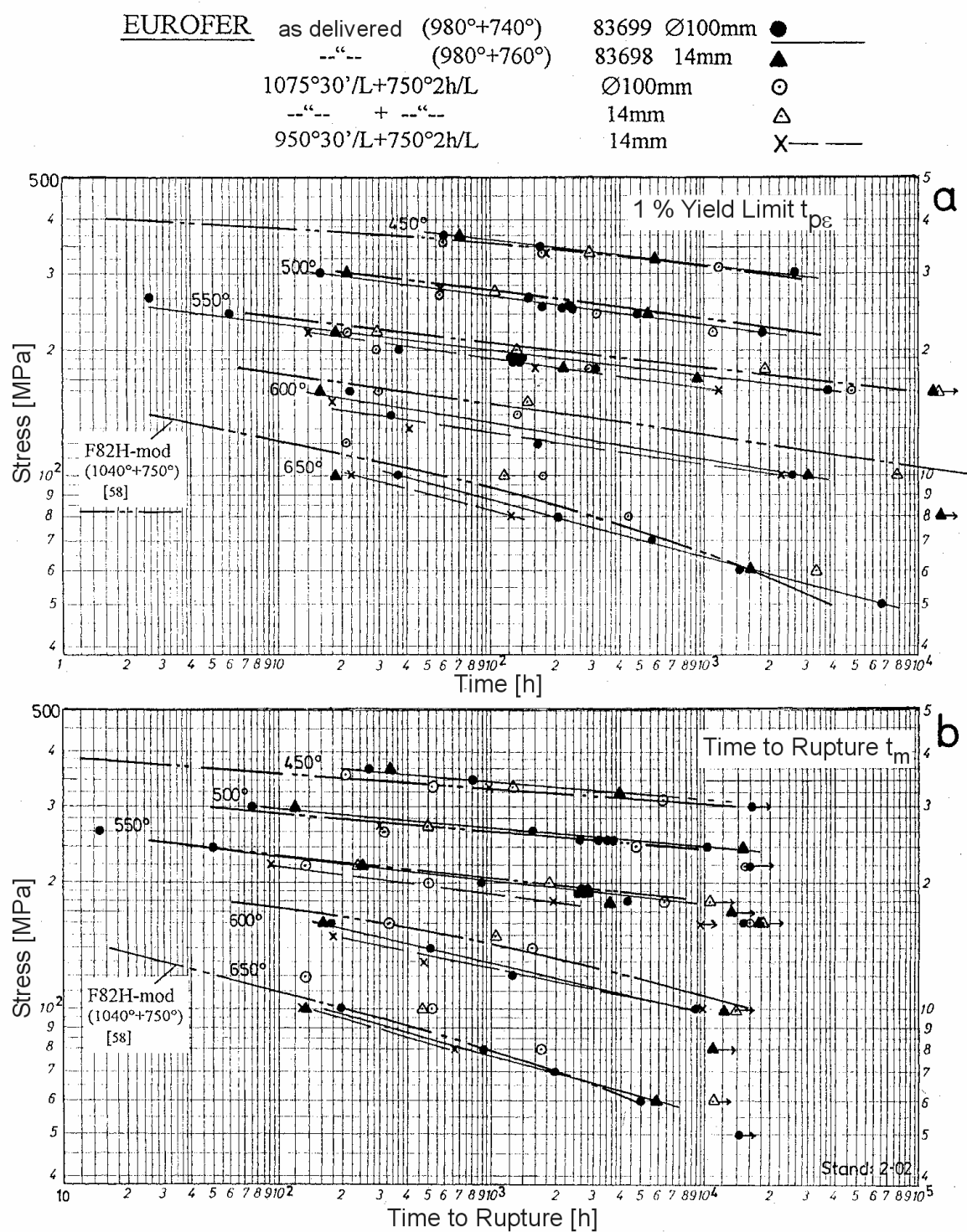


Fig. 24: Influence of annealing treatment on time to rupture and 1 % yield limit

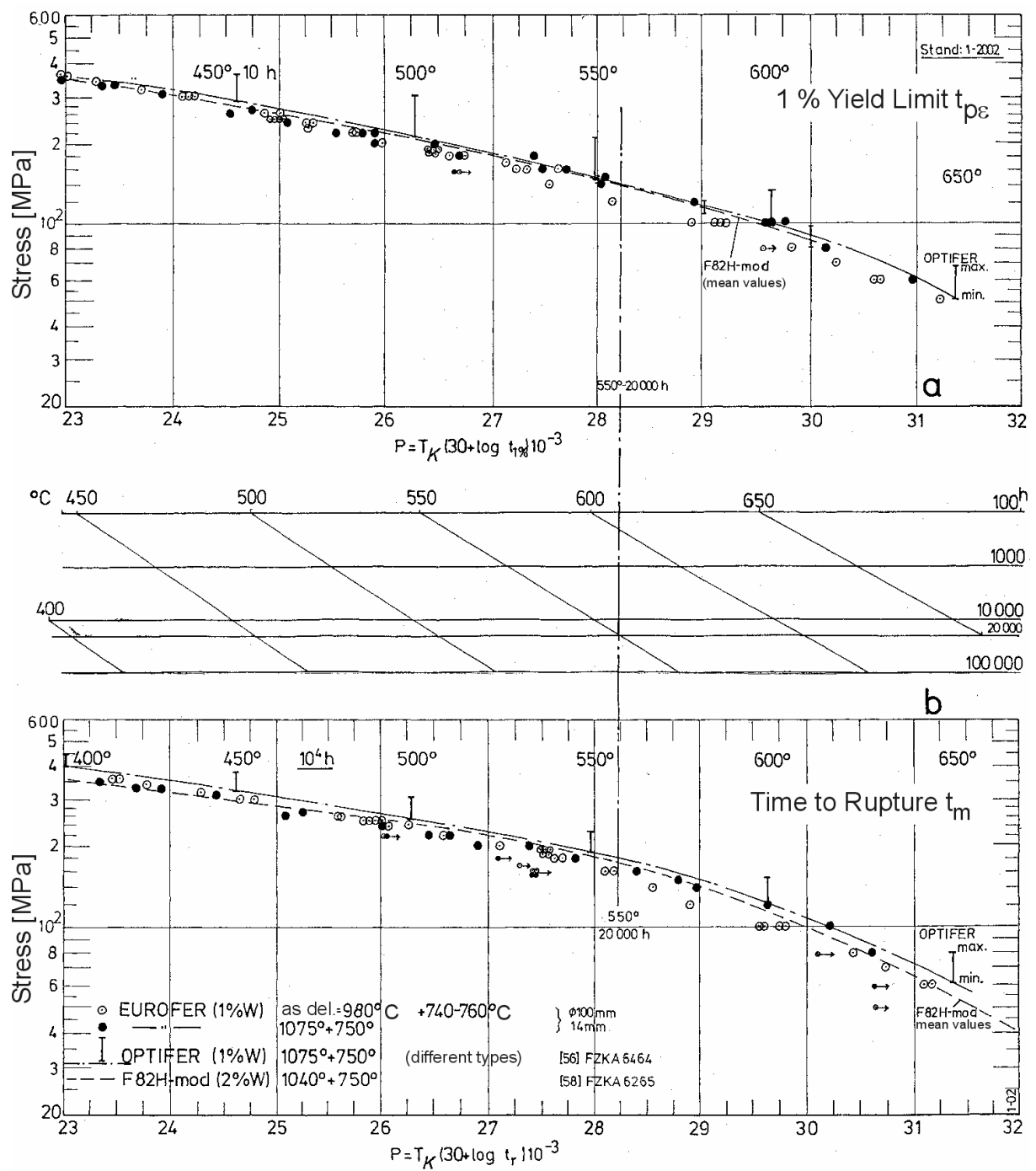


Fig. 25: Creep Rupture Master Curve (Larson-Miller Parameter)

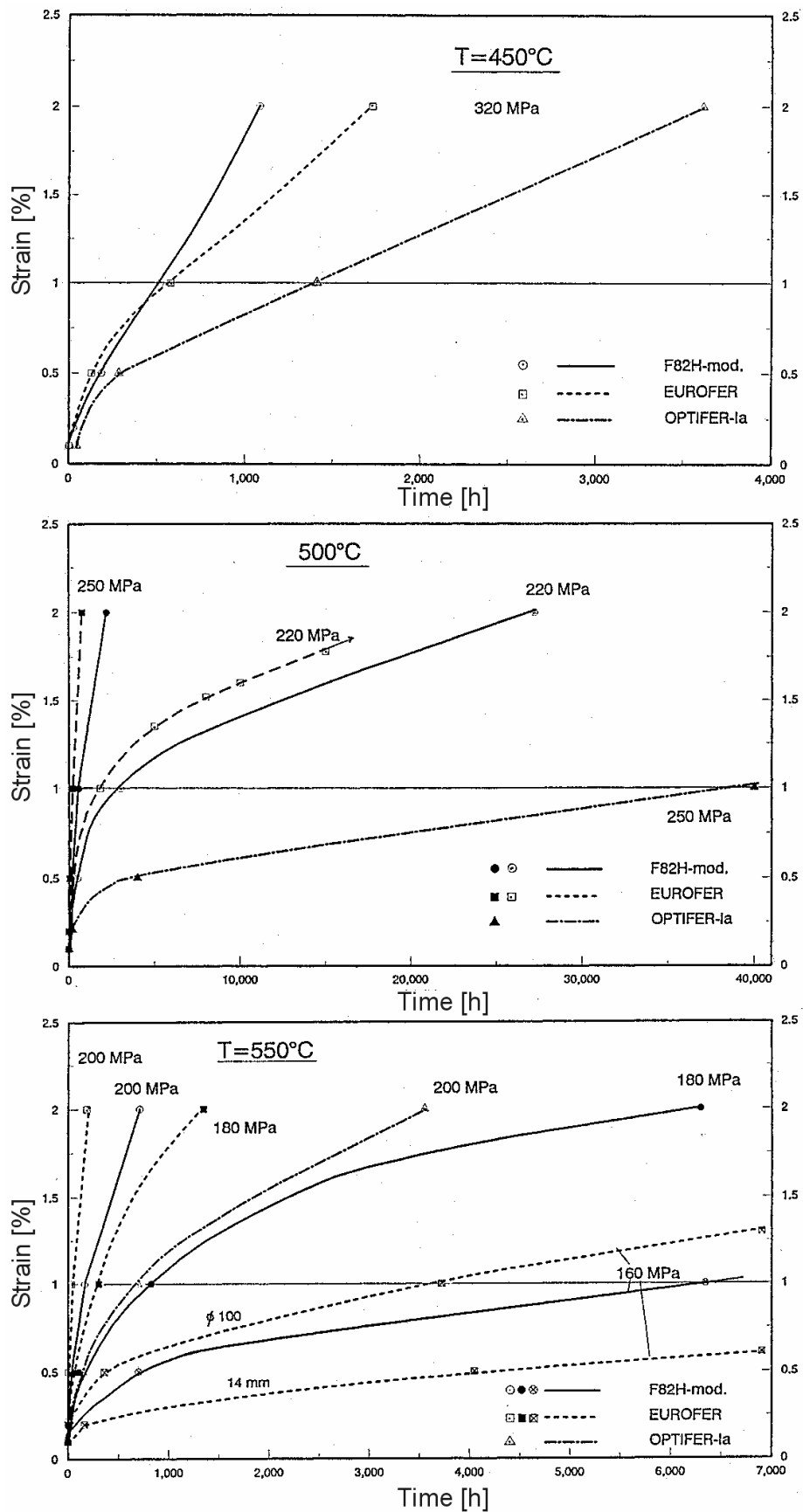


Fig. 26: Comparison of the primary creep range

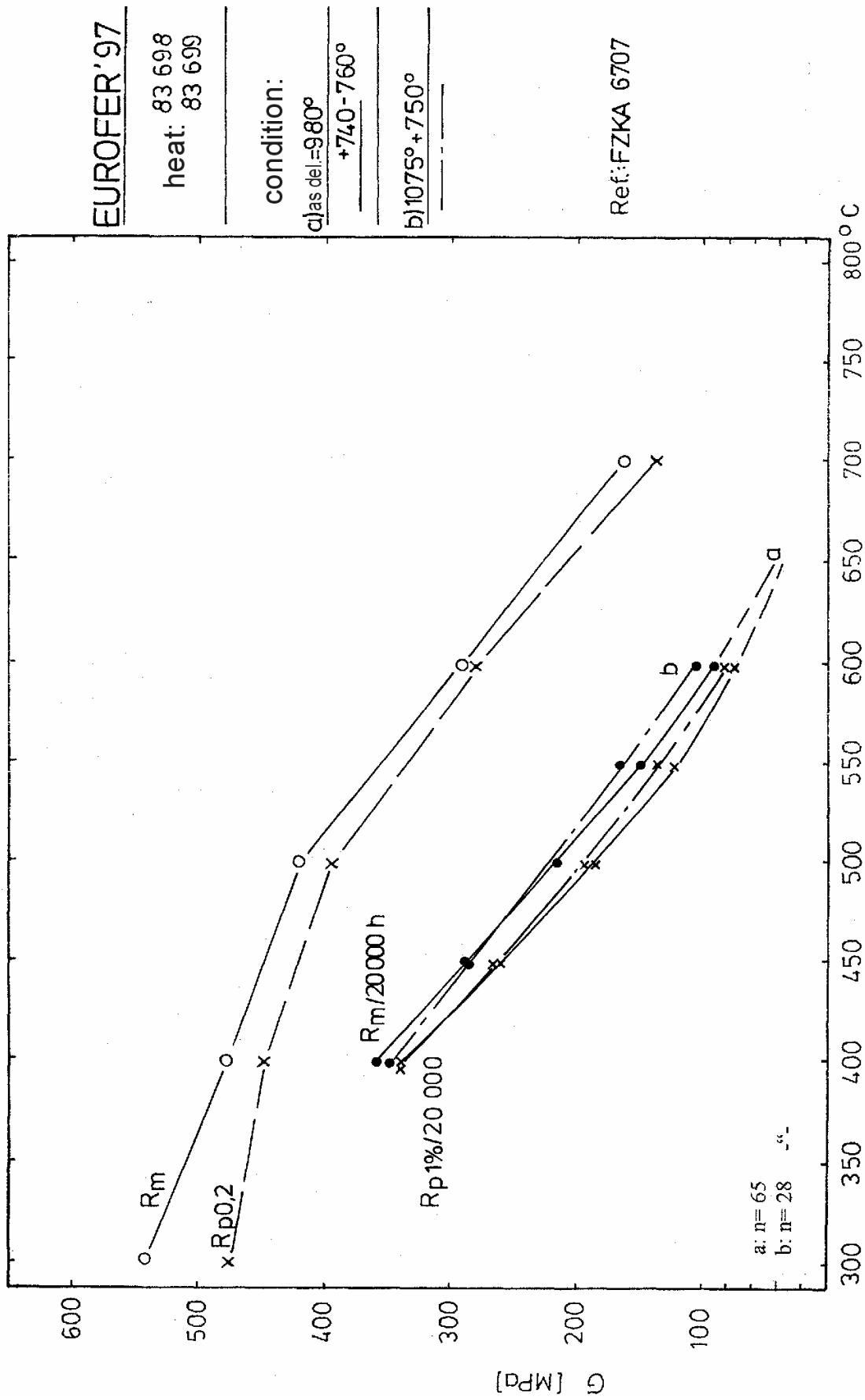


Fig. 27: Temperature Dependency of Tensile, Yield and Creep Strength as well as the 1% Yield Limit

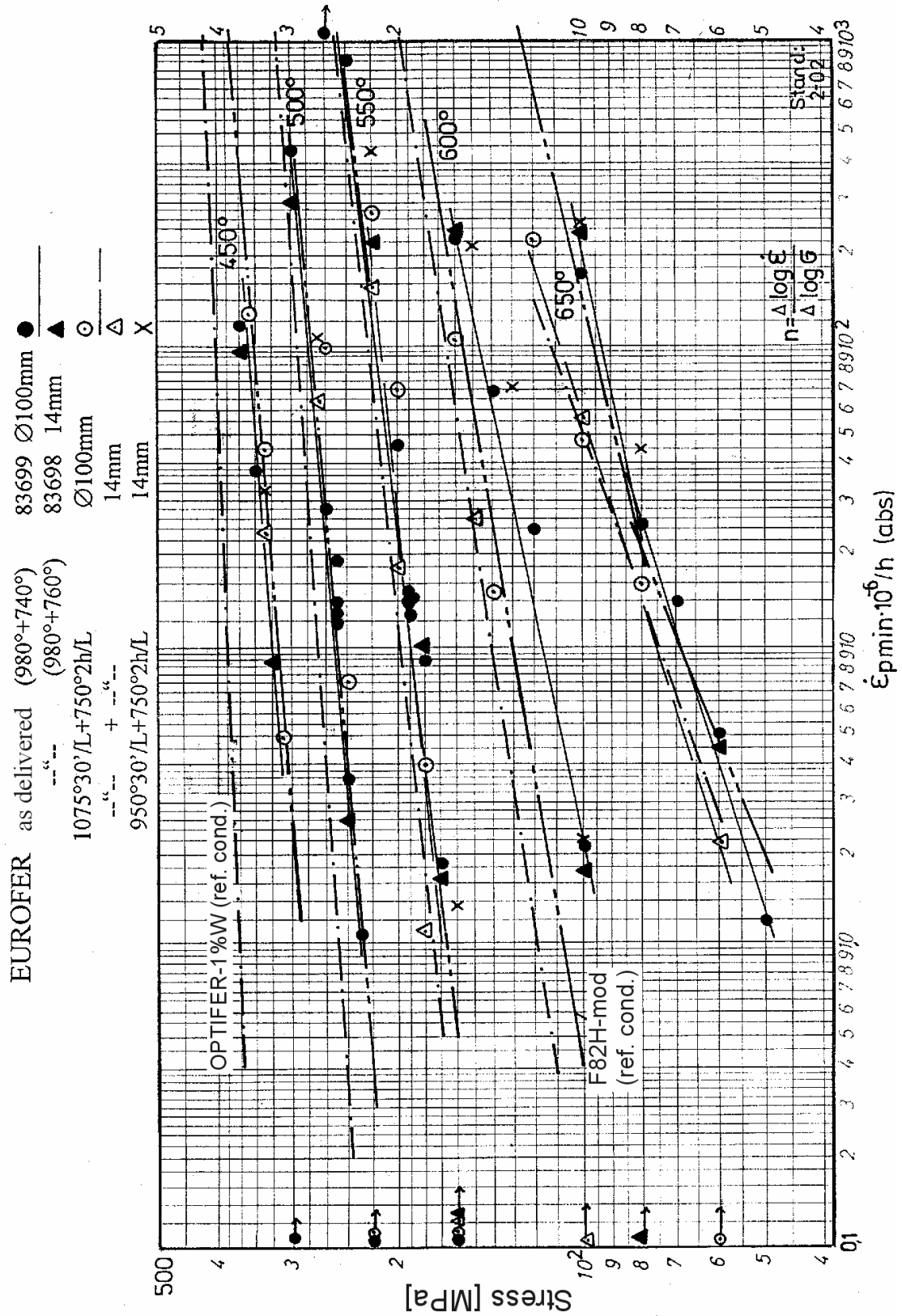


Fig. 28: Minimum creep rate dependent on stress (influence of annealing and comparison with OPTIFER and F82H-mod)

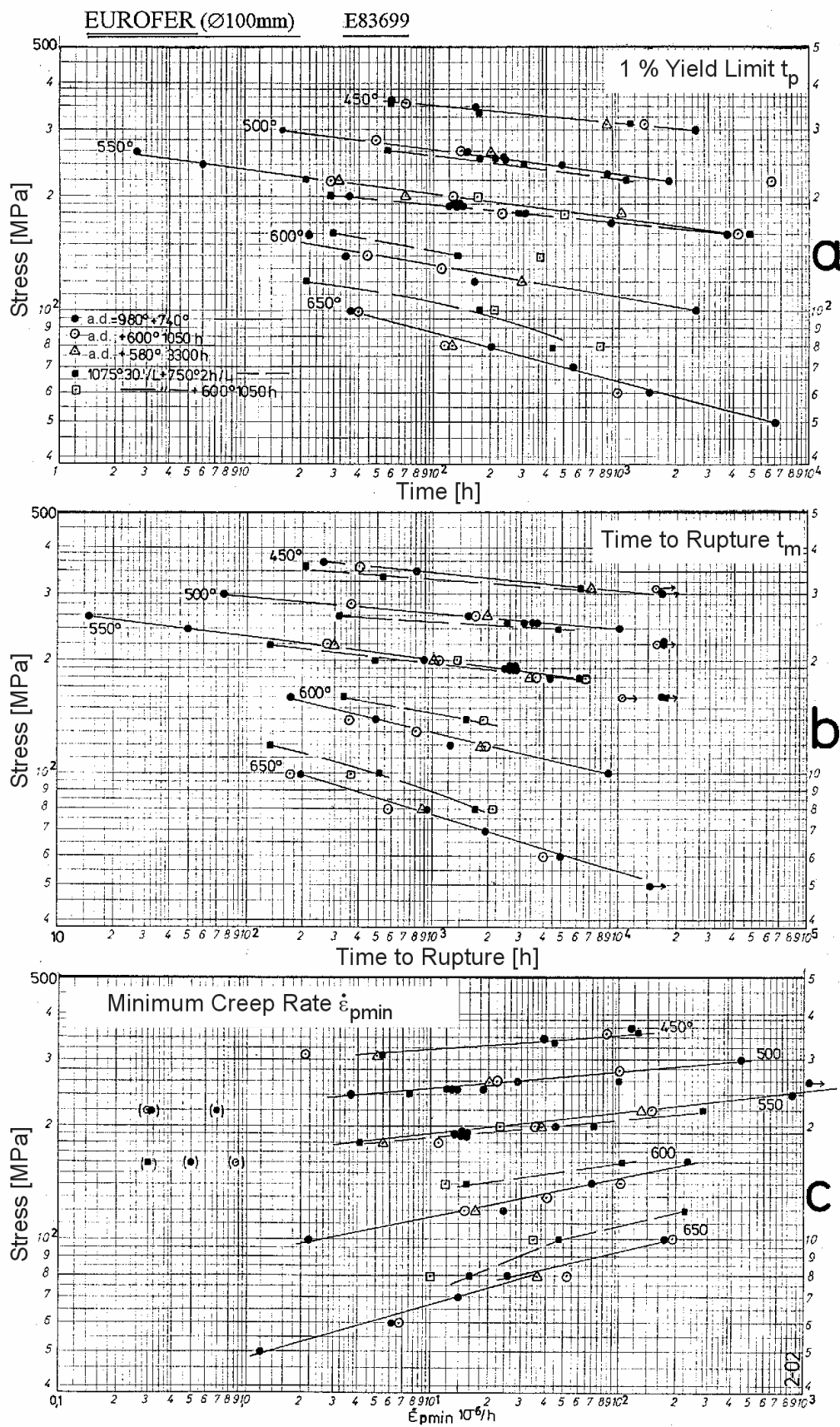


Fig. 29: Influence of ageing on creep properties

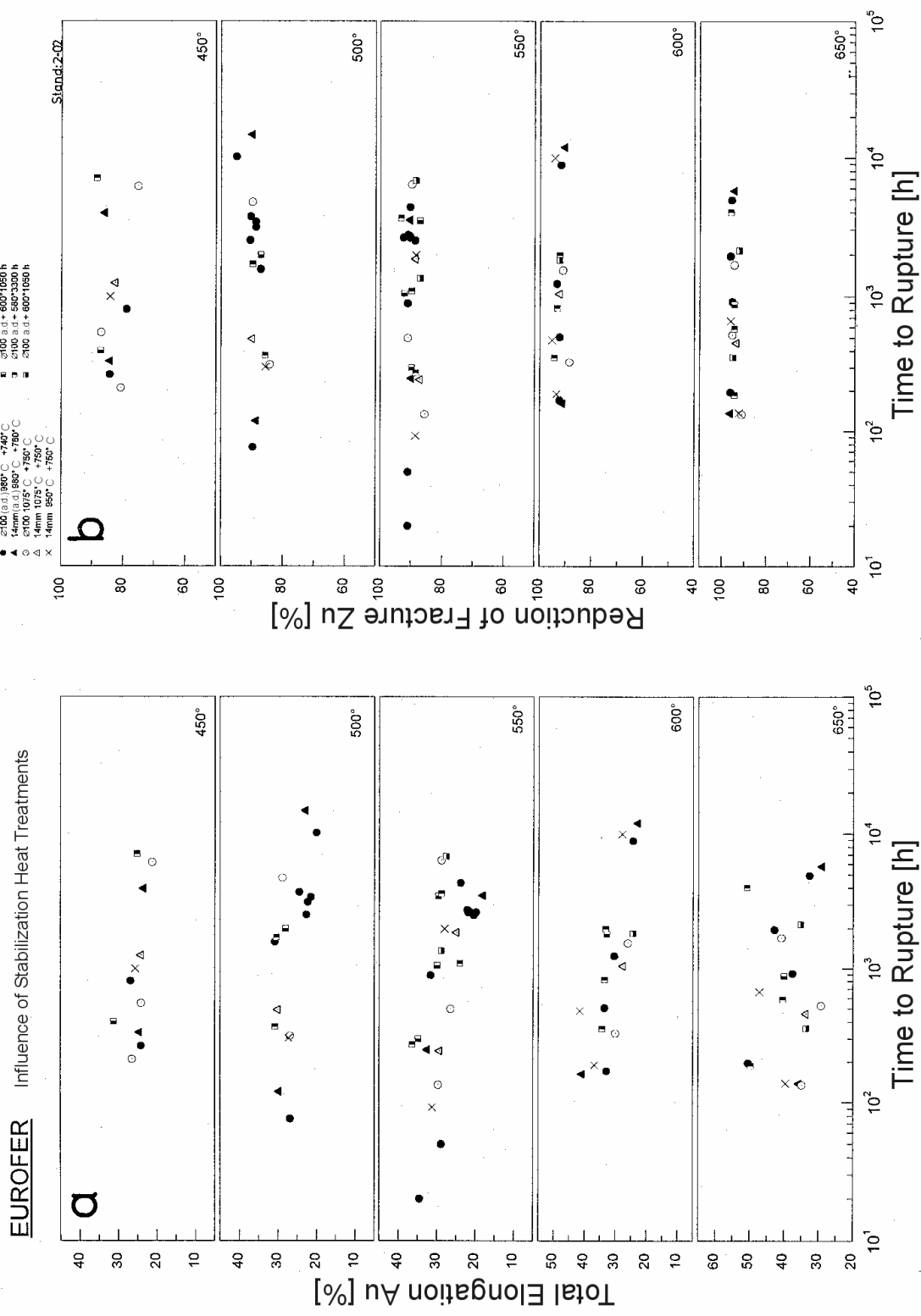


Fig. 30: Total elongation and reduction of fracture dependent on time to rupture

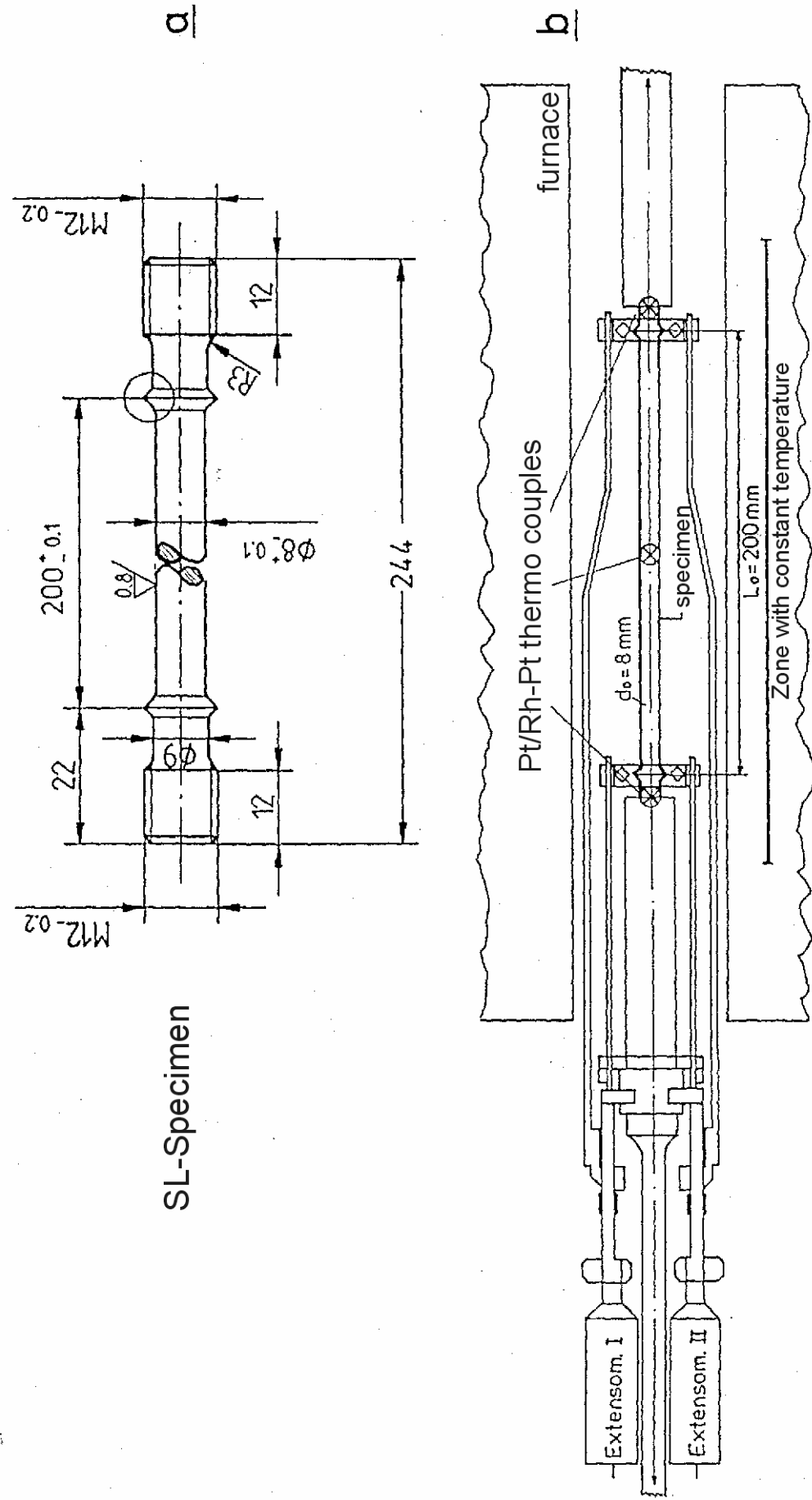


Fig. 31: Creep specimen and device for long-term creep tests at low stresses

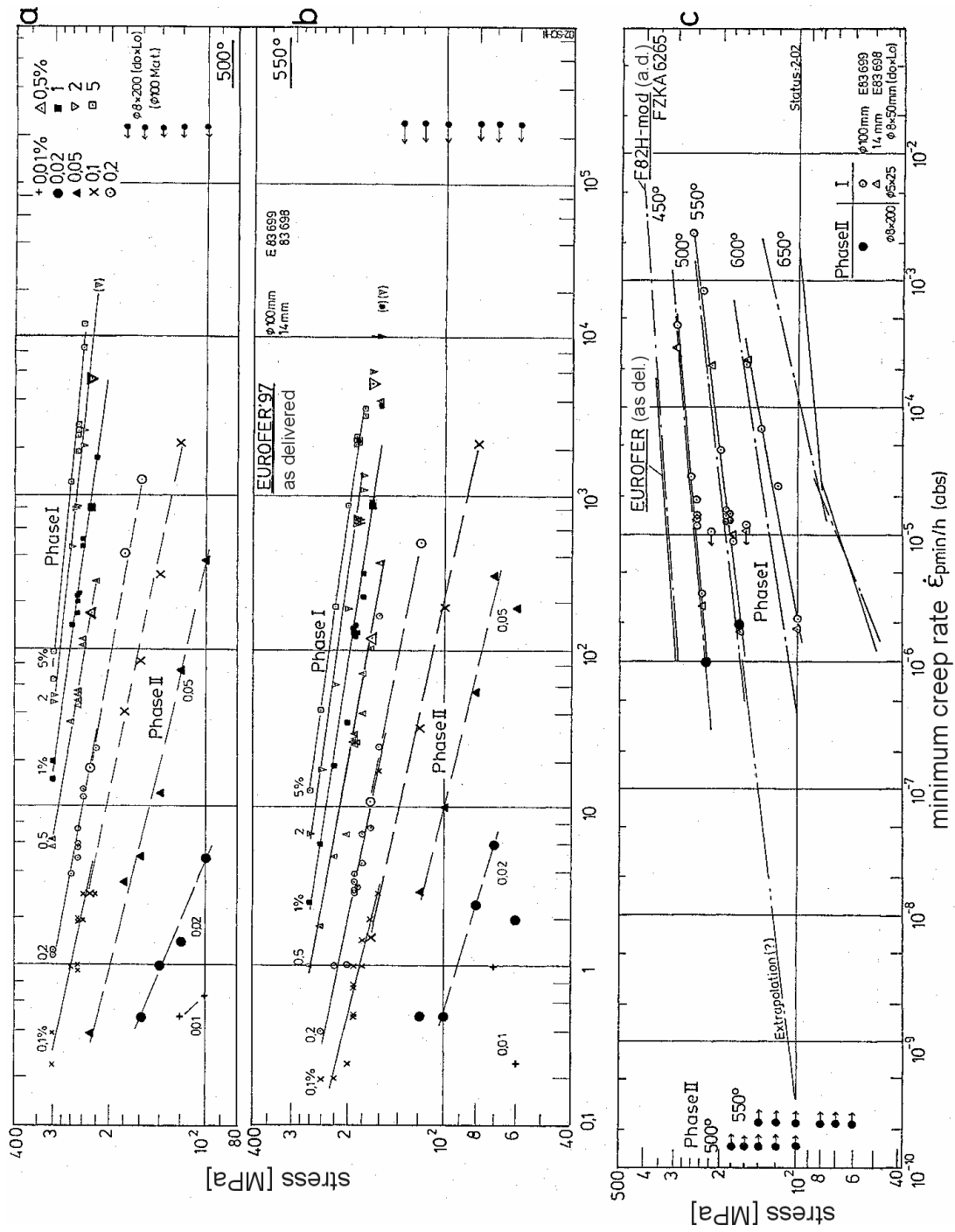


Fig. 32: Yield limits and minimum creep rate

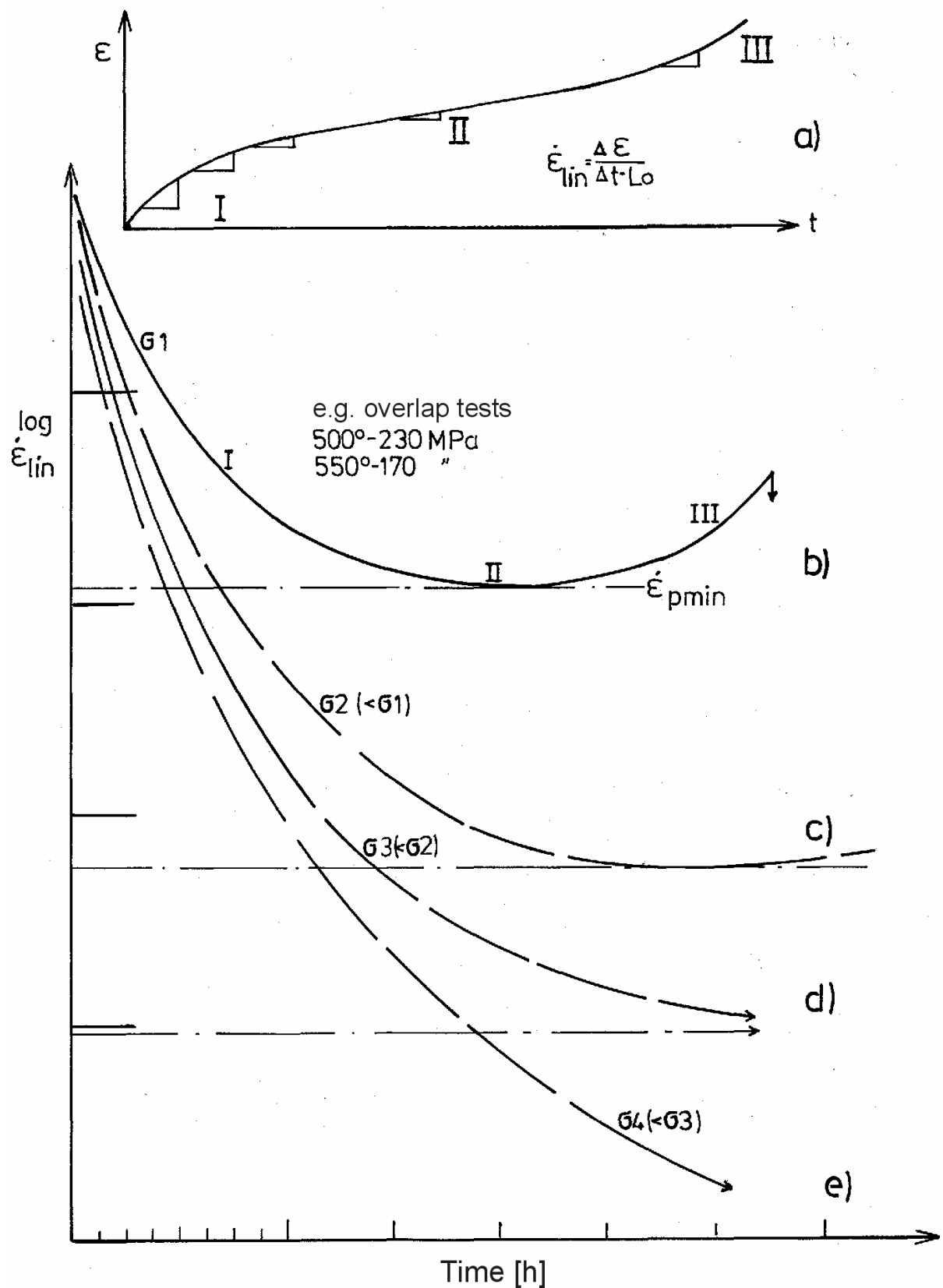


Fig. 33: Schematic drawing of creep curves

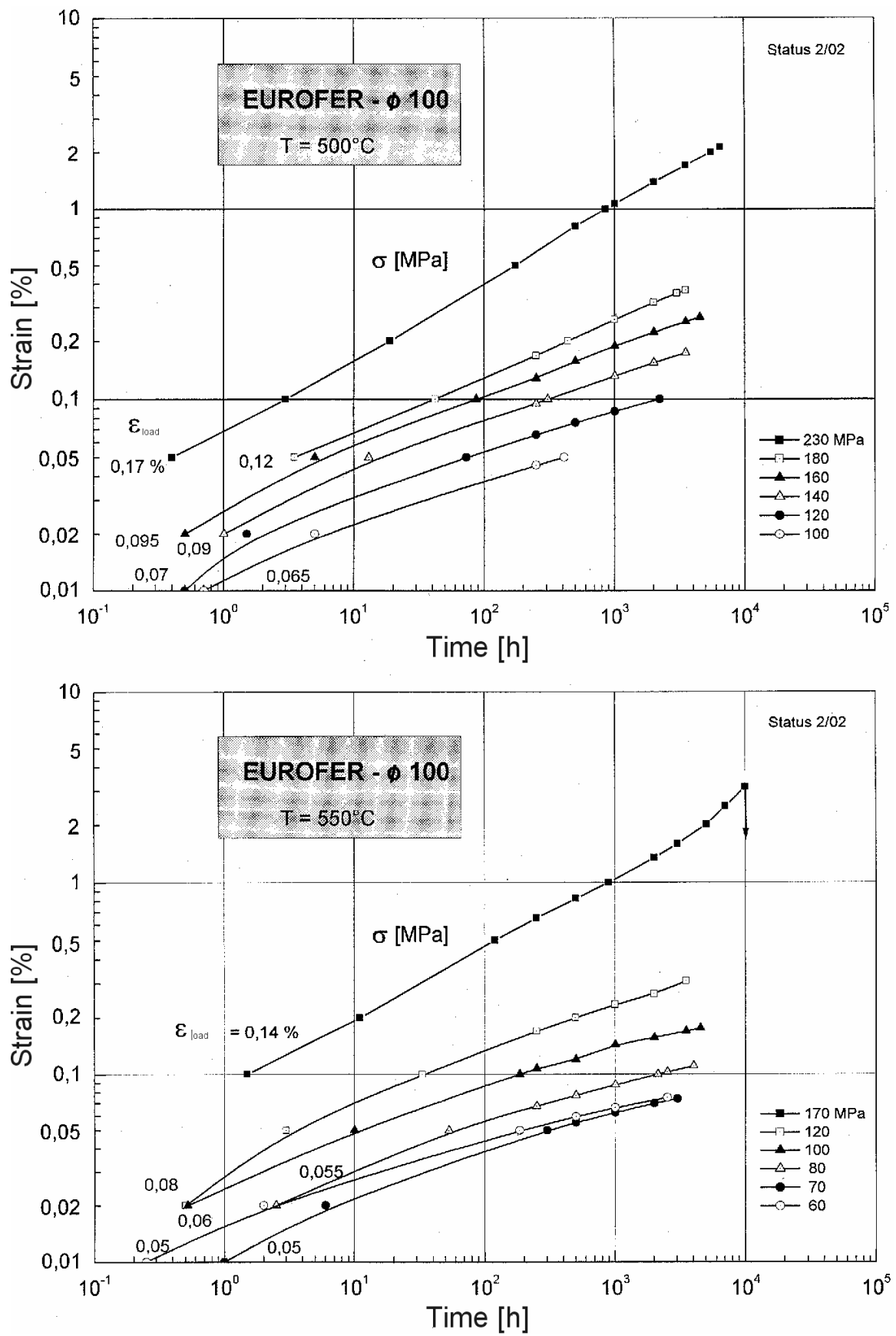


Fig. 34: Present state of the long-term creep tests with EUROFER 97

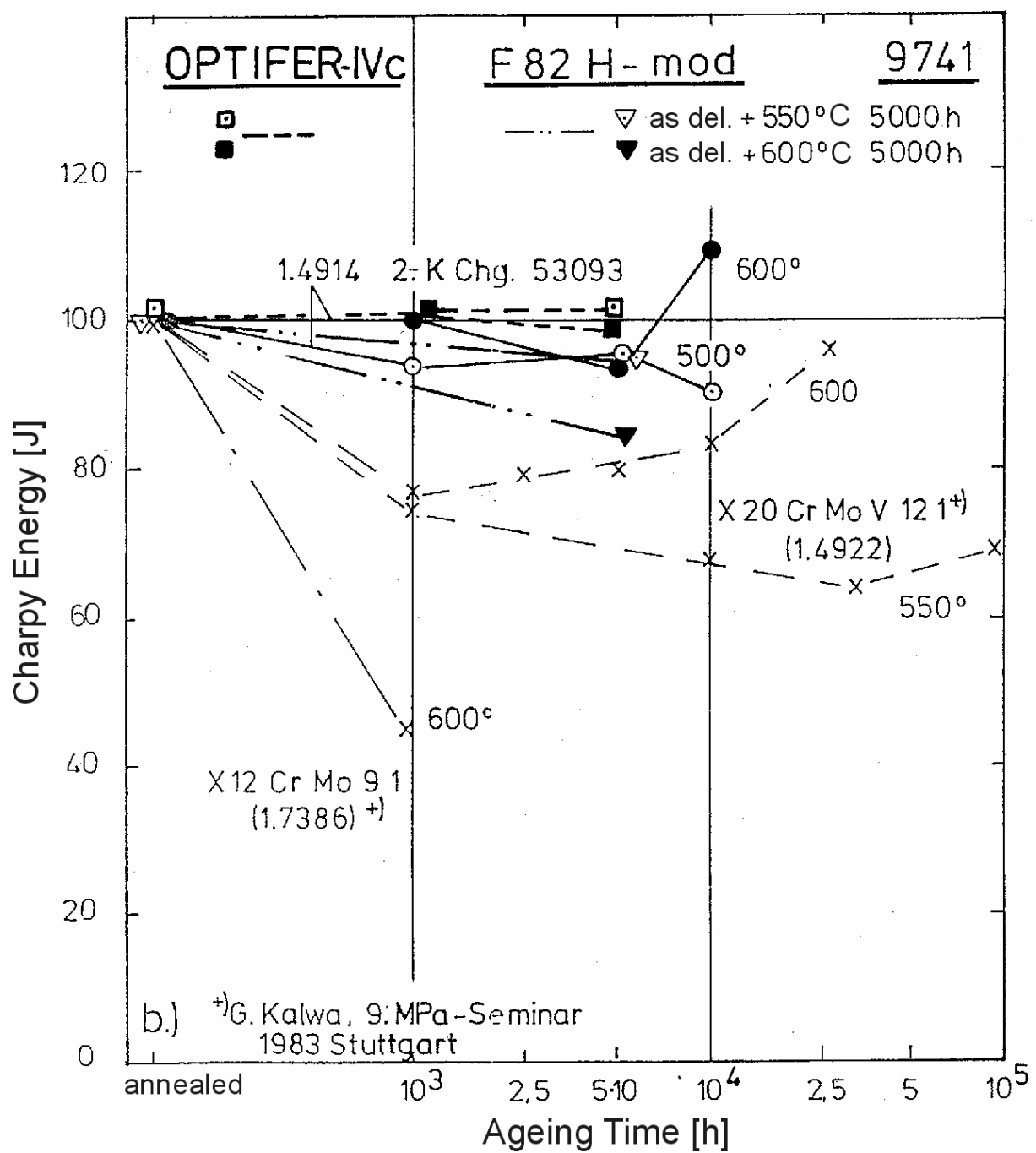
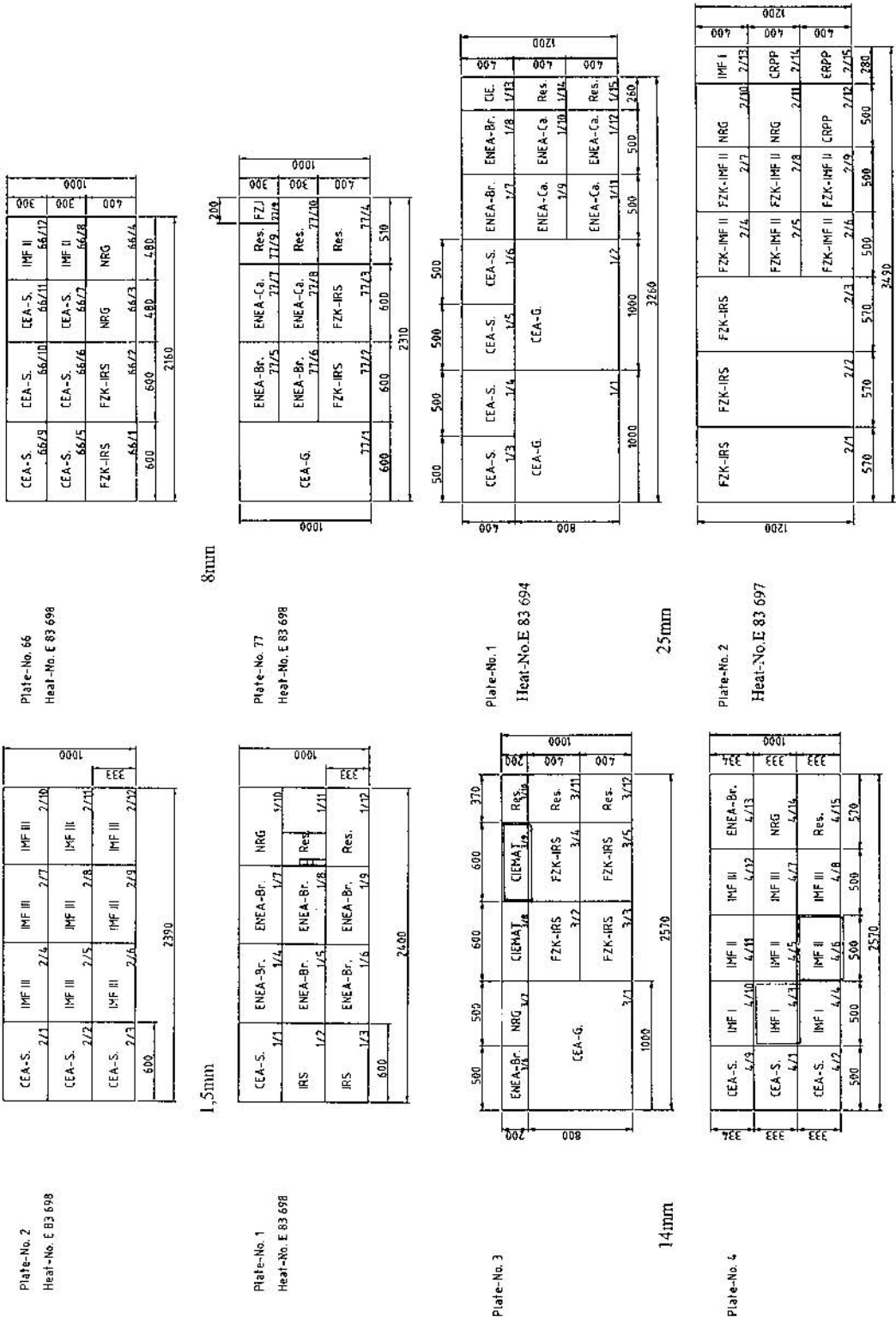


Fig. 35: Charpy energy dependent on ageing time



Marking on bottom right corner, direction of last roll indicated \rightarrow WR \leftrightarrow

Fig. 36: Distribution of EUROFER plates